

**UNCLASSIFIED**

---

---

**AD 297 370**

*Reproduced  
by the*

**ARMED SERVICES TECHNICAL INFORMATION AGENCY  
ARLINGTON HALL STATION  
ARLINGTON 12, VIRGINIA**



---

---

**UNCLASSIFIED**

NOTICE: When government or other drawings, specifications or other data are used for any purpose other than in connection with a definitely related government procurement operation, the U. S. Government thereby incurs no responsibility, nor any obligation whatsoever; and the fact that the Government may have formulated, furnished, or in any way supplied the said drawings, specifications, or other data is not to be regarded by implication or otherwise as in any manner licensing the holder or any other person or corporation, or conveying any rights or permission to manufacture, use or sell any patented invention that may in any way be related thereto.

~~297 370~~

**297 370**

63-2-5

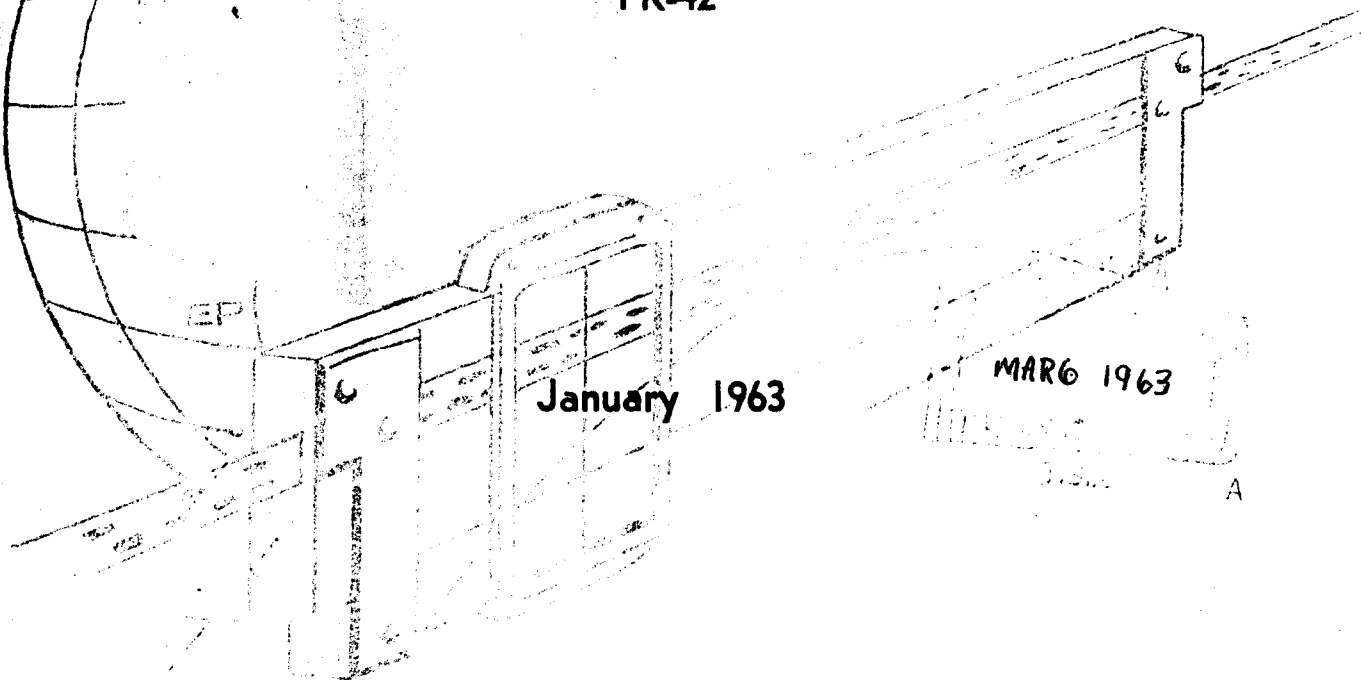
CATALOGED BY ASTIA

ASAP 297370

UNIVERSITY OF NEW MEXICO  
ALBUQUERQUE

**ENGINEERING EXPERIMENT  
STATION**

1962 PROGRESS REPORT  
ON  
**SUBMARINE COMMUNICATIONS  
RESEARCH**  
PR-42



Prepared Under  
Contract Nonr 278(01) (FBM)

**Best Available Copy**

1962 PROGRESS REPORT ON SUBMARINE  
COMMUNICATIONS RESEARCH [CONTRACT Nonr 2798(01)(FBM)]

Summaries of Reports Presented to the U.S. Navy

18 and 19 February 1963

at

The Naval Research Laboratory  
Washington, D. C.

PR-42

Department of Electrical Engineering  
University of New Mexico  
Albuquerque, New Mexico

Prepared under  
Contract Nonr 2798(01)(FBM)

## TABLE OF CONTENTS

	<u>Page</u>
<b>Table of Contents</b>	<b>1</b>
<b>Introduction</b>	<b>2</b>
<b>Summary of General Progress</b>	<b>3</b>
<b>The Effect of the Rough Air-Sea Interface on ELF/VLF Electromagnetic Wave Propagation</b>	<b>9</b>
<b>The Nature of the Sea Surface</b>	<b>9</b>
<b>The Boundary Value Problem for E.M. Fields in the Presence of the Rough Air-Sea Interface</b>	<b>20</b>
<b>Electromagnetic Radiation in Magneto-Ionic Media for VLF and VHF Spectra</b>	<b>34</b>
<b>Background Study for the Calculation of the Driving-Point Impedance of a Cylindrical Antenna in the Anisotropic Ionosphere</b>	<b>62</b>
<b>Air-to-Subsurface VLF Propagation</b>	<b>68</b>
<b>I Air-to-Submarine Communications</b>	<b>68</b>
<b>II Electric Field Components in the Sea</b>	<b>73</b>
<b>Investigation of Parallel-Wire and Coaxial Side- Loaded Transmission Lines as a Trailing Wire Antenna</b>	<b>95</b>
<b>Experimental Investigations</b>	<b>119</b>
<b>Plans for 1963</b>	<b>138</b>
<b>Index of Reports and Memoranda Issued under Contract Nonr 2798(01)(FBM) since October 1961</b>	<b>145</b>

## INTRODUCTION

This is an interim progress report on Contract Nonr 2798(01)(FBM) covering the work done on submarine communications at the University of New Mexico during the last three months of 1961 and the calendar year 1962. It was prepared to supplement the oral presentation to be given to the Navy Department at the Naval Research Laboratory on February 18 and 19, 1963. A similar, oral and written, report was rendered to the U. S. Navy on October 13, 1961. It summarized the progress on the contract up to October, 1961.

Bimonthly progress reports are submitted to ONR except for the months of July and August, when monthly progress reports are rendered. These reports give a detailed account of the work as it progresses. The purpose of this report is not to itemize the work done on the project during the period reported upon, but to summarize and highlight the work on the tasks on which more significant progress was made. For more detailed information reference should be made to the reports published on the contract. Such list appears elsewhere in this report.

It should be noted that this is a progress report and, therefore, the results and/or conclusions presented should not be taken as final. Changes in the findings may have to be made as additional information and data become available.

## SUMMARY OF GENERAL PROGRESS

During the last three months of 1961 and the calendar year 1962 the investigations conducted under Contract Nonr 2798(01)(FBM) continued in general along the same lines as the year before. However, our goals became clearer, our tasks better oriented and our studies directed toward the solution of certain more defined problems. Several tasks were completed, others were modified and several new ones initiated.

From the general approach to the problem of investigating submarine communications, the work at UNM on the ELF/VLF portion of the frequency spectrum can be divided into three general areas; these are:

1. Study of ELF/VLF propagation in air, sea and the ionosphere.
2. Investigation of ELF/VLF antennas in these media.
3. Modeling and experimentation to confirm results of the theoretical investigations.

Each of these areas is subdivided into a number of tasks with specific goals. A general summary of our progress on each task follows.

1. The study of ELF/VLF propagation consisted of the following tasks:

a. Undersea Propagation. The main effort under this task consisted of evaluating the effect that a rough sea surface (wave height and length) has on the amplitude and phase of an electromagnetic wave transmitted from the air to the sea; this is to be followed by a study of the effect such a surface may have on a wave going from the sea to the air. In other words, the purpose of this task is to develop a technique by means of which the fields near the interface can be calculated when the fields some distance from the interface are known. The initial phase of this task consisted of defining or describing the surface of the sea, including its various states of roughness. Having done this, the second phase is to solve the boundary value problem. We have made some progress on this task and a more detailed report on it follows.

b. Subterranean Propagation. This task, whose goal was to investigate the feasibility of long-range low frequency propagation in the earth's crust, was concluded. Based on experiments, we found that even under the best of conditions low frequency propagation in the earth's crust beyond the range of several hundred miles was not feasible. We will give a concluding report on this task.

c. Satellite-Submarine Propagation. The purpose of this task is to investigate ELF/VLF propagation in the ionosphere in order to determine the feasibility of propagating ELF/VLF signals radiated from satellite antennas.

The initial effort consisted of studying the general theory associated with propagation in anisotropic media such as the ionosphere. Approximate solutions were developed for the radiation field from a dipole source in the ionosphere. Then power relations and radiation resistance for elementary dipoles operating at VLF in the ionosphere were derived. We found that the same approach applies to the VHF portion of the spectrum. We will go into more detail on the progress on this task.

d. Study and Measurement of Noise in Sea.

The initial effort under this task consists of finding a suitable method to evaluate sensors in a conducting medium such as sea water. This includes the coaxial type (both shorted and open), the loop type of several configurations and the toroidal type. Expressions are being derived for the open circuit voltage for the three types of sensors. This requires an expression for the self-impedance of each type of sensor. As of this date the work on this task has not progressed sufficiently to report on it in more detail.

2. Our investigations of antennas covered five separate tasks. The first one consisted of:

a. Submerged Antennas. Following the work that Dr. Anderson did several years ago on submerged ELF antennas, we are reconsidering our approach to this task. Anderson, in his study, made some simplifying assumptions and approximations. His results are applicable only at large distances.

Anderson felt that some kind of a numerical process would have to be used to remove these limitations. Further study showed that the whole problem was much more complicated than at first anticipated. It appeared that integrals of the type Anderson used occur frequently in electromagnetic and acoustic problems involving layered media. There was a need to evaluate such expressions and it appeared desirable to find a computer technique to make the solution of such integrals routine. After some study of the problem, the conclusion was reached that to solve these integrals for the variation of the several parameters involved would be an enormous task. It has been shown that without the ionosphere a submerged horizontal electric dipole can be replaced by another horizontal electric dipole at the air-sea boundary. It appears that such an approach to the problem may be superior and more direct to that of evaluating the integrals on a computer. We are looking into this approach further.

Under this task we have also continued the study of coaxial and toroidal receiving antennas in sea water. This phase of the task will be covered in more detail.

b. ELF Antennas for Launching Waves in Air. A sub-task, which consisted of the study of the feasibility of using an island-sea configuration as a natural slot (aperture) antenna for operation in the ELF electromagnetic spectrum, was closed out in 1961 when it became apparent that others have already investigated the problem. The concluding report on this phase of the task was published last year as TM-6.

An investigation was initiated in September 1962 to determine if certain subsurface antenna configurations could be used to launch ELF waves in air in a manner comparable to the above-the-surface vertical antennas. The configuration now under consideration is a toroid excited by one or more current windings. This task has not progressed sufficiently to report on it in more detail.

c. Air-to-Submarine Antennas. The purpose of this task is to evaluate the effectiveness of a horizontal against a vertical airborne antenna from the standpoint of radiation at very long ranges. The study has centered at 15 kc/s. The problem has required the development of a technique to determine field strengths at long ranges. Also, the effect of anisotropy of the ionosphere on the propagation of VLF waves is being investigated. We will describe our progress on this task in more detail.

d. Satellite-to-Submarine Antennas. This task is the second phase of the satellite-to-submarine propagation study. This phase has centered on the calculation of approximate expressions for the fields in a region immediately adjacent to a finite antenna structure in an anisotropic homogeneous ionosphere. These will be used in an attempt to determine the driving-point impedance of a cylindrical structure radiating in such an ionosphere. We will go into more detail on the progress on this phase of the task.

e. VLF Airborne Antennas. This task had as its goal the determination of the advantages, if any, that a parallel wire side-loaded transmission line may have if used as a trailing-wire antenna and to suggest a design for a practical form of this type of an antenna for use in the VLF spectrum. The first phase of this task, that is the evaluation of the advantages of a side-loaded trailing-wire transmission line and a method of analysis of such an antenna, has been completed. The results of the experimental work on a scaled model were quite successful. However, the second phase, the design of a practical and flyable antenna, is still under way. We will present our progress on this task in more detail.

3. The third area of our work was in experimentation, modeling and testing. To confirm the results or conclusions of our studies some experimental data is required. It is also needed to get some concept of how the dependent parameters vary when the independent variables are changed. Because of the tremendous effort that would be involved in any full-scale experimental work at ELF/VLF, any work of this type that we do must be appropriately scaled. Our work of this type is limited in scope and restricted only to a back-up for our investigations. It consists of laboratory scaled models of antennas, of the two- and multi-layer problems and of scaled impedance measuring circuitry. We will cover this phase of our work in more detail.

## THE EFFECT OF THE ROUGH AIR-SEA INTERFACE ON ELF/VLF ELECTROMAGNETIC WAVE PROPAGATION

The problem of E.M. wave propagation near the rough air-sea interface falls naturally into two parts:

1. The description of the air-sea interface (i.e., the sea surface);
2. The solution of the boundary value problem for the E.M. fields in the presence of the rough interface.

As Part One is necessary in order to define clearly the problem considered in Part Two, the present state of knowledge about the mathematical description of the sea surface is first briefly reviewed. Then the problem of Part Two is considered in light of this description.

### The Nature of the Sea Surface

Even casual observation shows the great irregularity of the sea surface; no single wave retains its identity long; the period, form, etc., vary greatly even for consecutive waves. Indeed, the sea surface, in a rough sea, seems to vary almost randomly both in time and space.

Presented below is a very brief review of the present state of knowledge about the nature of the sea surface. However, the study of the sea surface continues and changes continue to be made in the theories and mathematical formulations; many questions about the sea surface still remain unanswered and no known theory is in any sense complete.

The study of the sea surface can, for our purpose, be placed into three general categories:

- a. The study of the sea surface by classical hydro-dynamics.
- b. The study of the sea surface by statistical methods.

In this category only the linearized problem will be considered as this allows us to obtain general results. By assuming a linearized free-surface boundary condition, the problem becomes linear and the sea surface can then be described by a known random process (stationary Gaussian process).

c. Other theories which consider the non-linear effects of the sea surface. In this case the results obtained are far less useful for a description of the sea surface than the results of Category b. However, such results place the limitations of Category b in the correct perspective.

Before going into a more detailed study of the sea surface a few general comments are appropriate. First, the present theories assume a fixed meteorological condition. Then the description of the sea surface given by the theory holds only as long as this assumption is approximately true. A theory based on the correlation of the changes in meteorological conditions with changes in the sea surface could be used but would be somewhat complex; however, in some cases this may be necessary. Second, the known theories consider only the gross meteorological conditions (e.g., average wind velocity, average fetch, etc.). In practice this is all that can be assumed without making the problem inordinately complex. Third, no current theory is

complete in the description of the sea surface. Under certain meteorological conditions one theory may be approximately correct; however, it fails when meteorological conditions change. It should be noted that no theory now available gives the complete description of the detailed properties of the sea surface; only the gross features can be accurately described mathematically. A brief discussion of the three general categories follows:

a. Classical Hydrodynamics. When the depth of the sea is large, a solution of the hydrodynamic equations which represent the sea surface is a trochoidal wave [1,2]. The parametric equation of the trochoid is:

$$x = r\theta - a \sin \theta$$

$$z(x) = r - a \cos \theta$$

where

$r$ ,  $a$  - fixed parameters for a given trochoid.

$\theta$  - parameter that varies (i.e., generates the curve).

The trochoid is a two-dimensional wave, which "could exist" in a swell. Using the trochoid to describe the sea surface makes such a surface regular and uniform while, in fact, the sea surface is very irregular even in a swell.

A more general model of the sea state would include the irregularity of the sea; however, such a formulation is too complex for practical use. We consider this model as some of the results will be used later. Leaving out the details, the following equation of a simple harmonic progressive wave is a solution to the linearized hydrodynamic equations:

$$\xi(x, y, t) = A \cos \left[ \frac{2\pi}{L} (x \cos \theta + y \sin \theta) - \frac{2\pi}{T} t + \epsilon \right] \quad (1)$$

where

$\xi$  - sea surface

A - amplitude of the simple harmonic progressive wave

T - period of the simple harmonic progressive wave

L - wavelength of the simple harmonic progressive wave

c - velocity of the simple harmonic progressive wave

$\theta$  - direction of propagation measured with respect to the  $+x$  axis

$\epsilon$  - phase at  $x = y = t = 0$  (arbitrary)

If we let:

$\vec{r} = x\hat{x} + y\hat{y}$  - position vector in the horizontal plane

$\vec{k} = k_x\hat{x} + k_y\hat{y}$  - propagation vector in the horizontal plane

$k = |\vec{k}| = \frac{\omega^2}{g} = \frac{2\pi}{L}$  - wave number [3]

$g$  - acceleration due to gravity

$\omega = \frac{2\pi}{T}$  - radian frequency of the wave

then:

$$\xi(\vec{r}, t) = A \cos (\vec{k} \cdot \vec{r} - \omega t + \epsilon) \quad . \quad (2)$$

If we assume that the waves are progressing in the  $+x$  direction (i.e.,  $k_x \geq 0$ ) which is reasonable if the wind is in the  $+x$  direction, the general solution is [4]:

$$\xi(\vec{r}, t) = \int_{-\pi/2}^{\pi/2} \int_0^{\infty} [a(\omega, \theta) \cos (\vec{k} \cdot \vec{r} - \omega t) + b(\omega, \theta) \sin (\vec{k} \cdot \vec{r} - \omega t)] d\omega d\theta \quad (3)$$

where

$a(\omega, \theta)$  and  $b(\omega, \theta)$  are the spectra of  $\xi(\vec{r}, t)$

If  $\xi(0, y, t)$  is known, we can obtain  $a(\omega, t)$  and  $b(\omega, t)$  and therefore  $\xi(x, y, t)$ . However, it is clear that the deterministic model of the sea surface as given above is not practical. As has been the case with many problems whose complexity defy deterministic solution, one next attempts to formulate the problem in probabilistic terms. We will now consider such an attempt.

b. Statistical Description of the Sea Surface. In the past few years there has been an increased tendency to treat many natural phenomena as random processes. The main feature of such a process is an indeterminacy in the expected behavior of a single occurrence coupled with strong statistical properties for a large number of occurrences. The "indeterminacy" in the sea surface comes from the complexity of its mathematical description [e.g., finding  $\xi(0, y, t)$ ].

Chronologically, experimental data first lead to the assertion that the sea surface could be represented approximately as a stationary multivariate Gaussian process. From a theoretical view, it can be shown by using equation (2) with the assumption that the random variable  $\epsilon(\omega, \theta)$  has a uniform distribution, that the general solution for the sea surface is [4]:

$$\xi(\vec{p}, t) = \int_0^{\infty} \int_{-\pi}^{\pi} \cos [\vec{k} \cdot \vec{p} - \omega t + \epsilon(\omega, \theta)] \sqrt{A^2(\omega, \theta)} d\omega d\theta \quad (4)$$

This expression is a multivariate Gaussian process, where  $A^2(\omega, \theta)$  is the energy density spectrum. This (as does (2))

assumes linearized equations and boundary conditions; if these assumptions hold, the surface is given by (4). However, as stated above the experimental data implies that the surface is only approximately Gaussian, the error being due in large measure to the nonlinear effects neglected by this theory.

The same results can be given in a standard notation such as used in reference [3]

$$\xi(\vec{r}, t) = \int_{-\pi}^{\pi} \int_0^\infty A(\omega, \theta) \cos(\vec{k} \cdot \vec{r} - \omega t + \epsilon(\omega, \theta)) d\omega d\theta \quad (5)$$

where:

$$\frac{1}{2} A^2(\omega, \theta) = E(\omega, \theta) \text{ is the energy density spectrum.}$$

Using this Gaussian model of the sea surface, many of the general properties of the "sea state" have been calculated. [4,5,6]. The basic question to be resolved is: Can the multivariate Gaussian process describe accurately the real sea surface? If not, from what standpoint is it deficient?

To answer this question, we consider a specific model of the sea surface (i.e., a given spectrum  $E(\omega, \theta)$ ) and then compare this random process with the known properties (experimental data) of the sea surface. Naturally, for a different spectrum, the properties of the sea predicted by the random process will be different. The best known spectrum of the "sea surface" is a semi-empirical expression given by Neumann for a fully developed sea [4]:

$$E(\omega) d\omega = \frac{\pi}{2} \frac{c}{\omega^6} e^{-2g^2/\omega^2 v^2} d\omega \quad (6)$$

where  $v$  is the velocity of the wind "generating" the "sea".

The total energy  $E$  for this spectrum then becomes:

$$E = \int_0^{\infty} E(\omega) d\omega = \frac{c \pi^{3/2}}{2^{13/2} g^5} 3v^5 \quad (7)$$

This seems to be in agreement with some experimental data if  $c = 3.05 \text{ m}^2/\text{sec}^5$ . To study in detail what this model predicts, we will consider the shape of the spectrum and some of its results.

Neumann's spectrum rises rapidly at  $\omega = \frac{g}{1.6v}$  and has a maximum at  $\omega = \sqrt{\frac{2}{3}} g/v$ . For large  $\omega$ ,  $E(\omega) \approx \omega^{-6}$  and for small  $\omega$ ,  $E(\omega) \approx e^{-2g^2/\omega^2 v^2}$ ; therefore, there is very little energy in the low frequency (long wavelength) part of the spectrum.

Neumann's spectrum is for a fully developed sea only. In actuality, of course, the sea may not be fully developed. The growth of the sea waves depends upon the fetch (distance over which the wind blows), the duration (length of time the wind has been blowing) and naturally, the wind velocity. There are methods that consider the problem of duration-limited and fetch-limited seas (but only approximately).

From empirical data an approximate directed spectrum (which depends on the direction relative to the wind as well as on the duration and fetch of the wave) is [4]:

$$E(\omega, \theta) = \begin{cases} c \frac{e^{-2g^2/\omega^2 v^2}}{\omega^2} \cos^2 \theta & \text{for: } -\frac{\pi}{2} < \theta < \frac{\pi}{2} \text{ and } \omega_i < \omega < \infty \\ 0 & \text{otherwise} \end{cases} \quad (8)$$

where

$\theta$  - polar angle with reference to the x axis (the wind is blowing in the +x direction).

$\omega_i$  - intersection radian frequency (a function of duration and fetch).

The above model is at best an approximation to the sea surface and accurate only under certain conditions. There are better models [3,7]; they are, however, more complex concerning the directional part of the formula; other inaccuracies have also been noted in all the models. This is particularly true for high sea states where the sea may not be fully developed. Other empirical formulas are available to represent the sea surface in this case [8]. It is still not conclusively known how well the statistical results of this model hold for actual sea waves.

Neumann's model of the sea surface contains some energy in the high frequency part of the spectrum and predicts the sea to be "completely covered by short wavelength ripples." Physically, this seems reasonable even though the above spectrum is known to be deficient in the high frequency range. The error in the high frequency part of the spectrum is due to the fact that non-linear effects are prevalent at these frequencies; we consider this effect in the next section.

c. The Generation of the Sea Surface and Non-Linear Effects. Phillips [9] has described the generation of the sea surface by considering turbulent fluctuation of the air (wind) above the air-sea interface. At present this theory seems to be accepted as correct for the "original" formation

of the sea surface. However, once the waves have been formed, their growth occurs through other mechanisms.

At present there are two principal theories on the growth of waves:

(a) Phillips' resonance theory. [10]

(b) Miles' sheer-flow instability theory. [11]

These two theories do not agree in many respects (e.g., Phillips' theory gives a "growth rate" proportional to time and Miles gives a "growth rate" exponential with time). While both mechanisms play a role in the growth of waves, Phillips has recently given a description of the domains of dominance of each mechanism. These theories, while they do give some understanding of the sea surface, are unfortunately of no qualitative help at present in describing the sea surface.

We will consider only one other mechanism of energy transfer, the breaking of the waves. Under sufficiently high winds, the energy transfer from the breaking of waves reaches an equilibrium; then for that range of frequencies where the non-linear (breaking) effects are important the energy spectrum is given by:

$$E(\omega) = \alpha g^2 \omega^{-5} \text{ where } \alpha = 7.4 \times 10^{-3} \text{ (empirical constant)}$$

The same basic conclusions (under basically the same restrictions) were obtained by Mikhailov [12], who used the theory of turbulence. There is close agreement between these theories [Phillips has  $E(\omega) \sim \omega^{-5}$ , Mikhailov cites experimental work which gives  $E(\omega) \sim \omega^{-4}$  to  $\omega^{-6}$ ; both theories are within these bounds. Note Neumann in this range has  $E(\omega) \sim \omega^{-6}$ ].

Tick [13,14] has considered the problem of non-linear effects from a perturbation point of view. He adds to the "linear (Gaussian) spectrum" a correction due to the non-linear effects. However, the statistics of the "non-linear" spectrum are not known.

All theories (as those above) which do not directly consider capillary waves (waves of very short wavelength) do not hold for frequencies in the "capillary" range. While much work on capillaries has been done, at present there is nothing available on correlating this theory with the overall sea surface. And there is no correct information available on the "capillary" range of the energy density spectrum. Work on radar return and light reflection [15] from the sea surface has shown that the slopes of the sea surface are nearly Gaussian and that the sea surface curvature is highly non-Gaussian. The usual experimental data taken for description of the sea surface does not include frequencies in the "capillary" range.

The complexity of the air-sea interface alone is enough to make one resort to statistical analysis; however, the fact that both the linear model and the experimental data give a Gaussian process for the gross features of the sea surface implies that a useful model would be a statistical one.

If one is willing to neglect the non-linear effects of the sea surface and use the Gaussian model, the Ergodic theorem [4] implies that the ensemble analysis of statistical properties is the same as space (or time) analysis of the statistical properties (note that this requires a stationary

process, i.e., an equilibrium state). There are questions as to the validity of the Gaussian model as regards the statistical properties of the sea surface. However, if one is only interested in the gross statistical features, then the Gaussian description may be adequate. However, such description will give only the "smooth average" shape of the sea without any details such as ripples or minor variations. The experimental data on sea surface variation is meagre; the processing of such data for meaningful results is long and costly; therefore, it is doubtful if an accurate description of the sea surface can be readily obtained. The shape of the surface of the sea depends upon past as well as upon present conditions; however, to a degree of approximation, past effects though still significant may be discounted. Also by describing the sea condition by means of only a few average parameters, the sea surface will not be represented accurately in every detail, but from the practical approach, this may be all that can be done. This is the point of departure for the study of propagation of electromagnetic waves near the air-sea interface.

The Boundary Value Problem for E.M.  
Fields in the Presence of the Rough Air-Sea Interface

"In the mathematical sense the problem at hand is extremely complex, since it is impossible to use the method of separation of variables to obtain a solution of the wave equation which satisfies the boundary conditions specified on the uneven surface. The methods for obtaining an accurate solution of this problem in general form has (sic) not yet been found. However, there are a number of theoretical papers (which have appeared essentially during the last 5-6 years) in which a number of approximate methods for computing the field have been developed." This is a quotation from a survey paper: "Theory of the Scattering of Waves at Periodically Uneven Surfaces," by Iu. P. Lysanov [16]. This paper treats for the most part the problem of a scalar field in the presence of a periodically uneven (rough) surface with "natural" boundary conditions. When the boundary conditions of the actual problem are not the "natural" ones, the "natural" boundary conditions are used as an approximation. The "interface" boundary conditions are not considered. The problem treated is then the simplest problem considering a rough surface; even then, this problem is not solvable using known techniques. Although work on this problem has continued for a number of years, little advancement has been made; no new methods or theories have resulted; and the investigation has generally been confined

to refinement of techniques given in Lysanov's paper and experimental data. The theory (techniques of "solution") for the rough surface (or interface) problem is reviewed with the discussion limited to the inadequacy of the "solutions".

Basically Lysanov's approach will be followed. He considers six general classifications (or techniques):

1. Rayleigh's Method. This is the oldest approach and due to Rayleigh. Rayleigh assumed that the reflected (scattered) field could be represented as a sum of outward (from the surface) directed plane waves. However, this is only true for the fields above the highest point of the surface. Lippmann [17] showed that the assumption of Rayleigh was not quite correct; unfortunately, he could not obtain an "accurate" solution to the problem by the use of his variational technique.

Barantsev [18] has also obtained the same result by use of Laplace transforms. In Barantsev's approach to the problem, as in Rayleigh's, an infinite number of algebraic equations must be solved. In the case where the irregularities are small (the maximum height of the surface wave is much smaller than a wavelength of the radiation field) Rayleigh obtained a solution for the first mode (specular reflection); this agrees quite well with experimental data in the "far field", however, near the interface many evanescent (surface) waves are present and an accurate solution is not practicable (even if Rayleigh's assumption were to be considered correct) [19,25].

2. The Method of Small Perturbations. The boundary conditions are specified on the uneven surface,  $z = \xi(x)$ , and then

are transferred to the plane  $z = 0$  by means of an expansion into a power series with respect to  $\xi$ . It has been shown by Lysanov that this method leads to solutions identical to Rayleigh's results. It was used by Feinberg for solving the problem of propagation of radio waves along the earth's surface and more recently by Senior [20] who considered the effect of surface roughness on the reflection of E. M. waves. Senior was able to replace surface roughness by a change in the impedance at the boundary. The surface impedance is then a function of position. Hessel [21] and others have also considered the problem of varying surface impedance; Hessel seems to account for Wood's anomaly this way; however, this method is useful only in the far field. Bass [22] also uses the method of perturbations to obtain results parallel to Senior, these again are valid only in the far field. Lysanov [23], has extended this theory to point sources.

3. The Method of L. M. Brekhovskikh. This is the method of physical optics [24]. As in this method the fields on the surface are assumed, the problem becomes one of evaluation of an integral [25] which cannot be readily accomplished for the region near the surface.

A related approach, the Kline-Luneberg theory, has been recently used to calculate the fields on a rough dielectric surface [26]. A special case of the Kline-Luneberg theory, referred to as geometric optics, has been applied by Leontovich to the case of a highly conducting medium in which the wavelength is "small," and then extrapolated to the problem of a rough interface [27].

For the frequency range that we are interested in (ELF/VLF) the use of geometric or physical optics does not appear generally valid.

4. The Integral Equation Method. The problem of the scalar boundary value problem with "natural" boundary conditions can, by use of Green's theorem, be formulated conveniently as an integral equation. This equation is exact; however, it cannot be solved without making some approximations. If the rough surface satisfies certain conditions (is not too rough), an approximate integral equation is obtained, which can be solved. There is a difference in the field assumed on the surface by geometric optics and the field on the surface obtained by the integral equation method [28]. Unfortunately, the solution to the integral equation is not at present known to be accurate enough for our purpose.

5. The Method of Images. The method of images can be used to investigate the fields in the presence of an uneven surface with a sufficiently simple shape; this has been done by Twersky for a perfectly reflecting plane covered with half-cylinders or hemispheres (with little interaction between scatterers). Biot [29] considered the perfect conduction plane covered by hemispheres with strong interaction (as there would be in the case of the sea surface). Twersky also has considered multiple scattering in a very general way. This method could be used to find the fields on the surface, assumed to be a plane covered with hemispheres; however, to obtain a more realistic model of the sea surface would involve higher multi-pole expansions and this does not seem practical (though Biot thought this

method could be used for the air-sea interface problem). It does give a good idea of what is happening to the E.M. field in the air near the air-sea interface (where Biot uses a static solution).

6. Method of Matching Fields. This method can be used only in the case where the rough surface is such that the space may be separated into regions in which the wave equation allows solution by the method of separation of variables (when the wave equation is written in an appropriate coordinate system). As this is not possible for the air-sea interface, we will not consider this method further.

Lysanov references several papers on experimental work, since then papers covering similar work have been published which seem to imply Rayleigh's theory (including the second mode) is approximately correct for the low frequency problem except near  $\lambda_r = \lambda_w$  ( $\lambda_r$ , wavelength of radiation;  $\lambda_w$ , wavelength of the surface) [19]. Since 1958 many papers on the statistical analysis of the reflection of sound from the rough sea surface have been published; these use either Rayleigh's assumption or Kirchhoff's approximation for the solution of the boundary value problem and as such are only useful in the far field [30,31].

One of the few papers considering "interface" boundary conditions on an irregular surface was published by Wait [32] in 1959; this paper has been used to calculate the effect of the rough surface on the E.M. fields in the sea. Wait bases his approach on the work of Leontovich [27] and obtains the field on a plane in the sea; he then solves the wave equation in the

sea with this as a boundary condition. A short discussion of this work is given in a paper by Whalen [32]. It is noted there that the model of the sea as used in Wait's paper was not too realistic. Because of his approximation, Wait uses a "local boundary condition" which is not exact.

Another paper of interest is by Bass [34], who considers non-local boundary conditions, but uses a perturbation method which invalidates the theory near the interface. He also considers the effect of the variation with time of the rough surface.

Lastly, we note a number of papers on radar scattering from rough surface including the surface of the sea as given by Lysanov. These usually use Kirchhoff's approximation which is reasonable in this frequency range. An excellent discussion of the radar problem is given by Kerr [2]. The most frequently used method is: "The construction of the phenomenological theory starting from the statistical properties of the received signal." [35]

The basic limitation of currently known theories of propagation of E.M. waves in the presence of a rough interface is that no theory holds accurately near the interface. Wait's approach applies the "non local" effects after the waves are below the interface and not at the interface; this introduces some inaccuracy. The use of Kirchhoff's approximation at ELF and VLF can be questioned. No known theory can be considered sufficiently accurate at the interface, so that the fields on the surface can be used as sources (following Huygen's Principle)

for the fields in the sea. Even if we knew the fields on the interface, the use of Huygen's Principle in its usual form may not be very practical (could involve a large amount of numerical integration).

As noted, the known attempts to solve the problem for the field near a rough fixed surface in analytic form have not been very successful. The question, if any of the many approximate methods (of which the method of small perturbation seems most popular at present) are "sufficiently accurate" near the surface, cannot be answered categorically as no bounds can be set on the errors. Efforts to correct this have not been successful and it is felt that little, if any, success would be made by continuing this approach. While further work on a general analytic solution to this problem has continued, no progress can be reported. In light of the quotation from Lysanov, it seems that other methods of solution should be attempted collaterally with a general analytic study. In the past, numerical solutions to a number of special problems have furnished material for a general theory. In this case, the numerical solutions to some special cases may give enough insight to do the same (i.e., give intuitive or the "needed accurate assumption"). This would also make it possible to compare the results from the many approximate methods with the "correct" result and obtain bounds on the error. Numerical solutions could also give the "general effect" of surface roughness.

It, therefore, seems reasonable to turn to other methods to solve the problem numerically. A short outline of such

methods is available in literature [36]. The use of the following two general methods has been considered:

1. Analog (simulation)
2. Numerical (finite difference)

An extensive study of analog simulation is given by Karplus [37]. The use of analog computers does not seem suited to the problem. However, the use of network analogs, based on the finite difference approximations, does appear to apply. Because of its cost, this method will be considered only after other methods are found unapplicable.

The numerical solution of differential equations has been under extensive study for the last several years. This has produced many excellent papers and books [38,39] on the subject. There are many techniques for rapidly obtaining solutions to boundary value problems; however, these methods are not applicable near a rough interface. At present our calculations are limited to two-dimensional problems (the solution for one scalar function). Even in this case, the work involved is extremely long.

#### CONCLUSION

While the available mathematical descriptions of the sea surface are not accurate at very long and very short lengths of sea waves, the available expressions for energy density spectra give the correct gross features of the sea surface. When using the finite difference method for the determination of the electromagnetic fields near a rough sea surface, only the gross

features of the sea surface are required. It appears "best" to use "average" values. The finite difference method appears at present to be the best mathematical approach to the rough interface problem. Use of this method does not require detailed knowledge of the very short wavelength ripples or capillary waves. It also appears reasonable to assume that the statistical properties of the gross features of the sea surface are given by a joint Gaussian distribution for low sea states; for high sea states the non-linear effects predominate and the statistics are not known.

The first case considered using the finite difference method was a two-dimensional sinusoidal surface. The result agrees with other theoretical studies [32] near the surface or the water. Using this method, calculations will be made to see if the same conclusion applies to rougher surface under more general assumptions. The method can in theory be used for three dimensional problems; we will see if this can be done practically. Such an approach to the problem will require some correlation with experimentally determined data.

### Some Useful Formulae

For reference some useful relations pertaining to the sea surface are given below.

If  $\xi(\vec{r}) = A \cos (\vec{k} \cdot \vec{r} - \omega t)$  is a solution to the linearized hydrodynamic equations, then:

$$\omega^2 = gk \tanh kh$$

for  $kh \gg 1$  (large depth)

$$\omega^2 = gk \quad (1)$$

where

$$k = \frac{2\pi}{L}$$

$$\omega = \frac{2\pi}{T}$$

We then have for a single harmonic wave in deep water:

$$v_p = \frac{L}{T} = \frac{\omega}{k} = \frac{g}{2\pi} T$$

$$v_g = \frac{d\omega}{dk} = \frac{1}{2} v_p = \frac{g}{4\pi} T \quad (2)$$

$$L = \frac{g}{2\pi} T^2$$

For relatively "regular" seas (after they have consolidated into a "regular" series of connected troughs and crests).

$$\frac{H}{L} \text{ (height)}: \frac{1}{12} < \frac{H}{L} < \frac{1}{35}$$

(some references give  $\frac{1}{7} < \frac{H}{L} < \frac{1}{20}$ , where  $\frac{1}{7}$  is the theoretical limit for stability (greater slopes will "break")).

$$\text{For a swell: } \frac{1}{35} < \frac{H}{L} < \frac{1}{200}$$

Using Neumann spectrum for a fully developed sea [40] :

$$E = .242 \left( \frac{v}{10} \right)^5 \quad v - \text{knots}$$

$$T_{ave} = .285 v \quad T - \text{sec.}$$

$$L_{ave} = \frac{2}{3} (5.12) T_{ave}^2 \quad L - \text{ft.}$$

## REFERENCES

1. Lamb, H., Hydrodynamics, Dover Publications, Inc., New York, 1945, p. 423.
2. Kerr, D. E., Propagation of Short Radio Waves, McGraw-Hill, New York, 1951.
3. Longuet-Higgins, M. S., "The Directional Spectrum of Ocean Waves, and Processes of Wave Generation," Proceedings of the Royal Society, Vol. 265, No. 1322, Jan. 30, 1962, p. 286.
4. Pierson, W. J., Jr., "Wind Generated Gravity Waves," Advances in Geophysics, Vol. II, 1955, Academic Press, New York, p. 93.
5. Longuet-Higgins, M. S., "The Statistical Analysis of a Random Moving Surface," Trans. Royal Society of London, Series A. Vol. 249, 1956-57, p. 321.
6. Longuet-Higgins, M. S., "Statistical Properties of an Isotropic Random Surface," Trans. Royal Society of London, Series A. Vol. 250, 1957-58, p. 157.
7. Pierson, W. J., Jr., (Ed.), "The Directional Spectrum of a Wind Generated Sea as Determined from Data Obtained by the Stereo Wave Observation Project," New York University Meteorological Papers, Vol. 2, No. 6, June 1960, (unpublished).
8. Pierson, W. J., Jr., "A Study of Wave Forecasting Methods and of the Height of a Fully Developed Sea," Deutsche Hydrographische Zeitschrift, Vol. 12, No. 6, 1959, p. 244.
9. Phillips, O. M., "On the Generation of Waves by Turbulent Wind," Journal of Fluid Mechanics, Vol. 2, 1957, p. 417.
10. Phillips, O. M., "Resonance Phenomena in Gravity Waves," Proc. of Symposia in Applied Math, Vol. XIII, Amer. Math. Society, McGraw-Hill, New York, 1962, p. 91.
11. Miles, J. W., "Generation of Surface Waves by Shear Flows," Proc. of Symposia in Applied Math, Vol. XIII, Amer. Math. Society, McGraw-Hill, New York, 1962, p. 79.

12. Mikhailov, V. I., "On the Theory of Scattering of Electro magnetic Waves on the Sea-Surface," Bulletin, Academy of Science, U.S.S.R., Geophysics Series, 1960, p. 818.
13. Tick, L. J., "A Non-Linear Random Model of Gravity Waves I," Journal Math. and Mech., Vol. 8, 1959, p. 643.
14. Pierson, W. J., Jr., "A Note on the Growth of the Spectrum of Wind-Generated Gravity Waves as Determined by Non-Linear Considerations," Journal of Geophysical Research, Vol. 64, No. 8, August, 1959, p. 1007.
15. Cox, C., and W. Munk, "Slopes of the Sea Surface Deduced from Photographs of Sun Glitter," Bulletin of the Scripps Institution of Oceanography, Vol. 6, No. 9, p. 401-488, University of California Press, 1956.
16. Lysanov, Iu. P., "Theory of the Scattering of Waves at Periodically Uneven Surfaces," Soviet Physics Acoustics, Vol. 4, No. 1, Jan.-March, 1958, p. 1.
17. Lippmann, B. A., "Variational Formulation of a Grating Problem," Nuclear Development Associates, Inc., Report No. NDA-18-8, 1952-53 (unpublished).
18. Barentsev, R. G., "Plane Wave Scattering by a Double Periodic Surface of Arbitrary Shape," Soviet Physics Acoustics, Vol. 7, No. 2, Oct.-Dec., 1961, p. 123.
19. La Casce, E. O., "Some Notes on the Reflection of Sound from a Rigid Corrugated Surface," Journal of Acoustical Society of America, Vol. 33, No. 12, Dec. 1961, p. 1772.  
La Casce, E. O., B. D. McCombe, R. L. Thomas, "Measurements of Sound Reflection from a Rigid Corrugated Surface," Vol. 33, No. 12, Dec., 1961, p. 1768.
20. Senior, T. B. A., "Impedance Boundary Conditions for Imperfectly Conducting Surfaces," Applied Science Research, Section B, Vol. 8, 1960, p. 418.  
Senior, T. B. A., "Impedance Boundary Conditions for Statistically Rough Surfaces," Applied Science Research, Section B, Vol. 8, 1960, p. 437.  
Hiatt, R. E., T. B. A. Senior, and V. H. Weston, "Studies in Radar Cross Sections XL," -- "Surface Roughness and Impedance Boundary Conditions," the University of Michigan Research Institute, Ann Arbor, Mich., July, 1960 (Unpublished).

21. Hessell, A., A. A. Oliver, "On the Theory of Wood's Anomalies, in Progress Report No. 19," R. 452.19 61, Polytechnic Institute of Brooklyn (unpublished), AD 256 809.
22. Bass, F. G., V. G. Bocharov, "On the Theory of Scattering of Electromagnetic Waves from a Statistically Uneven Surface," Radiotekhnika Elektronika, Vol. 3, No. 2 1958, p. 180.
23. Lysanov, Iu. P., "On the Field of a Point Radiator in a Laminar-Inhomogeneous Medium Bounded by an Uneven Surface," Soviet Physics-Acoustics, Vol. 7, No. 3, Jan.-March, 1962, p. 255.
24. Mentzer, J. R., Scattering and Diffraction of Radio Waves, Pergamon Press, New York, 1955.
25. Senior, T. B. A., "The Scattering of Electromagnetic Waves by a Corrugated Sheet," Canadian Journal of Physics, Vol. 37, 1959, p. 787 (AD 238 810).
26. Jacobson, A. D., "Luneberg-Kline of Scattering from a Sinusoidal Dielectric Interface," IRE Trans. on Antennas and Propagation, AP-10 #6, Nov. 1962, p. 715.
27. Leontovich, M. A., "Approximate Boundary Conditions for the Electromagnetic Fields on the Surface of a Good Conductor," Diffraction, Refraction and Reflection of Radio Waves, p. 383 (AD 117 276).
28. Meecham, W., "On the Use of the Kirchhoff Approximation for the Solution of Reflection Problems," J. Rational Mech. Analysis, Vol. 5, p. 323, 1956.
29. Boit, M. A., "Some New Aspects of the Reflection of Electromagnetic Waves on a Rough Surface," Journal Applied Physics, Vol. 28, Dec., 1957.  
Boit, M. A., "On the Reflection of Electromagnetic Waves on a Rough Surface," Journal Applied Physics, Vol. 29, June, 1958, p. 998.
30. Proud, J. M., Jr., R. T. Beyer, and Paul Tamarkin, "Reflection of Sound from Randomly Rough Surfaces," Journal of Applied Physics, Vol. 31, No. 3, March, 1960, p. 543.
31. Marsh, H. W., "Exact Solution of Wave Scattering by Irregular Surfaces," Journal of the Acoustical Society of America, Vol. 33, No. 3, March, 1961, p. 330.

- Marsh, H. W., M. Schulkin and S. G. Kneale, "Scattering of Underwater Sound by the Sea Surface," Journal of the Acoustical Society of America, Vol. 33, No. 3, March, 1961, p. 334.
32. Wait, J. R., "The Calculation of the field in a Homogeneous Conductor with a Wavy Interface," Proceeding IRE, Vol. 47, No. 6, June, 1960, p. 1155.
33. Whalen, J. L., "Measured Effects of Ocean Waves on the Phase and Amplitude of VLF Electromagnetic Radiation Received Below the Waves," USL Tech. Memorandum No. 941.1-67-61, 3 August, 1961 (unpublished).
34. Bass, F. G., "On the Theory of Combination Scattering of Waves on a Rough Surface," Izvestia VUZ, Radiofizika, Vol. 4, No. 1, 1961, AD 262 417.
35. Braude, S. Ya, N. N. Komarov, I. E. Ostrovskii, "On the Statistical Nature of Scattering of Centimetre Waves from the Disturbed Surface of the Sea," Radiotekhnika i Elektronika, Vol. 3, No. 2, p. 172, 1958.
36. Moon, P., D. E. Spencer, Field Theory for Engineers, D. Van Nostrand, Princeton, New Jersey, 1961.
37. Karplus, W. J., Analog Simulation, McGraw-Hill, New York, 1958.
38. Collatz, L., The Numerical Treatment of Differential Equations, Springer, Berlin, 1960.
39. Forsythe, G. E., W. R. Wasow, Finite-Difference Methods for Partial Differential Equations, John Wiley, New York, 1960.
40. Pierson, W. J., Jr., G. Neumann, R. W. James, "Observing and Forecasting Ocean Waves," H. O. Publication No. 603, 1958.

ELECTROMAGNETIC RADIATION IN MAGNETO-IONIC  
MEDIA FOR VLF AND VHF SPECTRA

A method of analysis is presented for obtaining approximate solutions to Maxwell's equations pertaining to current sources in an homogeneous magneto-ionic medium. The analysis is applied to the radiation of electromagnetic energy in the VLF and VHF spectra [1].

The analysis is directed toward the development of a set of potential functions for describing the electromagnetic fields of finite electric current sources. The gauge conditions associated with the potential functions are discussed and the limitations of a particular gauge condition, the tensor Lorentz gauge, are discussed in detail. The analysis is then restricted to specific frequency spectra and regions of the ionosphere which are applicable for communications to and from space vehicles within such regions. It is found that approximate solutions of Maxwell's equations may be obtained from a potential function which satisfies the tensor form of Helmholtz's equation. Such solutions are applicable to current sources in the VLF and VHF spectra in or above the F-layer of the ionosphere (i.e., equal to or greater than 150 kilometers above the earth's surface).

Closed form solutions for the potential function are then derived for both electric and magnetic dipoles in a homogeneous ionosphere by use of Fourier analysis and the associated Green's functions.

Results are presented for the radiation characteristics of electric and magnetic dipoles arbitrarily oriented with respect to the static magnetic field or the gyrotropic axis of the magneto-ionic medium. Main emphasis is placed on the field structure in the radiation zone. From the field structure the Poynting vector is determined for the VLF and VHF spectra, and hence the net radiated power from the dipole. Radiation phenomena are compared with those for free space for the same dipole.

The first general solution for the radiation of a finite current distribution in a homogeneous anisotropic medium was given in an elegant presentation by F. V. Bunkin [2]. Bunkin considered only monochromatic source functions and assumed the anisotropic medium was characterized by a general permittivity tensor, the permeability being a known scalar. He then considered only the partial differential equation satisfied by the electric field vector as required by Maxwell's equations:

$$\nabla(\nabla \cdot \vec{E}) - \nabla^2 \vec{E} - k^2 \hat{\epsilon} \vec{E} = \frac{4\pi k}{ic} \vec{j} \quad (1)$$

$\hat{\epsilon}$ : complex dielectric tensor

$k$ : free space propagation constant in CGS units,

$\vec{j}$ : specified current distribution

$c$ : speed of light

Utilizing the linearity of the above differential equation, Bunkin assumed that the electric field vector could be expressed in the integral form:

$$\vec{E} = \frac{4\pi k}{ic} \int_{v_1} \hat{T}(\vec{r}, \vec{r}_1) \vec{J}(\vec{r}_1) dv_1 \quad (2)$$

where  $\hat{T}(\vec{r}, \vec{r}_1)$  is a tensor of second rank depending on the coordinates of the point of observation ( $\vec{r}$ ) and the source point ( $\vec{r}_1$ ).

In a concise but rigorous manner he then achieved the formal solution for the electric field of a general current distribution in a homogeneous anisotropic medium. He then directed his attention to a magneto-ionic medium such as the ionosphere for evaluation of the integrals.

#### Restrictions of Bunkin's Solution

Because of the complexity of the integral solutions, Bunkin was forced to restrict his attention to the radiation zone, where asymptotic methods could be applied to obtain a formal evaluation of the integrals. This procedure produced a multipole expansion of the electric field due to an arbitrary current distribution in a magneto-ionic medium.

Although his formal solution was valid for any current distribution and any point of observation, numerical evaluation of such a solution was restricted to the electric dipole distribution. Furthermore, expressions for the electric field vector were given in terms of a parameter introduced through the use of the method of steepest descent (the saddle point), whose value is not easily determined for any medium and point of observation. More specifically, the parameter

is a function of the angle between the observation point and the static magnetic field as well as the elements of the permittivity tensor.

In conclusion, Bunkin considered only two orientations of the dipole; and for each orientation he discussed only the solutions at particular observation points which produced simplified values of the parameters introduced in his analysis.

Although Bunkin's presentation was quite elegant, it did not manifest itself as a working paper for further use in the radiation characteristics of an electric dipole in an anisotropic medium.

During the year 1960 Kogelnik and Kuehl published certain results for the radiation characteristics of an electric dipole in an anisotropic medium which utilized the formulation of Bunkin [3, 4]. Kogelnik determined the quadratic form for the radiated power of an electric dipole with specific orientations relative to the static magnetic field. Through the aid of electronic computers, he was able to obtain numerical data for the power relations of an electric dipole but did not explicitly evaluate the electromagnetic field structure.

Kuehl's paper was essentially a reworking of Bunkin's presentation with the exception that it was developed in much greater detail and did provide asymptotic expressions for the far-zone fields of an electric dipole in an homogeneous anisotropic plasma. However, Kuehl's results were also restricted to two particular problems.

His first result was a highly theoretical situation in which it was assumed that the external magnetic field was infinitely large such that the integral solutions were considerably simplified. This condition does not occur in the ionosphere and hence is not applicable to any physically realizable problem of radiation in the earth's atmosphere.

Kuehl's other result was for a magneto-ionic medium in which the normalized plasma, normalized gyro and normalized collision frequencies were much less than one. Physically this corresponds to source functions operating in the VHF spectrum and distances above the earth's surface exceeding 150 kilometers. Indeed this result is applicable to communication problems for space vehicles.

#### The Need for Further Investigation of the Radiation Problem

Recent experimental work in the ionosphere has required a knowledge of radiation phenomena in the VLF spectrum. However, a review of the literature reveals that little information is available on the radiation of electromagnetic energy in the VLF spectrum as applied to the ionosphere.\* Theoretical investigations have essentially been restricted to those discussed above which are not readily applicable to the VLF spectrum. A detailed investigation of the work of Bunkin and Kuehl revealed that the application of this type

---

\* The paper by R. Mittra, "Solution of Maxwell's Equations in a Magneto-Ionic Medium with Sources," U. of Ill., had not yet become available when K. R. Cook finished his work.

of analysis to the VLF case is prohibitive in view of the complex integrations required. In view of these conclusions, and the need for information pertaining to radiation phenomena in the VLF spectrum, it was apparent that a different method of analysis was required if useful results were to be obtained.

The following approach describes a new method of analysis for obtaining approximate solutions for both the electromagnetic fields and radiated power for current sources in the VLF and VHF spectra in a magneto-ionic medium.

Considering only monochromatic source functions, Maxwell's equations for anisotropic media may be expressed by the following system:

$$\nabla \times \vec{E} + i\omega\mu_0 \vec{H} = \vec{0} \quad (3)$$

$$\nabla \times \vec{H} - i\omega\epsilon_0 \vec{E} = \vec{J} \quad (4)$$

$$\vec{D} = \epsilon_0 \vec{E}, \quad \vec{B} = \mu_0 \vec{H} \quad (5)$$

$$\nabla \cdot \vec{D} = \rho, \quad \nabla \cdot \vec{H} = 0 \quad . \quad (6)$$

Thus we see, as in isotropic media, the magnetic field intensity represents a solenoidal vector field. Therefore, we may conclude that there exists a vector  $\vec{A}$  such that

$$\vec{H} = \nabla \times \vec{A} \quad . \quad (7)$$

From Maxwell's equations it follows that the electric field is representable as,

$$\vec{E} = - (i\omega\mu_0 \vec{A} + \nabla\phi) \quad . \quad (8)$$

The potentials  $\vec{A}$  and  $\varphi$  must satisfy the differential equations,

$$\nabla^2 \vec{A} + k_o^2 \hat{\kappa} \vec{A} = - \vec{J} + \nabla \nabla \cdot \vec{A} + i\omega \epsilon_o \hat{\kappa} \nabla \varphi \quad (9)$$

$$\nabla \cdot (\kappa \nabla \varphi) + i\omega \mu_o \nabla \cdot (\hat{\kappa} \vec{A}) = - \rho / \epsilon_o \quad (10)$$

We now assume that  $\vec{A}$  and  $\varphi$  satisfy the following gauge condition,

$$\nabla(\nabla \cdot \vec{A}) + i\omega \epsilon_o \hat{\kappa} \nabla \varphi = \vec{0} \quad (11)$$

However, we find the assumed gauge condition imposes restrictions on the vector potential  $\vec{A}$ . To show this we premultiply (11) by the inverse permittivity matrix  $\hat{\kappa}$ , to produce the result,

$$\nabla \varphi = \frac{1}{\omega \epsilon_o} \hat{\kappa} \nabla (\nabla \cdot \vec{A}) \quad (12)$$

Therefore, it follows that the vector potential must satisfy the condition,

$$\nabla \times [\hat{\kappa} \nabla (\nabla \cdot \vec{A})] = \vec{0} \quad (13)$$

From the above equations we find that under the assumed gauge condition the vector potential must also satisfy the equation

$$\nabla^2 \vec{A} + k_o^2 \hat{\kappa} \vec{A} = - \vec{J} \quad (14)$$

In general equations (13) and (14) will not be satisfied identically by the vector  $\vec{A}$  for a given source function.

For a magneto-ionic medium with the gyrotropic axis parallel to the  $x_3$ -axis, the inverse permittivity matrix will have the canonical form,

$$\hat{\mathbf{A}} = \begin{bmatrix} \gamma_{11} & \gamma_{12} & 0 \\ -\gamma_{12} & \gamma_{11} & 0 \\ 0 & 0 & \gamma_{33} \end{bmatrix} \quad (15)$$

For notation purposes we define  $\mathbf{f} = \nabla \cdot \hat{\mathbf{A}}$  and use the subscript notation to denote partial derivatives of  $\mathbf{f}$ .

Combining the above results we find that the gauge condition requires the following set of homogeneous equations to be satisfied for a given set of parameters describing the magneto-ionic medium,

$$\begin{bmatrix} f_{23} & -f_{13} & -f_{23} \\ f_{13} & f_{23} & -f_{13} \\ 0 & f_{11} + f_{22} & 0 \end{bmatrix} \begin{bmatrix} \gamma_{11} \\ \gamma_{12} \\ \gamma_{33} \end{bmatrix} = \begin{bmatrix} 0 \\ 0 \\ 0 \end{bmatrix} \quad (16)$$

If non-trivial solutions are to exist for the parameters  $\gamma_{11}$ ,  $\gamma_{22}$ , and  $\gamma_{33}$  it is necessary that the determinant of the coefficient matrix vanish. Therefore we have the characteristic equation,

$$\begin{bmatrix} f_{23} & -f_{13} & -f_{23} \\ f_{13} & f_{23} & -f_{13} \\ 0 & f_{11} + f_{22} & 0 \end{bmatrix} = 0 \quad (17)$$

Indeed the determinant does vanish and there are non-trivial solutions. However, it is also apparent that it is necessary that

$$(f_{11} + f_{22})\gamma_{12} = 0 . \quad (18)$$

In terms of the vector potential function this requires

$$\nabla_t^2(\nabla \cdot \vec{A}) = 0 \quad (19)$$

where

$$\nabla_t^2 = \frac{\partial^2}{\partial x_1^2} + \frac{\partial^2}{\partial x_2^2}$$

Therefore, we conclude that for  $\gamma_{12} \neq 0$  the divergence of  $\vec{A}$  must satisfy Laplace's equation in the plane transverse to the gyrotropic axis.

However, we also realize that if  $\gamma_{12} = 0$ , then the characteristic equation is satisfied identically and the solution of (14) represents exact solutions of Maxwell's equations. This condition, of course, reduces the medium to an isotropic medium.

From the structure of the mathematical system and some a priori knowledge of the ionosphere we are motivated to consider the possibility of obtaining solutions of (14) for values of the plasma parameters which will give the conditions

$$\begin{aligned} \gamma_{11} &\rightarrow \gamma_{33} \\ \gamma_{12} &\rightarrow 0 \end{aligned} \quad . \quad (20)$$

These restrictions are necessary so that the imposed gauge condition yields closed form solutions representing approximate solutions to Maxwell's equations.

#### Useful Approximations for the Permittivity Matrix Pertaining to a Homogeneous Ionosphere

Restricting our attention to the regions of the ionosphere and frequency spectrum for which,

$$\begin{aligned} 10^4 &\leq f < 10^5 \\ h &\geq 160 \text{ km} \\ N &\geq 10^5 \text{ electrons/c.c.} \end{aligned} \tag{21}$$

we find the following approximations to be applicable to the elements of the inverse permittivity matrix:

$$\begin{aligned} \chi_{11} &\doteq -1/X \\ \chi_{12} &\doteq -i Y/X \quad X \gg Y^2 \gg i \gg z \\ \chi_{33} &\doteq -1/X \end{aligned} \tag{22}$$

X: Normalized Plasma Frequency Squared

Y: Normalized Gyro Frequency

Z: Normalized Collision Frequency

Therefore, we find that the conditions stipulated in (20) are approximately satisfied. This provides sufficient validity for the use of (14) as determining the potential function from which the electric and magnetic fields may be determined from (7) and (8). It is noted that the frequency range specified in (21) contains the VLF spectrum so the approximations in (21) are hereafter designated as the "VLF approximations."

The theory is also applicable to a frequency spectrum for which

$$f > 10^6 \text{ cps.} \tag{23}$$

Combining this restriction with the altitude range given in (21) we find that the elements of the inverse permittivity matrix may be approximated as

$$\begin{aligned} \chi_{11} &\doteq \frac{1}{1-x} \\ \chi_{12} &\doteq -ixy \quad x \ll 1; \quad y^2 \ll 1; \quad z \ll 1. \\ \chi_{33} &\doteq \frac{1}{1-x} \end{aligned} \quad (24)$$

The approximations stated in (24) shall hereafter be designated as the "VHF approximations."

#### Solution for the Vector Potential for the VLF and VHF Spectrum

The above discussion has provided sufficient validity for the use of the following set of equations for describing the radiation of current sources in the ionosphere:

$$\nabla^2 \vec{A} + k_o^2 \hat{k} \vec{A} = - \vec{J} \quad (25)$$

$$\vec{H} = \nabla \times \vec{A} \quad (26)$$

$$\vec{E} = \frac{1}{i\omega\epsilon_0} [k_o^2 \vec{A} + i\nabla(\nabla \cdot \vec{A})] \quad (27)$$

We now seek a solution for the vector  $\vec{A}$  in terms of a dyadic Green's function. Due to the linearity of the above equations, we assume the vector potential may be expressed as,

$$\vec{A}(\vec{x}) = \int_{\text{v}'} \hat{G}(\vec{x}, \vec{x}') \vec{J}(\vec{x}') d\vec{x}' \quad (28)$$

It is assumed that the source function  $\vec{J}(\vec{x}')$  is well defined over the source coordinates. Combining (25) and (28) it follows that the Green's function must satisfy

$$(\nabla^2 + k_o^2 \hat{k}) \hat{G}(\vec{x}, \vec{x}') = - \delta(\vec{x} - \vec{x}') I \quad (29)$$

Employing Fourier transform theory we find the elements of the dyadic Green's function to be

$$G_{11} = \frac{1}{8\pi} \left[ \frac{e^{-ik_1 R}}{R} + \frac{e^{-ik_2 R}}{R} \right], \quad (30)$$

$$G_{22} = G_{11}, \quad (31)$$

$$G_{12} = \frac{-i}{8\pi} \left[ \frac{e^{-ik_1 R}}{R} - \frac{e^{-ik_2 R}}{R} \right], \quad (32)$$

$$G_{21} = -G_{12}, \quad (33)$$

$$G_{33} = \frac{1}{4\pi} \left( \frac{e^{-ik_3 R}}{R} \right), \quad (34)$$

$$G_{13} = G_{31} = G_{23} = G_{32} = 0, \quad (35)$$

$$k_1 = k_o [\kappa_{11} + ik_{12}]^{1/2}; \quad k_2 = k_o [\kappa_{11} - ik_{12}]^{1/2}; \quad k_3 = k_o \kappa_{33}^{1/2} \quad (36)$$

$$R = |\vec{x} - \vec{x}'|.$$

Having determined the Green's function for the vector potential it is a simple matter to determine the electric and magnetic fields from (26), (27), and (28).

#### RADIATION FROM AN ELECTRIC DIPOLE IN A MAGNETO-IONIC MEDIUM

##### Radiation Fields of an Electric Dipole Operating in the VLF Spectrum

Applying the VLF approximations to the above results with the additional constraint that  $|k_n R| \gg 1$ , the electric and magnetic fields are given in spherical components as

$$E_R = \left( \frac{k_o^2 \sin \theta}{8\pi \epsilon_o} \right) e^{i\phi} \frac{e^{-ik_o \sqrt{X-Y} R}}{R} (P_1 - iP_2) \quad (37)$$

$$E_\theta = \left( \frac{k_o^2 \cos \theta}{8\pi \epsilon_o} \right) e^{i\phi} \frac{e^{-ik_o \sqrt{X-Y} R}}{R} (P_1 - iP_2) \quad (38)$$

$$E_\phi = \left( \frac{ik_o^2 \cos^2 \theta}{8\pi \epsilon_o} \right) e^{i\phi} \frac{e^{-ik_o \sqrt{X-Y} R}}{R} (P_1 - iP_2) \quad (39)$$

$$H_R = 0 \quad (40)$$

$$H_\theta = \frac{-i\omega k_o}{8\pi} \left(\frac{x}{-y}\right)^{1/2} e^{i\phi} \frac{e^{-ik_o\sqrt{X/-Y} R}}{R} (P_1 - iP_2) \quad (41)$$

$$H_\phi = \frac{\omega k_o \cos \theta}{8\pi} \left(\frac{x}{-y}\right)^{1/2} e^{i\phi} \frac{e^{-ik_o\sqrt{X/-Y} R}}{R} (P_1 - iP_2) \quad (42)$$

$$P_n = \frac{Idl}{i\omega} u_n$$

$u_n$  are directional cosines specifying the direction of the dipole with the coordinate axes.

#### VLF Radiation Patterns for an Electric Dipole

Defining the Poynting vector as

$$\vec{S} = 1/2 \operatorname{Re} \{ \vec{E} \times \vec{H}^* \} \quad (43)$$

the following components are obtained for an electric dipole operating in the VLF spectrum.

$$S_R = \frac{(Idl)^2 k_o^3 \cos^2 \theta}{64\pi^2 \omega \epsilon_o R^2} \left(\frac{x}{-y}\right)^{1/2} (u_1^2 + u_2^2), \quad (44)$$

$$S_\theta = - \frac{(Idl)^2 k_o^3 \sin \theta \cos \theta}{64\pi^2 \omega \epsilon_o R^2} \left(\frac{x}{-y}\right)^{1/2} \left(\frac{u_1^2 + u_2^2}{2}\right), \quad (45)$$

$$S_\phi = 0. \quad (46)$$

Normalized radiation patterns for the above results are plotted in Figure 1. The normalizing factor being

$$S_o = \frac{(Idl)^2 (u_1^2 + u_2^2) k_o^3}{32\pi^2 \omega \epsilon_o R^2} \quad (47)$$

which is the maximum value of the Poynting vector for the dipole in free space.

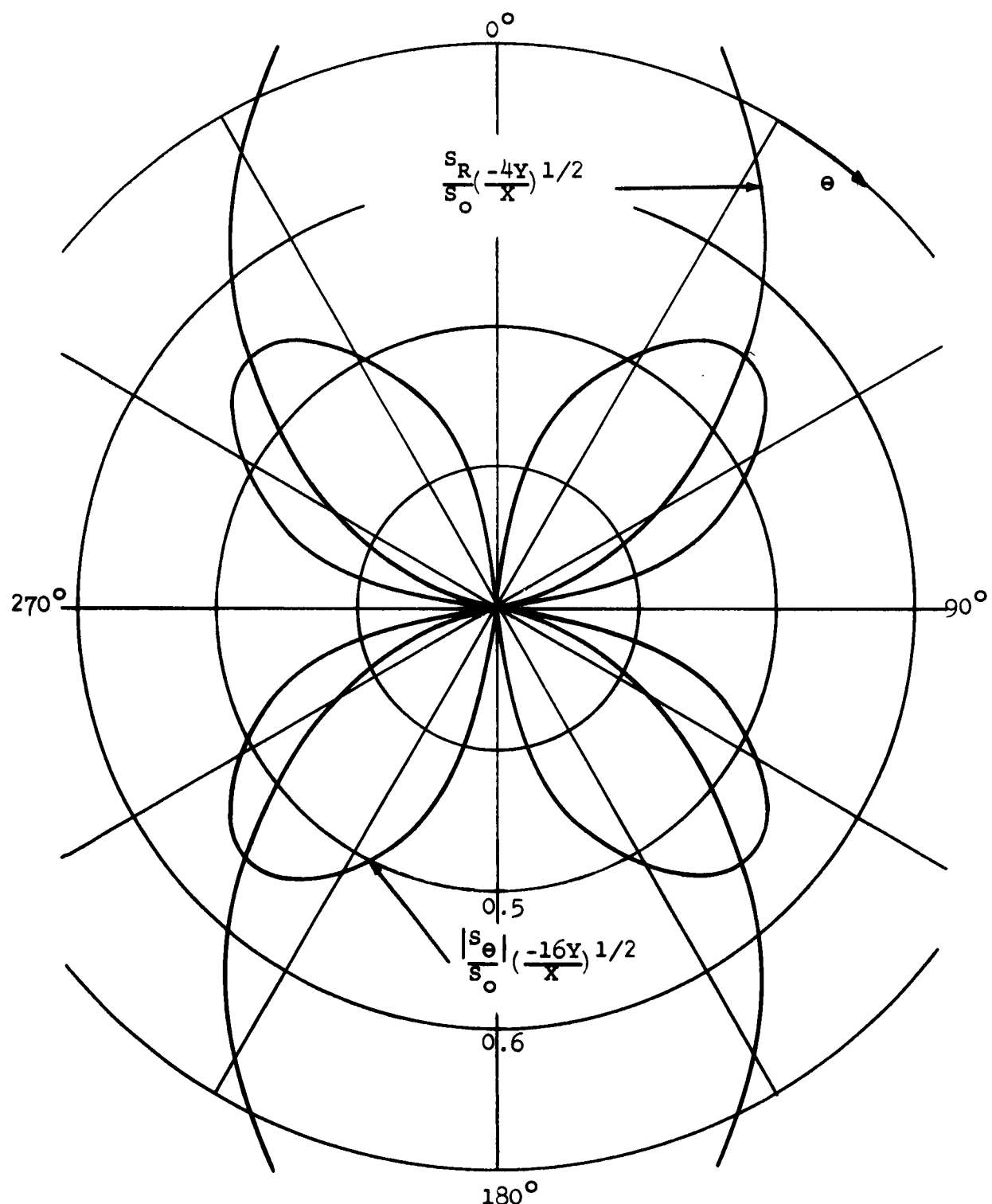


**Figure 1--VLF radiation patterns for an electric dipole transverse to the gyrotropic axis.**

Radiated Power for an Electric Dipole Operating in the VLF Spectrum

The net power radiated by the source dipole is defined by the integral,

$$P = \int_A \vec{S} \cdot \vec{n} dA , \quad (48)$$

where A represents any well defined closed surface enclosing the dipole source.

Putting the results of (44) through (46) into (48), the net radiated power for an electric dipole operating in the VLF spectrum is obtained.

$$P = \frac{(Idl)^2(u_1^2 + u_2^2)k_o^3}{48\pi\omega\epsilon_o} \left(\frac{X}{-Y}\right)^{1/2} \quad (49)$$

If we define the power radiated by the same dipole in free space as

$$P_o = \frac{(Idl)^2 k_o^3}{12\pi\omega\epsilon_o} , \quad (50)$$

the result in (49) becomes,

$$P = \left[ \left( \frac{u_1^2 + u_2^2}{4} \right) \left( \frac{X}{-Y} \right)^{1/2} \right] P_o \quad (51)$$

Since the coefficient in (51) is large we realize that the radiation of the dipole is enhanced by the presence of the ionosphere.

Radiation Fields for an Electric Dipole Operating in the VHF Spectrum

Applying the VHF approximations to the results obtained in (25) through (36), including the radiation zone restrictions, we obtain the electric and magnetic fields of an electric dipole operating in the VHF spectrum.

$$E_R = \frac{k_o^2 \sin \theta}{8\pi\epsilon_o} (XY) \left[ (P_1 - iP_2) \frac{e^{-i(k_1 R - \varphi)}}{R} - (P_1 + iP_2) \frac{e^{-i(k_2 R + \varphi)}}{R} \right], \quad (52)$$

$$\begin{aligned} E_\Theta &= \frac{k_o^2 \cos \theta}{8\pi\epsilon_o} \left[ (P_1 - iP_2) \frac{e^{-i(k_1 R - \varphi)}}{R} + (P_1 + iP_2) \frac{e^{-i(k_2 R + \varphi)}}{R} \right] \\ &\quad - \frac{k_o^2 \sin \theta}{4\pi\epsilon_o} \left[ \frac{e^{-ik_3 R}}{R} P_3 \right], \end{aligned} \quad (53)$$

$$\begin{aligned} E_\varphi &= \frac{ik_o^2}{8\pi\epsilon_o} \left[ [1 - XY(1-X+XY) \sin^2 \theta] \frac{e^{-i(k_1 R - \varphi)}}{R} (P_1 - iP_2) \right. \\ &\quad \left. - [1 + XY(1-X-XY) \sin^2 \theta] \frac{e^{-i(k_2 R + \varphi)}}{R} (P_1 + iP_2) \right. \\ &\quad \left. - 2 XY \sin \theta \cos \theta \frac{e^{-ik_3 R}}{R} P_3 \right], \end{aligned} \quad (54)$$

$$H_R = 0, \quad (55)$$

$$\begin{aligned} H_\Theta &= \frac{-ik_o\omega}{8\pi} \left[ (1 - X + XY)^{1/2} \frac{e^{-i(k_1 R - \varphi)}}{R} (P_1 - iP_2) \right. \\ &\quad \left. - (1 - X - XY)^{1/2} \frac{e^{-i(k_2 R + \varphi)}}{R} (P_1 + iP_2) \right], \end{aligned} \quad (56)$$

$$\begin{aligned} H_\varphi &= \frac{k_o\omega \cos \theta}{8\pi} \left[ (1 - X + XY)^{1/2} \frac{e^{-i(k_1 R + \varphi)}}{R} (P_1 - iP_2) \right. \\ &\quad \left. + (1 - X - XY)^{1/2} \frac{e^{-i(k_2 R + \varphi)}}{R} (P_1 + iP_2) \right] \\ &\quad - \frac{k_o\omega \sin \theta}{4\pi} \frac{e^{-ik_3 R}}{R} P_3. \end{aligned} \quad (57)$$

### VHF Radiation Patterns for an Electric Dipole

The components of the Poynting vector are readily obtained from the above field expressions.

$$\begin{aligned} S_R &= \frac{(Idl)^2 k_o^3}{32\pi^2 \epsilon_o R^2} \left[ (u_1^2 + u_2^2) \cos^2 \theta + u_3^2 \sin^2 \theta \right] \\ &\quad - \left( \frac{(Idl)^2 k_o^3 \sin \theta \cos \theta u_3}{16\pi^2 \omega \epsilon_o R^2} \right) \cos \beta_1 R \left[ u_1 \cos(\beta_2 R - \varphi) - u_2 \sin(\beta_2 R - \varphi) \right]. \end{aligned} \quad (58)$$

$$S_\theta = - \frac{(Idl)^2 k_o^3 \sin \theta u_3}{16\pi^2 \omega \epsilon_o R^2} (XY) \sin \beta_1 R [u_1 \sin(\beta_2 R - \varphi) + u_2 \cos(\beta_2 R - \varphi)], \quad (59)$$

$$S_\varphi = 0. \quad (60)$$

Normalized radiation patterns for the above results are plotted in Figure 2. The normalizing factor was given in (47).

#### Radiated Power for an Electric Dipole Operating in the VHF Spectrum

Evaluating the integral in (48) for the fields pertaining to the VHF spectrum gives the net power radiated by the dipole,

$$P = \left[ u_3^2 + \frac{u_1^2 + u_2^2}{2} \right] P_o \quad (61)$$

We note that the radiated power of a dipole oriented parallel to the gyrotropic axis is equal to the power radiated by the same dipole in free space. However, if the dipole is oriented transverse to the gyrotropic axis, the power radiated is one half that of free space.

#### RADIATION FROM A MAGNETIC DIPOLE IN A MAGNETO-IONIC MEDIUM

##### Radiation Fields of a Magnetic Dipole Parallel to the Gyrotropic Axis--VLF Spectrum

Omitting the details, the electric and magnetic field components for a magnetic dipole parallel to the gyrotropic axis and operating in the VLF spectrum are:

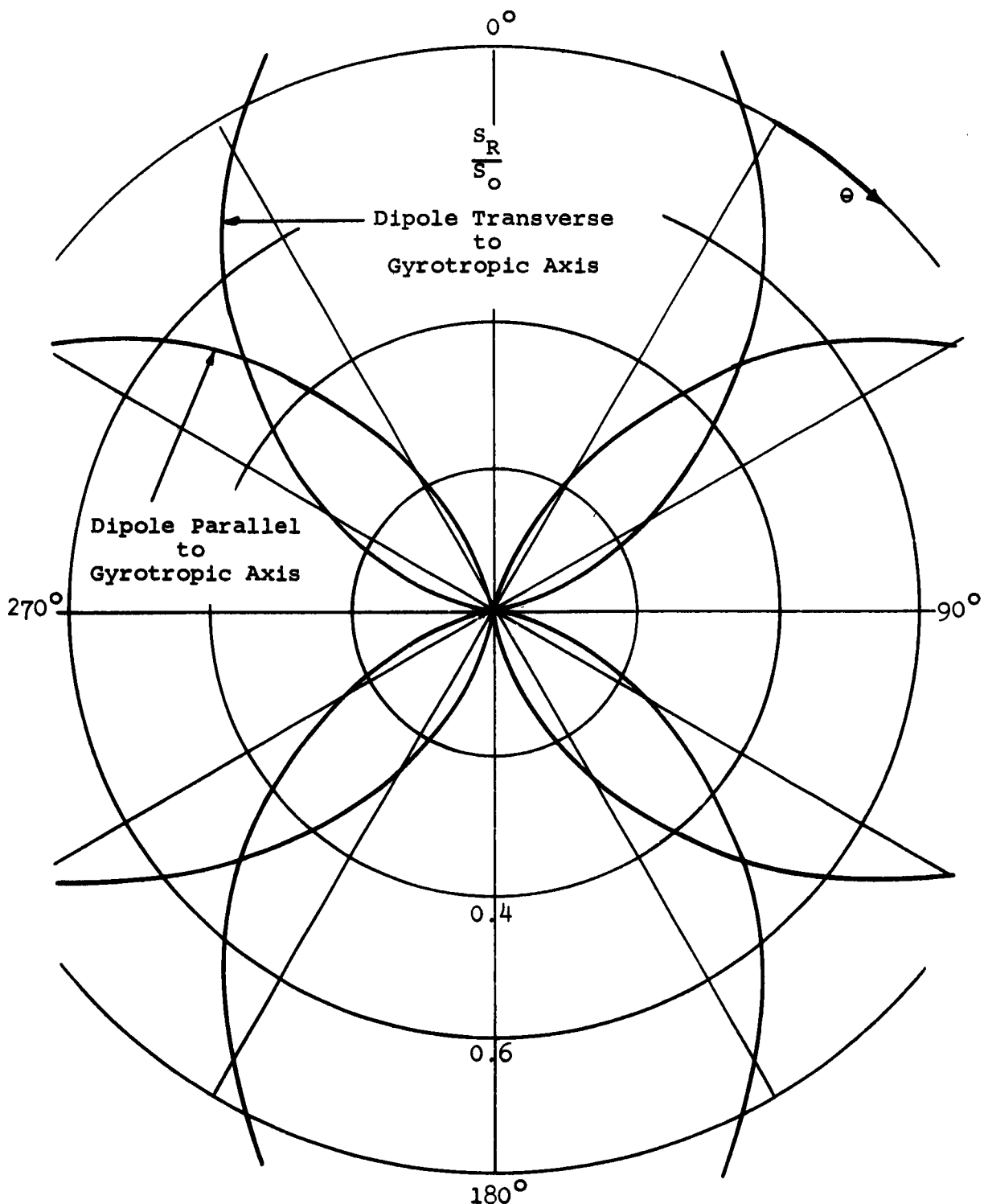


Figure 2--VHF radiation patterns for an electric dipole.

$$H_R = 0, \quad (62)$$

$$H_\theta = \frac{Mk_o^2 \sin\theta}{8\pi} (X/Y) \frac{e^{-ik_o\sqrt{X/-Y} R}}{R}, \quad (63)$$

$$H_\phi = i \frac{Mk_o^2 \sin\theta \cos\theta}{8\pi} (X/Y) \frac{e^{-ik_o\sqrt{X/-Y} R}}{R}, \quad (64)$$

$$E_R = \left( \frac{Mk_o^3 \sin^2\theta}{18\pi\omega\epsilon_o} \right) (X/-Y)^{1/2} \frac{e^{-ik_o\sqrt{X/-Y} R}}{R}, \quad (65)$$

$$E_\theta = \frac{Mk_o^3 \sin\theta \cos\theta}{18\pi\omega\epsilon_o} (X/-Y)^{1/2} \frac{e^{-ik_o\sqrt{X/-Y} R}}{R}, \quad (66)$$

$$E_\phi = \frac{Mk_o^3 \sin\theta}{8\pi\omega\epsilon_o} (X/-Y)^{1/2} [1/Y + \cos^2\theta] \frac{e^{-ik_o\sqrt{X/-Y} R}}{R}. \quad (67)$$

It is noted that the above field equations have the factor involving  $X/-Y$  which is much larger than one. It is also interesting to compare the above field structure with that for an electric dipole operating in the VLF spectrum and transverse to the gyrotropic axis.

#### VLF Radiation Patterns for a Magnetic Dipole Parallel to the Gyrotropic Axis

The components of the Poynting vector for a magnetic dipole parallel to the gyrotropic axis are readily obtained from the above equations.

$$S_R = \frac{M^2 k_o^5 \sin^2\theta}{64\pi^2 \omega \epsilon_o R^2} (X/-Y)^{3/2} (\cos^2\theta + \frac{1}{ZY}), \quad (68)$$

$$S_\theta = - \frac{M^2 k_o^5 \sin^3\theta \cos\theta}{128\pi^2 \omega \epsilon_o R^2} (X/-Y)^{3/2}, \quad (69)$$

$$S_\phi = 0. \quad (70)$$

Radiation patterns corresponding to these results are given in Figure 3. The normalizing factor being

$$S_0 = \frac{Mk_0^5}{16\pi^2 \omega \epsilon_0} . \quad (71)$$

#### Radiated Power for a Magnetic Dipole Parallel to the Gyrotropic Axis--VLF Spectrum

Defining  $P_0$  as the power radiated by a magnetic dipole in free space we readily find the power radiated to be

$$P = (P_0/4)(x/-Y)^{3/2}(1 + 3/2Y) \quad (72)$$

Due to the restrictions of the values of the plasma parameters in the VLF spectrum we realize that the radiation characteristics of the dipole are somewhat better than in free space.

#### Radiation Fields for a Magnetic Dipole Parallel to the Gyrotropic Axis--VHF Spectrum

For the VHF spectrum we find the electric and magnetic fields for a dipole parallel to the gyrotropic axis have the following form:

$$H_R = 0, \quad (73)$$

$$H_\theta = -\frac{Mk_0^5 \sin \theta}{8\pi} \left[ (1-X+XY) \frac{e^{-ik_1 R}}{R} + (1-X-XY) \frac{e^{-ik_2 R}}{R} \right], \quad (74)$$

$$H_\phi = \frac{Mk_0^5 \sin \theta \cos \theta}{18\pi} \left[ (1-X+XY) \frac{e^{-ik_1 R}}{R} - (1-X-XY) \frac{e^{-ik_2 R}}{R} \right], \quad (75)$$

$$E_R = \frac{Mk_0^3 \sin^2 \theta}{18\pi \omega \epsilon_0} (XY) \left[ \frac{e^{-ik_1 R}}{R} + \frac{e^{-ik_2 R}}{R} \right], \quad (76)$$

$$E_\theta = \frac{Mk_0^3 \sin^2 \theta}{18\pi \omega \epsilon_0} \left[ (1+XY) \frac{e^{-ik_1 R}}{R} - (1-XY) \frac{e^{-ik_2 R}}{R} \right], \quad (77)$$

$$E_\phi = \frac{Mk_0^3 \sin \theta}{8\pi \omega \epsilon_0} \left[ (1+XY \cos^2 \theta) \frac{e^{-ik_1 R}}{R} - (1-XY \cos^2 \theta) \frac{e^{-ik_2 R}}{R} \right], \quad (78)$$

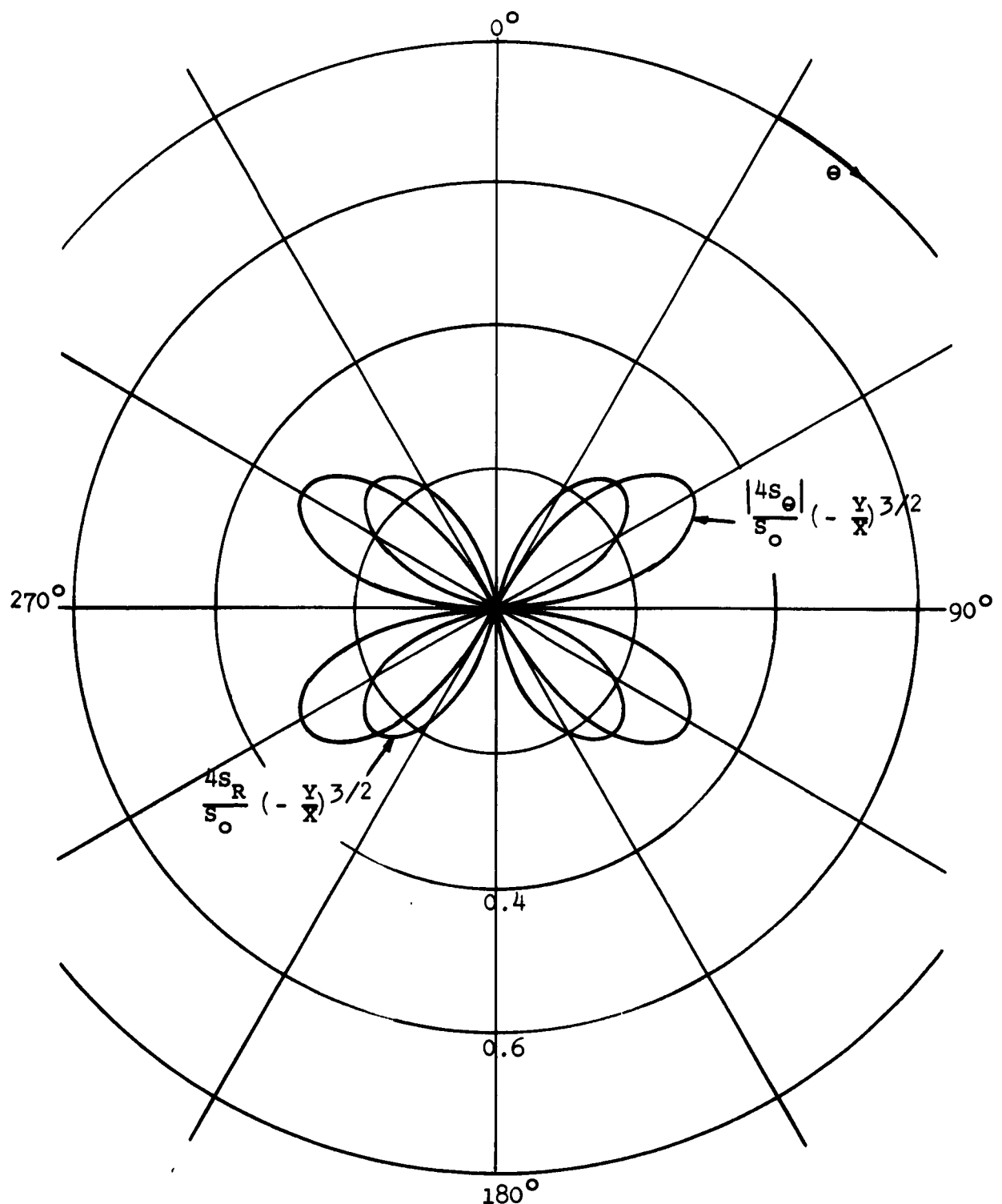


**Figure 3--VLF radiation patterns for a magnetic dipole parallel to the gyrotropic axis.**

Since the normalized plasma and gyro frequencies are much less than one it is apparent that the coefficients in the above expressions may be simplified somewhat; however, the effect of the ionosphere is evident in the phase factors of the propagating modes.

#### VHF Radiation Patterns for a Magnetic Dipole Parallel to the Gyrotropic Axis

The Poynting vector for the VHF spectrum has the following components:

$$S_R = \frac{M^2 k_0^5 \sin \theta}{64\pi^2 \omega \epsilon_0 R^2} [1 + \cos(k_1 - k_2)R + \frac{1}{2} \sin 2\theta(1 - \cos(k_1 - k_2)R)] , \quad (79)$$

$$S_\theta = - \frac{Mk_0^5 \sin^3 \theta \cos \theta}{64\pi^2 \omega \epsilon_0 R^2} (XY)^2 (1 + \cos(k_1 - k_2)R) , \quad (80)$$

$$S_\phi = - \frac{Mk_0^5 \sin^3 \theta}{64\pi^2 \omega \epsilon_0 R^2} (XY)^2 \sin(k_1 - k_2)R . \quad (81)$$

Radiation patterns for the above results are given in Figure 4.

The data for a magnetic dipole transverse to the gyrotropic axis (parallel to the  $x_1$ -axis) is given below in outline form.

#### Radiation Fields of a Magnetic Dipole Perpendicular to the Gyrotropic Axis--VLF Spectrum

$$H_R = 0 , \quad (82)$$

$$H_\theta = \frac{Mk_0^2 \cos^3 \theta}{8\pi} (X/Y) \frac{e^{-i(k_1 R - \phi)}}{R} , \quad (83)$$

$$H_\phi = i \frac{Mk_0^2 \cos^2 \theta}{8\pi} (X/Y) \frac{e^{-i(k_1 R - \phi)}}{R} , \quad (84)$$

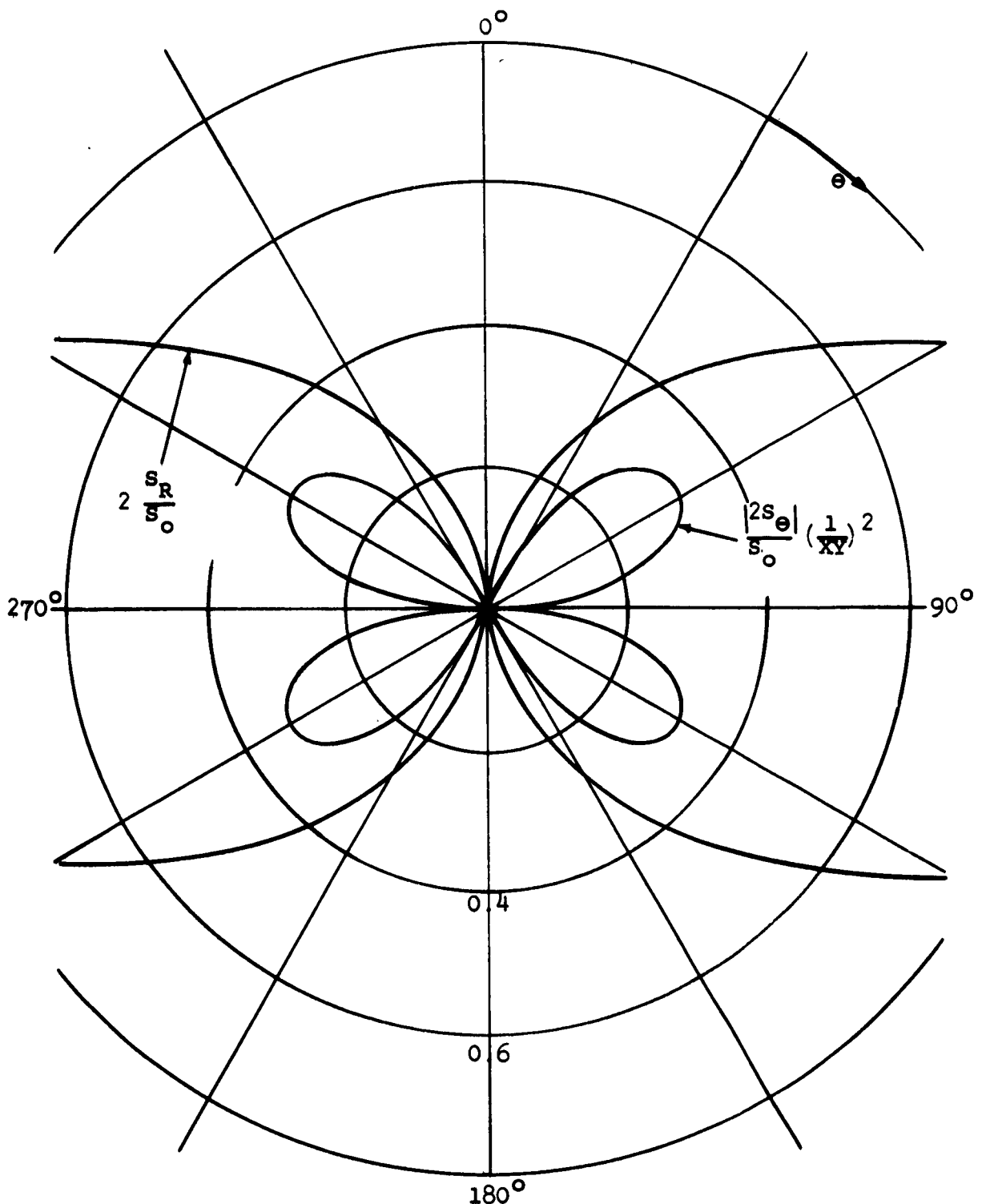


**Figure 4--VHF radiation patterns for a magnetic dipole parallel to the gyrotropic axis.**

$$E_R = - \frac{M k_o^3 \sin \theta \cos^3 \theta}{8\pi\omega\epsilon_o} (x/-y)^{1/2} \frac{e^{-i(k_1 R - \varphi)}}{R}, \quad (85)$$

$$E_\theta = - \frac{i M k_o^3 \cos^2 \theta}{8\pi\omega\epsilon_o} (x/-y)^{3/2} \frac{e^{-i(k_1 R - \varphi)}}{R}, \quad (86)$$

$$E_\varphi = \frac{M k_o^3 \cos^3 \theta}{8\pi\omega\epsilon_o} (x/-y)^{1/2} \frac{e^{-i(k_1 R - \varphi)}}{R}. \quad (87)$$

VLF Radiation Patterns for a Magnetic Dipole Perpendicular to the Gyrotropic Axis

$$S_R = \frac{M^2 k_o^5 \cos^4 \theta}{128\pi^2 \omega \epsilon_o^2 R^2} (x/-y)^{3/2} \left[ (x/-y) + \cos^2 \theta \right], \quad (88)$$

$$S_\theta = 0, \quad (89)$$

$$S_\varphi = \frac{M^2 k_o^5 \sin \theta \cos^6 \theta}{128\pi^2 \omega \epsilon_o^2 R^2} (x/-y)^{3/2}. \quad (90)$$

Radiation patterns are given in Figure 5.

Radiated Power for a Magnetic Dipole Perpendicular to the Gyrotropic Axis--VLF spectrum

$$P = 3/40 (x/-y)^{5/2} P_o \quad (91)$$

Radiation Fields of a Magnetic Dipole Perpendicular to the Gyrotropic Axis-VHF Spectrum

$$E_R = \frac{-i M \sin \theta \cos^3 \theta}{8\pi\omega\epsilon_o} (XY) \left[ k_1^3 \frac{e^{-i(k_1 R - \varphi)}}{R} + k_2^3 \frac{e^{-i(k_2 R + \varphi)}}{R} \right], \quad (92)$$

$$E_\theta = \frac{-i M}{8\pi\omega\epsilon_o} \left[ k_1^3 \cos^2 \theta \frac{e^{-i(k_1 R - \varphi)}}{R} - k_2^3 \cos^2 \theta \frac{e^{-i(k_2 R + \varphi)}}{R} \right. \\ \left. + i 2 k_3^3 \sin^2 \theta \sin \varphi \frac{e^{-i k_3 R}}{R} \right], \quad (93)$$

$$E_\varphi = \frac{M \cos \theta}{8\pi\omega\epsilon_o} \left[ k_1^3 \cos^2 \theta \frac{e^{-i(k_1 R - \varphi)}}{R} + k_2^2 \cos^2 \theta e^{-i(k_2 R + \varphi)} \right. \\ \left. - XY k_3^3 \sin^2 \theta \sin \varphi \frac{e^{-i k_3 R}}{R} \right], \quad (94)$$

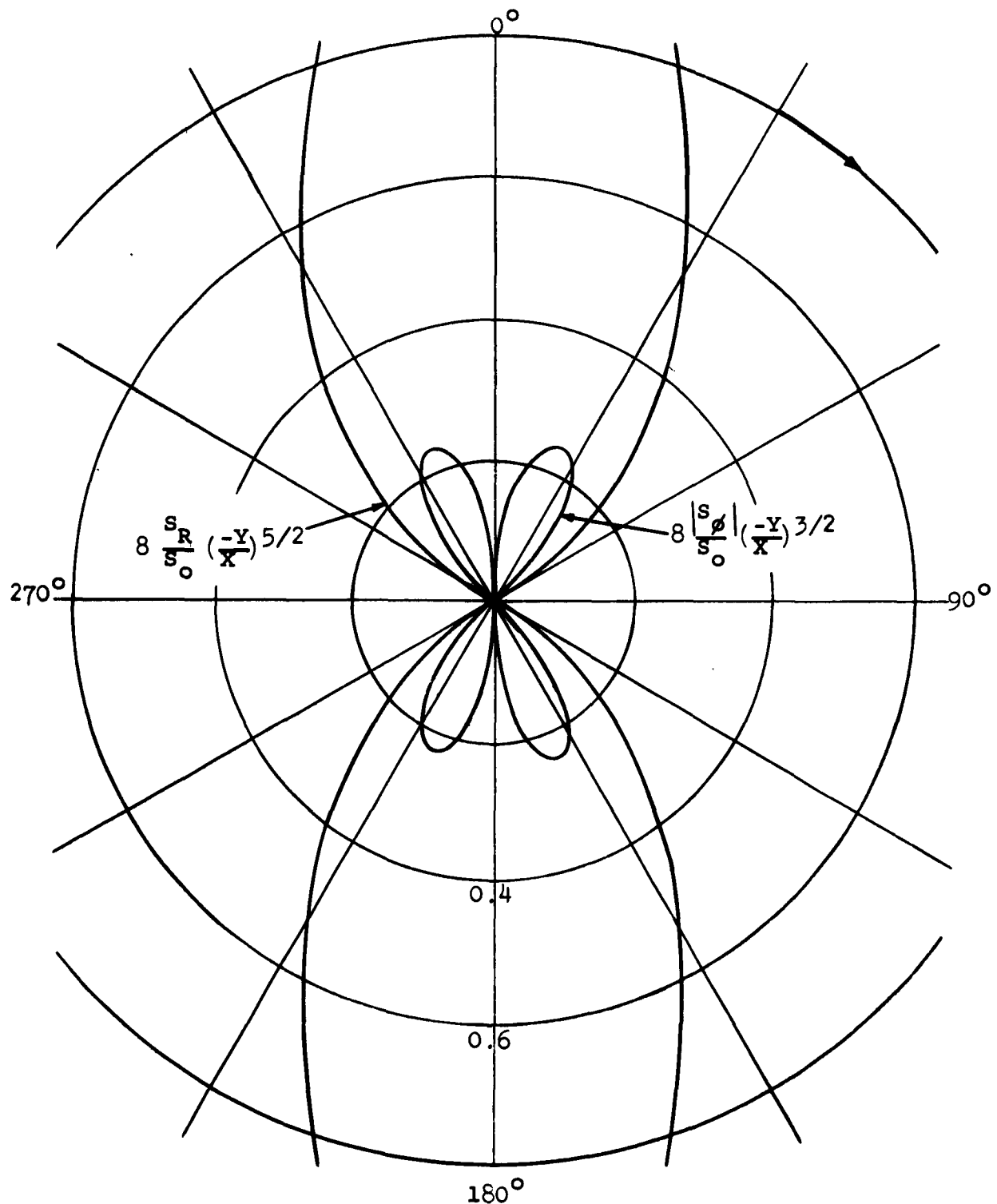


**Figure 5--VLF radiation patterns for a magnetic dipole transverse to the gyrotropic axis.**

$$H_R = 0 , \quad (95)$$

$$H_\Theta = - \frac{M \cos^3 \theta}{8\pi} \left[ k_1^2 \frac{e^{-i(k_1 R - \varphi)}}{R} + k_2^2 \frac{e^{-i(k_2 R + \varphi)}}{R} \right] , \quad (96)$$

$$\begin{aligned} H_\varphi = & - \frac{iM}{8\pi} \left[ k_1^2 \cos^2 \theta \frac{e^{-i(k_1 R - \varphi)}}{R} - k_2^2 \cos^2 \theta \frac{e^{-i(k_2 R + \varphi)}}{R} \right. \\ & \left. + i2k_3^2 \sin^2 \theta \sin \varphi \frac{e^{-ik_3 R}}{R} \right] . \end{aligned} \quad (97)$$

VHF Radiation Patterns for a Magnetic Dipole Perpendicular to the Gyrotropic Axis

$$S_R = \frac{M^2 \cos^4 \theta k_o^5}{64\pi^2 \omega \epsilon_o R^2} \left[ 1 + \cos^2 \theta + 2 \tan^4 \theta \sin^2 \varphi - \sin^2 \theta \cos 2(\beta_2 R - \varphi) \right. \\ \left. - XY \cos \beta_1 R \cos(\beta_2 R - \varphi) \right] , \quad (98)$$

$$S_\Theta = \frac{M^2 \sin^3 \theta \cos^3 \theta \sin \varphi k_o^5}{32\pi^2 \omega \epsilon_o R^2} (XY) \sin \beta_1 R \cos(\beta_2 R - \varphi) , \quad (99)$$

$$S_\varphi = 0 . \quad (100)$$

Radiation patterns are given in Figure 6.

Radiated Power for a Magnetic Dipole Perpendicular to the Gyrotropic Axis--VHF Spectrum

$$P = \left( \frac{15}{42} \right) P_o . \quad (101)$$

60

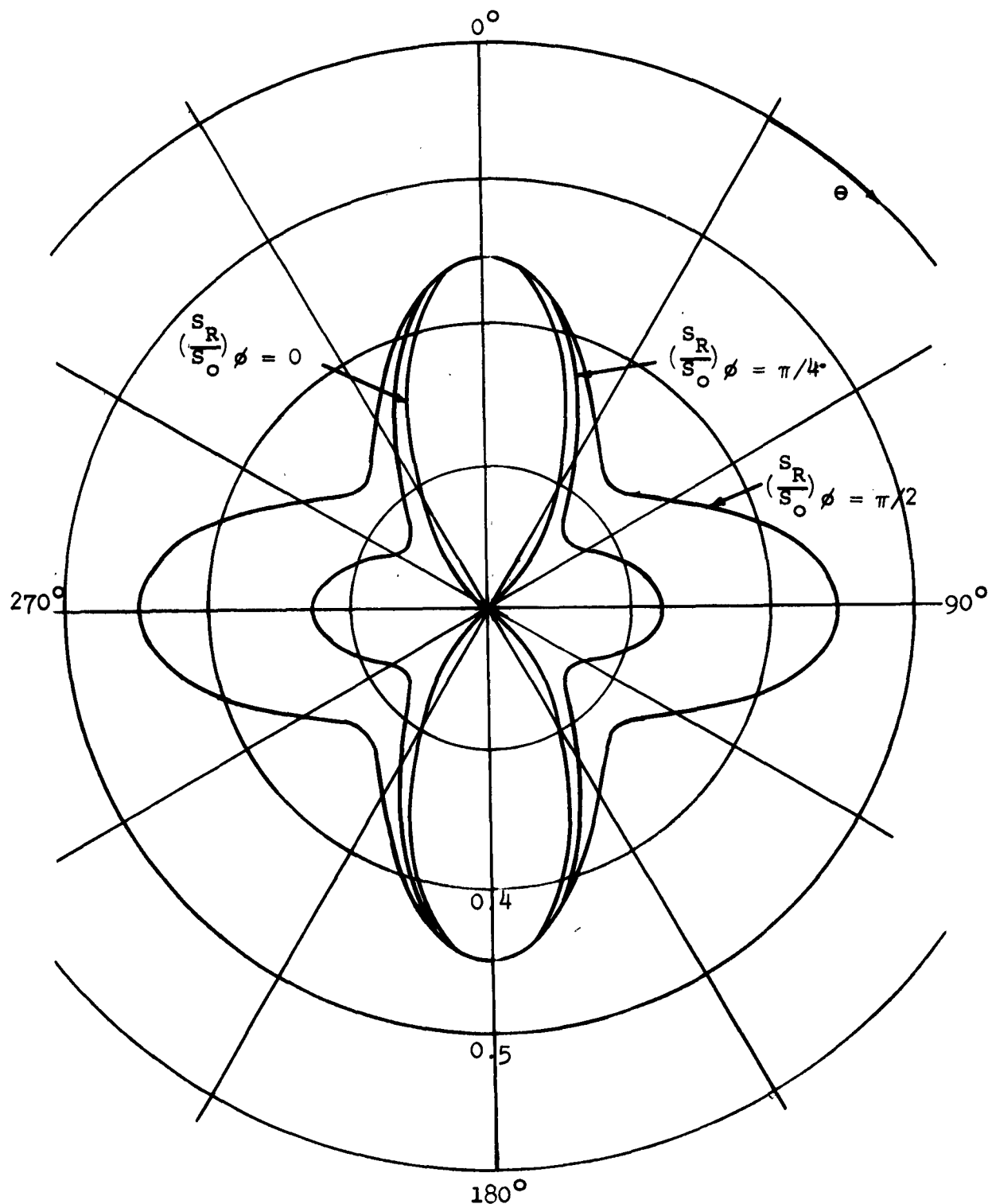


Figure 6--VHF radiation patterns for a magnetic dipole transverse to the gyrotropic axis.

#### REFERENCES

1. Cook, K. R., "Electromagnetic Radiation in Magneto-Ionic Media for VLF and VHF Spectra," Eng. Exp. Station, Report EE-76, Univ. of New Mexico, Albuquerque, (1962).
2. Bunkin, F. V., "On Radiation in Anisotropic Media," Journal of Experimental and Theoretical Physics, (USSR), Vol. 32, (1957), p. 338.
3. Kogelnik, H., "The Radiation Resistance of an Elementary Dipole in Anisotropic Plasmas," Fourth Intern. Conf. on Ionization Phenomena in Gases, North Holland Publishing Co., Amsterdam, (1960).
4. Kuehl, H. H., "Radiation from an Electric Dipole in an Anisotropic Cold Plasma," California Institute of Technology, Antenna Laboratory, Technical Report No. 24, (1960).

BACKGROUND STUDY FOR THE CALCULATION OF  
THE DRIVING-POINT IMPEDANCE OF A CYLINDRICAL  
ANTENNA IN THE ANISOTROPIC IONOSPHERE

The derivation of the driving-point impedance of any finite antenna in the ionosphere requires the calculation of the electromagnetic fields in the region directly adjacent to the surface of the antenna. The quasi-static fields (fields at a distance from the antenna much less than a wavelength) must be determined for the given ionospheric conditions surrounding the antenna, and for the given shape and material of the antenna. For the first approach, the ionosphere is chosen to be an infinite homogeneous, anisotropic, lossy (magneto-ionic) medium. The anisotropy is caused by the earth's magnetic field, whose effect is assumed uniform in the region of the antenna. The antenna is chosen to be a finitely long, thin, center-driven cylinder.

From a search of literature certain references have been found indirectly applicable to the problem of calculating the quasi-static fields at VLF radiating from a cylindrical antenna in the ionosphere. Progress in the mathematical formulation of this analysis has been made by Bunkin [1]; by Kuehl [2], who wrote a working paper based on Bunkin's analysis; and by Friedman [3], who considered propagation from a dipole in the ionosphere to the earth, using a spherical earth model. However, these three papers considered only dipole radiation

far from the antenna; and although the formulations are instructive, the solutions are not useful for practical applications of calculating impedances of antennas in the ionosphere. A recent mathematical formulation of the problem by Mittra [4] is more directly applicable. The best background reference is a book being published by McGraw-Hill [5].

Mittra formulated a mathematical technique by which one can derive the quasi-static Green's function solution to the tensor Helmholtz equation. Because of the ionospheric anisotropy, Maxwell's equations are written as a set of vector equations, which can be abbreviated in matrix form. If Cartesian coordinates are used with the z-axis aligned with the earth's magnetic field and  $e^{+j\omega t}$  is suppressed, then Maxwell's equations for an anisotropic ionosphere are as follows [6]:

$$\nabla \times \vec{E} + j\omega\mu_0 \vec{H} = \vec{0} \quad (a)$$

$$\nabla \times \vec{H} - j\omega\epsilon_0 \hat{\epsilon} \vec{E} = \vec{J} \quad (b)$$

$$\nabla \cdot \vec{H} = 0 \quad (c)$$

$$\nabla \cdot (\hat{\epsilon} \vec{E}) = \rho/\epsilon_0 \quad (d)$$

$$\hat{\epsilon} = \begin{bmatrix} \epsilon_{11} & -j\epsilon_{12} & 0 \\ j\epsilon_{12} & \epsilon_{11} & 0 \\ 0 & 0 & \epsilon_{33} \end{bmatrix} \quad (e) \quad (1)$$

where  $\vec{E}$ ,  $\vec{H}$  are the electric and magnetic field vectors, respectively;

$\mu_0$ ,  $\epsilon_0$  are the free-space permeability and permittivity, respectively;

$\vec{J}$  is the source electric current density;

$\rho$  is the volumetric source charge density;

$\omega$  is the radian frequency;

$\hat{\epsilon}$  is the (unitary) relative permittivity matrix;

$$\epsilon_{11} = 1 - \frac{x(1-jz)}{(1-jz)^2 - y^2} \quad (a) \quad x = \frac{Nq^2}{m\epsilon_0\omega^2} = \frac{\omega_p^2}{\omega^2} \quad (d)$$

$$\epsilon_{12} = \frac{xy}{(1-jz)^2 - y^2} \quad (b) \quad y = -\frac{B_0 q}{m\omega} = -\frac{\omega_q}{\omega} \quad (e) \quad (2)$$

$$\epsilon_{33} = 1 - \frac{x}{1 - jz} \quad (c) \quad z = \frac{\omega_r}{\omega} \quad (f)$$

$N$  is volumetric electron density;

$m$ ,  $q$  are electronic mass and charge (magnitude), respectively;

$B_0$  is earth's magnetic field;

$\omega_p$ ,  $\omega_q$ ,  $\omega_r$  are the plasma, cyclotron, and collision radian frequencies, respectively.

The use of the above forms of  $\epsilon_{11}$ ,  $\epsilon_{12}$ ,  $\epsilon_{33}$  presumes that the contributions of the ions can be neglected in comparison to the effect of the electrons. This should be a satisfactory assumption for frequencies of VLF and above and for ionospheric heights above the E-layer.

Substituting (1b) into (1a) yields the wave equation in matrix form (special case of the inhomogeneous, tensor Helmholtz equation):

$$\hat{C}\vec{E} - k_o^2 \hat{\epsilon} \vec{E} = -j\omega\mu_o \vec{J}, \quad (3)$$

where  $\hat{C}$  is the curl in Cartesian coordinates, written in matrix form; and

$$k_o^2 = \omega^2 \mu_o \epsilon_o .$$

The form of the matrix  $\hat{\epsilon}$  in (1e) can be diagonalized by a transformation and consequently will reduce the matrix form of (3) into a considerably simpler form [4]. This transformation is the key to obtaining an analytical solution to (3) in the quasi-static zone for the VLF spectra. As a result the quasi-static Green's function solutions can be derived.

The method by which we expect to derive the antenna driving-point impedance involves the following two steps:

(a) The calculation of the electromagnetic fields near the antenna, for an assumed current distribution,

(b) Computation of the driving-point impedance for an assumed current distribution using an "induced emf" technique or an iterative (Hallen) technique.

At this time, the "induced emf" technique appears simpler and will be attempted first. From this outlined approach, it will be necessary to develop basic theorems, stating the meaning of equivalence, reciprocity, duality, and the Poynting vector, in a magneto-ionic medium.

Recent results, which have yet to be checked and verified, show that the Green's function solutions for the electric fields are of the form of an operator,  $O(r,z)$  operating on a function of  $g(\epsilon_{11}, \epsilon_{33}, r, z)$  where  $r, z$  are the radial and longitudinal coordinates respectively in a cylindrical coordinate system whose  $z$ -axis is aligned with the earth's magnetic field, and  $r = (x^2 + y^2)^{1/2}$ . For example, with the antenna aligned with the earth's magnetic field (longitudinal orientation), the  $z$ -component of the electric field is the

following:

$$E_z^t = \frac{-j}{4\pi\omega\epsilon_0} \frac{\partial^2}{\partial z^2} (\epsilon_{11}^2 z^2 + \epsilon_{11}\epsilon_{33}r^2)^{-1/2}. \quad (4)$$

This expression reduces to the isotropic case by letting  $\epsilon_{11} = \epsilon_{33} = 1$ , in which case (4) simplifies as follows:

$$E_z = \frac{-j}{4\pi\omega\epsilon_0} \frac{\partial^2}{\partial z^2} (z^2 + r^2)^{-1/2}. \quad (5)$$

The equation (5) gives the correct  $E_z$  field component for the aforementioned antenna located in free space.

There is little theoretical work done describing propagation of electromagnetic energy through a magneto-ionic medium in quasi-static zone in the VLF spectrum. Consequently, a thorough investigation of fundamental concepts (e.g., the aforementioned equivalence, etc.) must be completed to insure that the analysis is valid. The study of these concepts is deliberate and necessary for our deriving valid results.

## REFERENCES

1. Bunkin, F. V., "On Radiation in Anisotropic Media," J.E.T.P., (Soviet Physics), USSR, Vol. 32, (1957), pp. 338-46.
2. Kuehl, Hans H., "Radiation from an Electric Dipole in an Anisotropic Cold Plasma," Tech. Report No. 24, California Inst. of Tech., Antenna Lab., AD 246 496.
3. Friedman, B., "Low Frequency Propagation," Boeing Airplane Co., Document No. D2-2302, (Seattle, Washington), 1 Nov. 1957.
4. Mittra, R., "Solution of Maxwell's Equations in a Magneto-Ionic Medium with Sources," Scientific Report No. 4, Engineering Experiment Station, University of Illinois, 18 January 1962, AD 274 083.
5. Brandstatter, J. J., The Propagation of Waves and Rays in a Plasma, McGraw-Hill (to be published 1963, probably in the Industrial Series of books).
6. Ratcliffe, J. A., The Magneto-Ionic Theory and its Applications to the Ionosphere, Cambridge Press (1959).

## AIR-TO-SUBSURFACE VLF PROPAGATION

### Part I - Air to Submarine Communications

The purpose of this paper, presented in two parts, is to report on the investigation into the relative merits of vertical versus horizontal airborne VLF antennas for communication with submerged submarines at large ranges. In this paper some qualitative aspects of the problem are considered, while the following paper is more quantitative. The physical model used here is a spherical earth enclosed by a concentric layer of air and a sharply bounded anisotropic ionosphere.

The basic antenna with which we are interested is a long wire trailed behind an aircraft at some height above the earth. In the frequency range of 10 - 30 kc the radiation pattern of such an antenna is not well known; the wire may be of the order of a wavelength while the aircraft, against which the wire is energized, will be a small fraction of a wavelength in dimensions. Therefore, the usual approximation of a sinusoidal current distribution may not be very accurate. In the absence of a precise radiation pattern, we assume that the antenna may be replaced by its equivalent electric dipole moment which will in general have a vertical as well as a horizontal component.

The field which the airborne trailing wire antenna will cause in sea water at large ranges can be computed from two

different theories--mode theory and ray theory. These two theories are equivalent but each possesses different practical advantages. To obtain a gross estimate of what is happening in the earth-air-ionosphere wave guide, mode theory is the easiest for computations if some approximations can be made. If a more accurate estimate is desired, then ray tracing provides the capability of variable ionospheric and earth reflection coefficients, enabling one to inject into the problem the transition from day to night, solar disturbances, and nuclear weapon perturbations. Both mode theory and ray theory are frequency sensitive; mode theory tending to be more tractable at ELF and ray theory at VLF. Ray theory is used in the following discussions since we are interested in a frequency range from 10 to 30 kc.

Some nomenclature that we use is illustrated in Figure 1. The plane of incidence is the plane of the paper and is defined by the great circle route between the airborne transmitter and the submerged receiver. Two representative rays between the transmitter and receiver are shown. Electric fields normal to the plane of incidence (horizontal

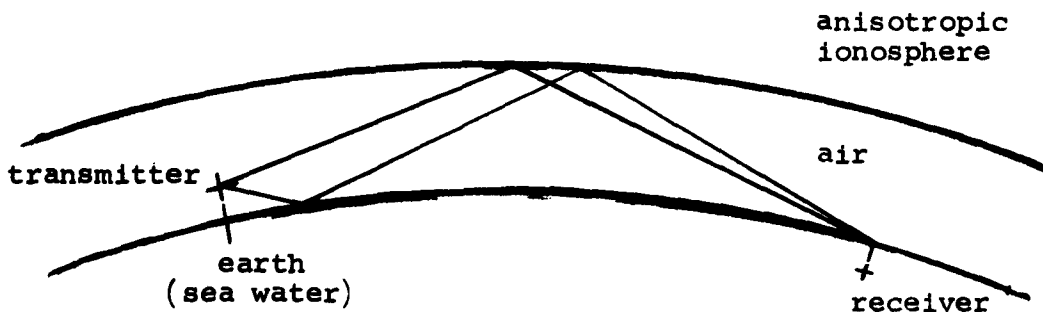


Figure 1.

polarization) are denoted by the subscript " $\perp$ ," and electric fields parallel to the plane of incidence (vertical polarization) are denoted by the subscript " $\parallel$ ."

The vertical dipole associated with the trailing wire antenna will radiate only vertically ( $\parallel$ ) polarized electric fields for any plane of incidence. The horizontal dipole will, however, radiate electric fields polarized vertically, horizontally, or a combination of the two depending on the orientation of the horizontal dipole with respect to the plane of incidence.

Part II will show more precisely the electric field components in sea water caused by vertical and horizontal dipoles at various heights above the earth. At this point, however, we merely state some of those results and discuss their possible implications for trailing wire antennas. Consider for a moment a receiver in sea water in a direction which is broadside to a trailing wire antenna. The effective vertical moment of the antenna will cause an electric field in sea water which is parallel to the plane of incidence.

See Figure 2.

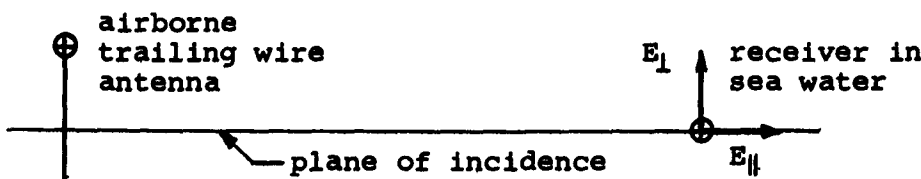


Figure 2. Top View of a Propagation Path.

The effective horizontal moment will cause an electric field in sea water which is normal to the plane of incidence. It is not unreasonable that  $E_{\perp}$  and  $E_{\parallel}$  could be of the same order of magnitude, and, in general, the phase of  $E_{\perp}$  and  $E_{\parallel}$  will be different. Thus the trailing wire antenna will cause fields in sea water which are elliptically polarized in a plane parallel to the sea surface. It therefore seems possible to make the submerged receiver more immune to noise by using polarization diversity. This phenomenon is not readily observable in the air above the sea water since the reflected  $E_{\perp}$  field virtually cancels the incident  $E_{\perp}$  field. However, the transmission coefficient for  $E_{\perp}$  is  $2n \cos \theta$  which is the same order of magnitude as the transmission coefficient for  $E_{\parallel}$  which is  $2n$ ; where  $n = (j\omega\epsilon_0\sigma^{-1})^{1/2}$  and  $\theta$  is the angle of incidence measured from the vertical. This indicates that if  $E_{\perp}$  and  $E_{\parallel}$  are of the same order of magnitude then  $E_{\perp}$  and  $E_{\parallel}$  received in sea water at large ranges will be roughly the same order of magnitude.  $E_{\perp}$  will tend to be less than  $E_{\parallel}$  because of the factor  $\cos \theta$  in the transmission coefficient for  $E_{\perp}$ , but this is partially offset by the fact that the magnitude of the reflection coefficients for  $E_{\perp}$  at the air-ionosphere boundary is greater than the corresponding reflection coefficient for  $E_{\parallel}$ .

It is, in general, true that the vertical component of the trailing wire antenna will cause a larger field strength in sea water (at large ranges) than the horizontal component if both components radiate the same power. However, this

phenomenon is partially offset, as will be shown in Part II, if the height of the trailing wire antenna above the earth is increased. The fields in sea water caused by the vertical component are relatively insensitive to antenna height while the fields caused by the horizontal component experience a very appreciable increase with antenna height.

It is also to be remarked that fields computed from ray theory tend to receive their greatest contribution from the first few, or the lowest order, rays. It is desirable, therefore, that these lowest order rays be incident on the earth in a region where the reflectivity is the greatest possible, e.g., sea water.

Finally, it is interesting to speculate on the possibility of increasing the directivity of an airborne trailing wire antenna. One possible method for doing this is suggested by the Yagi array. Thus, if a second aircraft carried a passive trailing wire antenna, as shown in Figure 3, then it is possible that the directivity in the direction of the receiver could be increased.

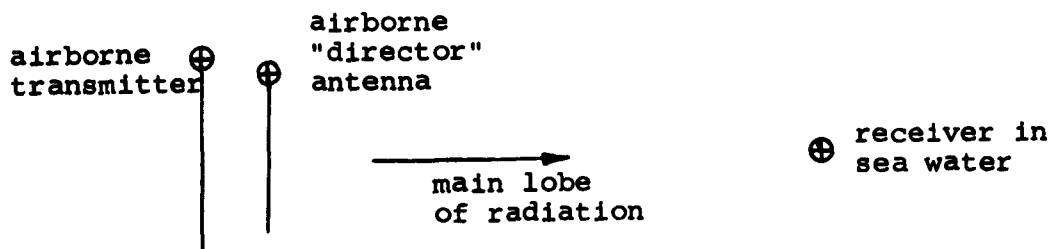


Figure 3.

## Part II. Electric Field Components in the Sea

The method chosen to obtain the electric field components in the sea from airborne vertical and horizontal antennas is a geometrical-optical technique based on a derivation by Bremmer [1]. Bremmer employed a saddle point evaluation in the complex plane of the original Sommerfeld-type integral equations. This method has been modified to include a re-evaluated convergence-divergence coefficient valid in the neighborhood of the caustic, a more accurate estimate of ionospheric reflection coefficients, and a "cut-back" factor which accounts for the effect of diffracted waves for receivers beyond the caustic.

The composition of the received electric field for airborne transmitting antennas is considered in the following paragraphs. Observations of the resultant field equations and results of the computer evaluation are discussed.

If a dipole is considered to be at a height,  $h$ , above an earth of effective radius,  $a$ , where the standard atmosphere has been assumed ( $a = 4/3$  times actual earth radius), and ionospheric height,  $H$ , two series of rays will reach a receiver on the surface of the earth. One ray will be reflected initially by the ionosphere (unprimed quantities) and the other ray will be reflected initially by the earth (primed quantities) as shown in Figure 1. The path length travelled by the rays will be slightly different, or  $d' > d$  for  $h > 0$ .

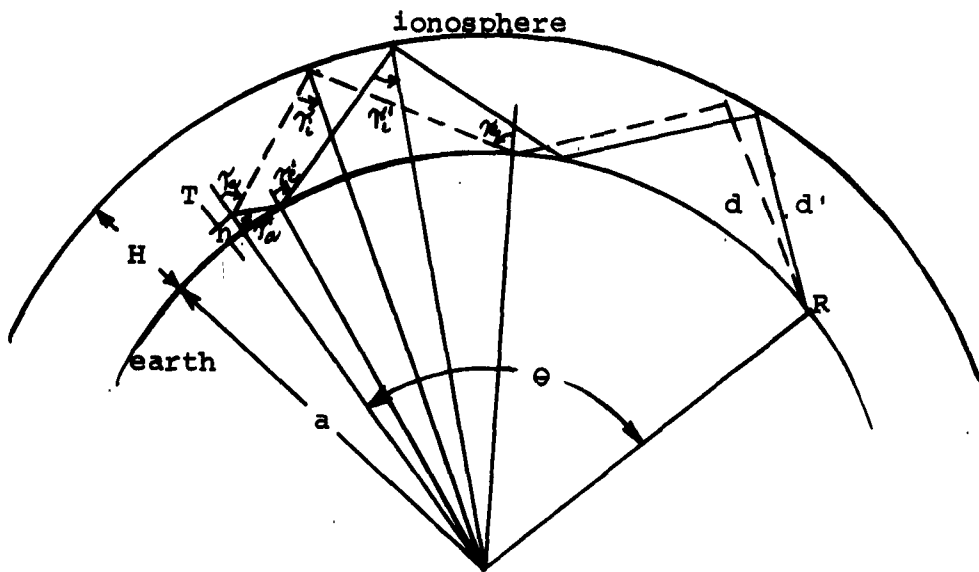


Figure 1.

The electric field at the receiver can be considered to consist of a modified free space field. In free space, the rms electric field in millivolts per meter at a distance,  $d$ , in kilometers from the transmitter can be written as

$$E = 150 \frac{e^{-ikd}}{d} \text{ mv/m/kw of radiated power,} \quad (1)$$

where the distance,  $d$ , is the total path length traversed by the ray and  $k$  is  $\frac{2\pi}{\lambda}$  the propagation constant in air. The coefficient (150) is obtained by evaluating the electric field at a distance of one kilometer from a short vertical dipole which radiates one kilowatt over a flat infinitely conducting surface.

Since, as shown in Figure 1, the path length of each ray is slightly different, the electric field for each ray will

in general be of about the same relative magnitude but of different phase. Since the phases will vary with  $d$  and  $d'$ , this will result in zones of strong and weak fields depending upon whether the phases add or subtract. This analysis can be extended to multihop rays, where the difference in magnitude of the rays is predominantly affected by the number of reflections by the ionosphere and earth since, at each reflection point, energy is lost in transmission across the boundary. This means that the more hops a ray experiences, the smaller the amplitude at the distant point compared to a ray which experienced less hops. Eventually, it can be seen that a limit will be reached where rays whose number of hops are greater than some number  $N$  will not contribute significantly to the total received electric field and can therefore be neglected.

The coefficient,  $\alpha$ , is defined as the ratio of the square root of the cross-sectional area of a pencil of rays which travel linearly from a transmitter to a receiver to the actual cross-sectional area of the rays arriving at the receiver. This coefficient takes into account the focusing of the ray on reflection from the ionosphere and the spreading caused on reflection from the earth. From the definition, if  $\alpha$  exceeds unity, it indicates convergence; if it is less than unity it shows divergence of the ray. If a spherical-earth concentric-ionosphere model is chosen and the receiver is

located at the earth's surface, the value of  $\alpha$  is always greater than unity.

From the definition of  $\alpha$ , the convergence coefficient for the  $j^{\text{th}}$  ray ( $\alpha_j$ ) can be described by the following formula:

$$\alpha_j = \frac{d_j}{a} \left( \frac{\tan \tau_{ej}}{\sin \theta} \left| \frac{d\tau_{ej}}{d\theta} \right| \right)^{1/2}$$

As shown in Figure 2,  $\tau_{ej}$  is the angle of incidence at both the transmitter and receiver.  $\theta$  is the angular distance of propagation measured at the earth's center,  $d_j$  is the total linear path length of the traversed ray, and "a" is the effective radius of the earth.

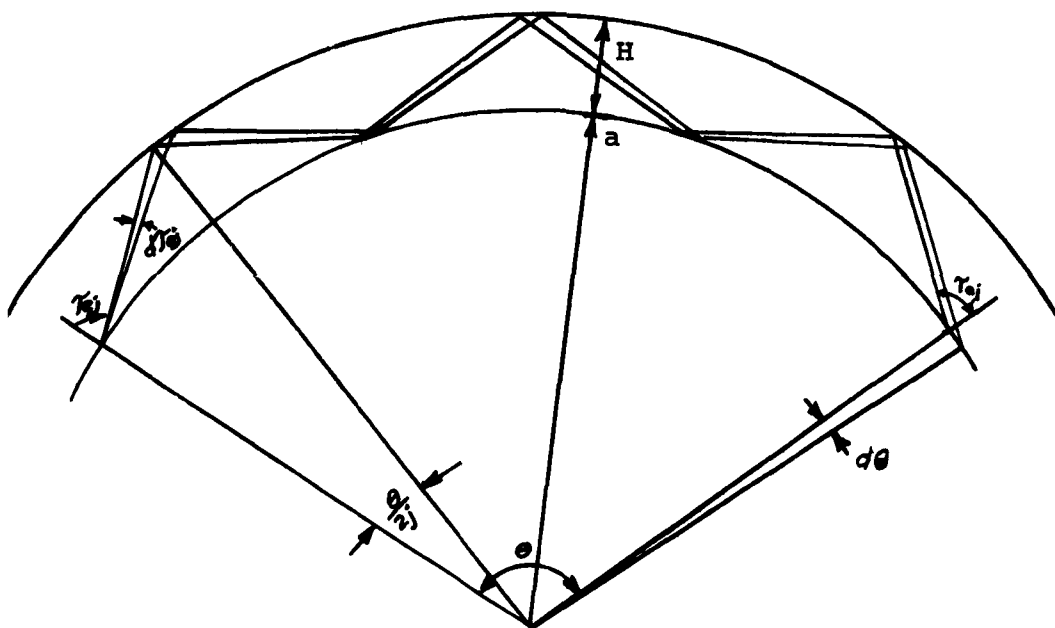


Figure 2.

From the geometry of Figure 2,

$$\tan \tau_{ej} = \frac{(a + H) \sin \frac{\theta}{2j}}{(a + H) \cos \frac{\theta}{2j} - a}$$

Using this relationship, the convergence coefficient becomes on evaluation

$$\alpha_j = \left( \frac{a+H}{a} \right) \left( \frac{2j \sin \frac{\theta}{ZJ}}{\sin \theta} \right)^{1/2} \left( \frac{a+H - a \cos \frac{\theta}{ZJ}}{(a+H) \cos \frac{\theta}{ZJ} - a} \right)^{1/2}$$

The convergence coefficient  $\alpha_j$ , as defined above, is valid for all regions except in the vicinity of the caustic, the region where the sky-wave leaves and returns to the earth tangentially. At this point,  $\cos \frac{\theta}{ZJ} = \frac{a}{a+H}$  and  $\alpha_j$  becomes infinite. This problem has been considered by Wait [2] who modified the convergence coefficient, valid in the vicinity of the caustic and beyond, by considering a third order approximation (Hankel approximation) of the original Sommerfeld-type integrals rather than the usual second order approximation (Debye expansion). For a rigorous development the reader is referred to Bremmer [1, page 182] and to Wait's original paper [2]. Application of this modification to the vicinity of the caustic allows the geometrical-optical calculation of the electric field to be continuous through the caustic zone.

At each reflection point, on the earth or at the ionosphere, the ray is modified in amplitude and phase dependent upon angle of incidence, the polarization of the incident wave and the index of refraction. The ratio of the electric field in the reflected wave to the electric field in the incident wave will be represented as four reflection coefficients:

$$R_{\parallel}, R_{\perp}, I_{\perp}, I_{\parallel}.$$

The first subscript denotes whether the incident electric field is parallel ( $\parallel$ ) or perpendicular ( $\perp$ ) to the plane of incidence and the second subscript denotes whether the reflected electric field is parallel or perpendicular to the plane of incidence. The reflection coefficients of the ionosphere can then be represented as the elements of a  $2 \times 2$  matrix,  $R$ . The reflection coefficients for an isotropic earth, designated as  $D(\tau_e)$ , on the other hand consist of only the terms  $\|R\|$  and  $\perp R\perp$  since  $\|R\perp$  and  $\perp R\|$  are zero for an isotropic medium.

Consider the  $j^{\text{th}}$  ray which is reflected initially from the ionosphere at an angle equal to its angle of incidence  $\tau_{ij}$ . The  $j^{\text{th}}$  ray will be reflected  $j$  times by the ionosphere and  $j-1$  times by the earth when considered at the earth's surface. The total reflection coefficient can be represented as a matrix product of ionospheric reflection coefficient matrices alternating with earth reflection coefficient matrices, as given by

$$Q_i = \prod_{k=1}^j D_{j-k+1}(\tau_{ej}) R_{j-k+1}(\tau_{ij}). \quad (2)$$

The total reflection coefficient matrix for those rays which are reflected initially by the earth ( $Q_s$ ) are similar in form to  $Q_i$  with the addition of a term  $D(\tau'_{ej})$  to the right side of the product,

$$Q_s = \prod_{k=1}^j D_{j-k+1}(\tau'_{ej}) R_{j-k+1}(\tau'_{ij}) D_o(\tau'_{ej}). \quad (3)$$

Note that  $Q_s$  is the same as  $Q_i$  except for slightly different angles of incidence and the term  $D_o(\tau'_{ej})$ .

The electric field that is of interest in submarine communication is the horizontal electric field at the boundary in the sea; therefore, if we pre-multiply the total reflection matrix by  $T(\tau_e)$ , the transmission coefficient matrix, the electric field parallel and perpendicular to the plane of incidence will be determined. The transmission coefficients as defined here are related to the reflection coefficients by the following relationships

$$T_{\parallel} = n(1 + R_{\parallel}) \quad (4)$$

and

$$T_{\perp} = 1 + R_{\perp} . \quad (5)$$

If the distance between transmitter and receiver is such that there are rays which do not geometrically reach the receiver, (the distance is greater than the distance to the caustic), a surface wave is created which diffracts along the surface of the earth to the receiver. The effect of such a diffraction can be accounted for by multiplying the electric field at the geometric limit by a "cut-back factor,"  $F$ . This factor was developed by Wait and Conda [3] to account for the influence of finite conductivity and earth curvature on the field pattern of receiving antennas. For waves approximately tangential to the surface of the earth,  $F$  degenerates to the factor  $(1 + R_g)$  where  $R_g$  can be  $R_{\perp}$  or  $R_{\parallel}$  depending upon the incident wave polarization.

The field patterns of the transmitting antenna,  $G_t(\tau_a, \phi)$ , and receiving antenna,  $G_r(\tau_e, \phi)$ , determine the magnitude of the radiated or received ray as a function of the incident and azimuth angles. The receiving antenna in the sea is assumed to be a trailing wire antenna whose field pattern is only a function of the azimuthal angle.

At VLF the ground wave is either dominant or of the same magnitude as the sky wave up to a distance of about 1000 kilometers. Van der Pol and Bremmer [1] developed asymptotic expressions for the electric field from a horizontal and a vertical dipole. These expressions will be used since they can be easily adapted to computer evaluation. The ground wave term will be symbolically represented as

$$E_o e^{-i\phi_o}$$

where  $E_o$  and  $\phi_o$  are the amplitude and phase of the ground wave.

From the preceding discussion, it is apparent that the total field at the receiver can be represented as the sum of a ground wave and two series of sky waves, one series corresponding to those rays initially reflected from the ionosphere and the other series corresponding to those rays initially reflected from the earth. Thus the horizontal electric field in the sea at the surface is

$$\begin{aligned}
 E = & E_0 e^{-i\varphi} + 150 \sum_{j=1}^N G_r(\varphi) F \alpha_j T_i Q_i G_t(\tau_a, \varphi) \frac{e^{-ikd_j}}{d_j} \\
 & + 150 \sum_{j=1}^N G_r(\varphi) F \alpha_j T_s Q_s G_t(\tau'_a, \varphi) \frac{e^{-ikd'_j}}{d'_j}
 \end{aligned} \quad (6)$$

Since the incident angles at the ionosphere and the incident angles at the earth are nearly equal for the two series of rays, for the  $j^{th}$  hop ray ( $\tau_{ij} \approx \tau'_{ij}$  and  $\tau_{ej} \approx \tau'_{ej}$ ), the transmission coefficients and reflection coefficients can be approximated as:

$$T(\tau_{ij}) \approx T(\tau'_{ij}) \quad (7)$$

and

$$Q_s(\tau'_{ij}, \tau'_{ej}) \approx Q(\tau_{ij}, \tau_{ej}) \begin{pmatrix} R_{||} & 0 \\ 0 & R_{\perp} \end{pmatrix}. \quad (8)$$

The transmitter antenna patterns for the two series of rays are also related; for the horizontal dipole

$$G_t(\tau'_a, \varphi) \approx \begin{pmatrix} -1 & 0 \\ 0 & 1 \end{pmatrix} G_t(\tau_a, \varphi) \quad (9)$$

and for the vertical dipole

$$G_t(\tau'_a, \varphi) \approx G_t(\tau_a, \varphi). \quad (10)$$

By representing the average path difference between the transmitter and receiver for the  $j^{th}$  ray as  $x_j$  and the average path length as  $s_j$ , where

$$x_j = \frac{1}{2}(d'_j - d_j) \quad (11)$$

and

$$s_j = \frac{1}{2}(d'_j + d_j), \quad (12)$$

the electric fields can be rewritten for the horizontal dipole as

$$E = E_0 e^{-i\varphi_0} + 300 \sum_{j=1}^N G_r(\varphi) F \alpha_j T Q_i \frac{e^{-ikx_j}}{s_j + x_j} \begin{pmatrix} a_{11} & 0 \\ 0 & a_{22} \end{pmatrix} G_t(\tau_a, \varphi) \quad (13)$$

and for the vertical dipole as

$$E = E_0 e^{-i\varphi_0} + 300 \sum_{j=1}^N G_r(\varphi) F \alpha_j T Q_i \frac{e^{-ikx_j}}{s_j + x_j} \begin{pmatrix} b_{11} & 0 \\ 0 & b_{22} \end{pmatrix} G_t(\tau_a, \varphi) \quad (14)$$

The composition of the coefficients is

$$\begin{aligned} a_{11} &= i \sin kx_j + \frac{x_j}{d_j} e^{ikx_j} + \frac{1}{2}(1 - R_{||}) e^{-ikx_j} \\ a_{22} &= i \sin kx_j + \frac{x_j}{d_j} e^{ikx_j} + \frac{1}{2}(1 + R_{\perp}) e^{-ikx_j} \\ b_{11} &= \cos kx_j + \frac{x_j}{d_j} e^{ikx_j} - \frac{1}{2}(1 - R_{||}) e^{-ikx_j} \\ b_{22} &= a_{22} \end{aligned} \quad (15)$$

For propagation over sea water, for some finite altitude of the transmitter, the terms  $(1 - R_{||})$  and  $(1 + R_{\perp})$  are negligible. When more than one ray is considered and the transmitting antenna is at some finite altitude, the contribution of the second and third term of the coefficients will be negligible compared to the magnitude of  $\sin kx_j$ . The received electric field can then be taken as

$$E = E_0 e^{-i\varphi_0} + 300i \sum_{j=1}^N G_r(\varphi) F \alpha_j T Q G_t(\tau_a, \varphi) \sin kx_j \frac{e^{-ikx_j}}{s_j + x_j} \quad (16)$$

Following the same analysis as given for the horizontal dipole, the received electric field from the vertical dipole becomes

$$E = E_0 e^{-i\varphi_0} + 300 \sum_{j=1}^N G_r(\varphi) F_a j T Q G_t(\tau_a, \varphi) \cos kx_j \frac{e^{-iks_j}}{s_j + x_j}. \quad (17)$$

### Discussion

Equation (16) and (17) indicate that each ray is composed of a standing wave which is a function of antenna height and to a lesser degree ionospheric height and propagation distance. As evident from the term  $\sin kx_j$ , the horizontal antenna has a definite antenna gain as the altitude is increased. For the small argument approximation applied to equations (13) and (14), the vertical antenna is found to have the same height-gain function as given by Bremmer [1], Eckersley and Millington [4], and more recently by Wait [5]; the horizontal antenna has the same height-gain function for the horizontally-polarized field component as given by Bremmer.

Considering again equations (13) and (14), as the transmitting antenna approaches the ground, the far field space wave function becomes identical to the space wave given by Norton [6] and more recently by Biggs [7] for a horizontal dipole in the earth near the surface (except for the attenuation due to depth of burial).

It is interesting to note that the conductivity of the earth in the region surrounding the transmitting antenna contributes markedly to the height-gain functions for both ground-based and airborne antennas. This is because those series of rays from the lower radiation quadrant are initially reflected by the earth in the immediate vicinity of the antenna. This region extends out to approximately a distance

of 100 miles for an antenna at 30,000 feet and a propagation distance of 3000 miles. At VLF and for small values of the argument ( $kx_j \approx kh \cos \tau_e < 1$ ) in the height-gain function, the vertically-polarized electric field from the vertical antenna will experience a reduction (maximum of 3 db) and then an increase in electric field strength. The horizontally-polarized electric field radiated by the horizontal dipole, on the other hand, experiences approximately a linear increase for small arguments of the height-gain function. The vertically-polarized component radiated by the horizontal dipole is dependent upon the incident angle at the earth's surface and does not have as large a gain as the horizontally-polarized component. At a sufficient altitude, the horizontally-polarized component radiated by the horizontal antenna appears to approach numerically that radiated by a ground-based vertical dipole.

The results of the modified ray theory for the spherical earth-anisotropic ionosphere model using the quasi-longitudinal approximation to obtain the ionospheric reflection coefficients (valid for median latitudes) at a propagation frequency of 15 kc compare favorably with available experimental data obtained by Bickel, Heritage, and Weisbrod [8] for ground-based vertical electric dipoles at 16.6 kc measured by an airborne receiver up to distances of 6000 km, see Figure 3. Comparison with actual airborne transmitting antennas has not been made but computer results for the vertical electric field component in air as shown in Figure 4

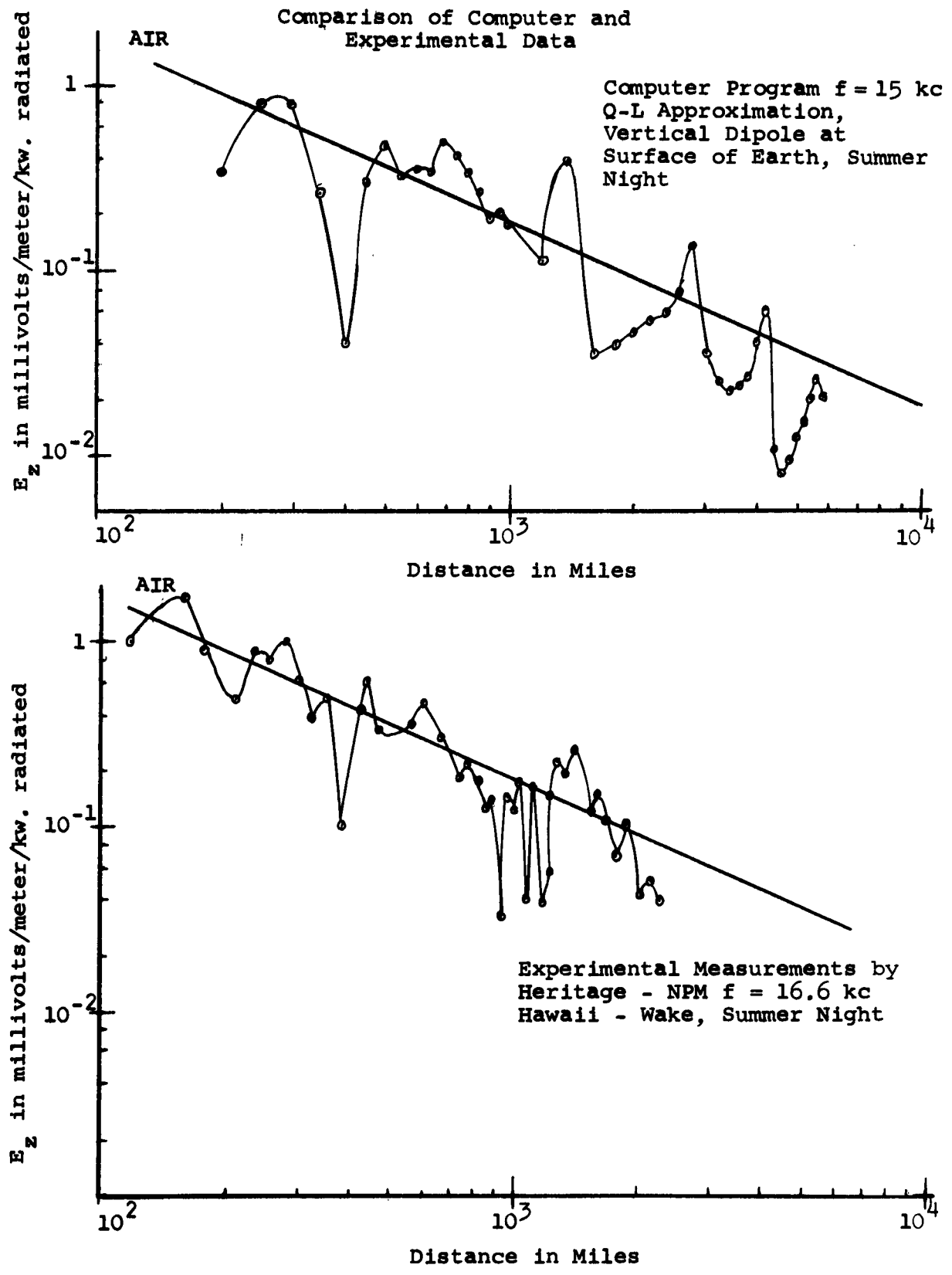


Figure 3.

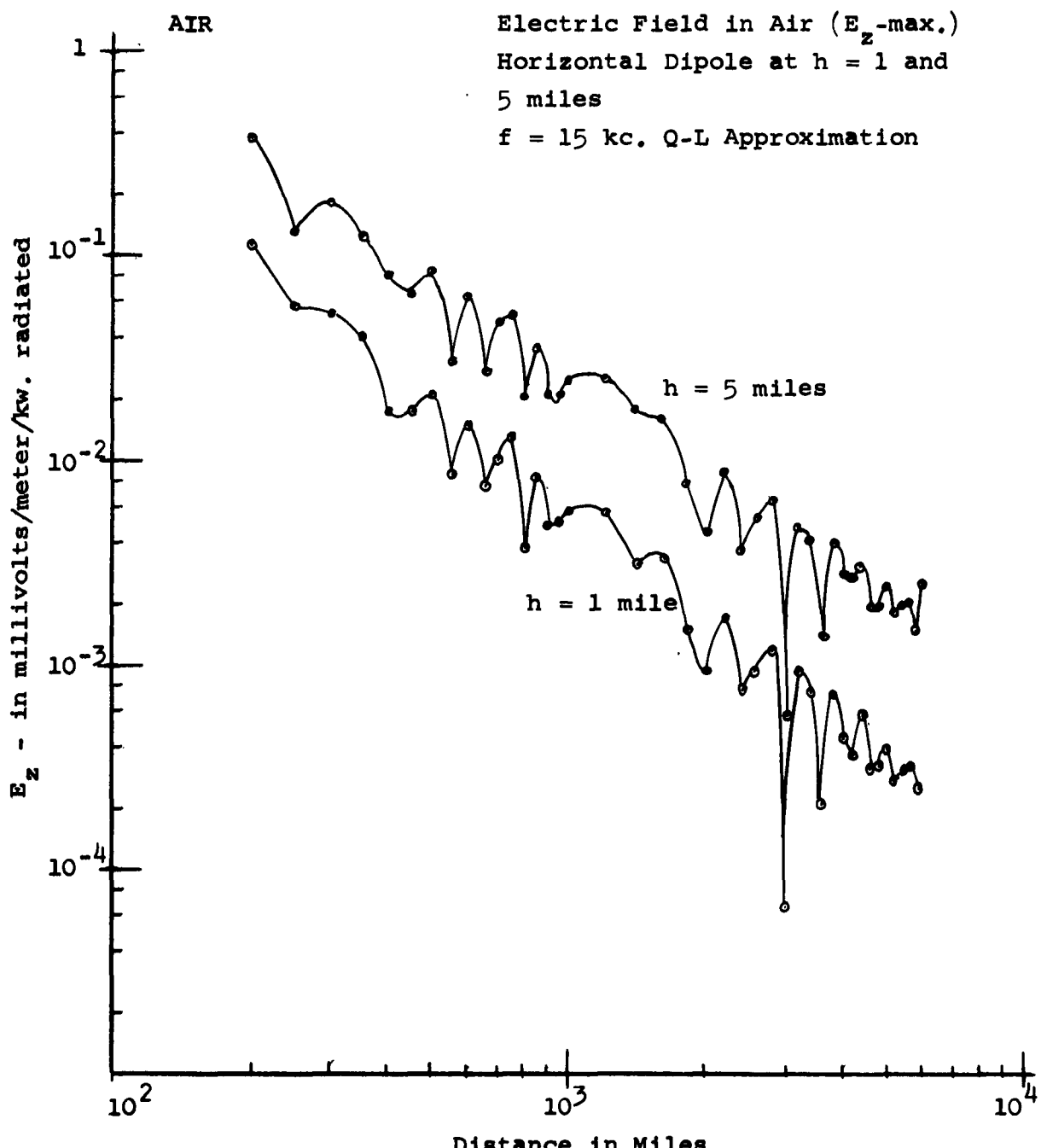


Figure 4.

indicate a definite increase of the electric fields radiated by the horizontal antenna of the order of 20 db per decade in height for altitudes greater than a skin depth (as a measure of conductivity) in earth in the vicinity of the transmitter, while the fields radiated by the vertical antenna, Figure 5, are essentially unchanged with height for the altitudes considered to date, 5 miles at one mile increments. The fields of the horizontal dipole are sinusoidal functions of azimuth as measured from the longitudinal axis of the antenna to the plane of propagation. The resultant graphs of electric field for the horizontal dipole are maximized with respect to azimuthal angle, which in turn determines the aircraft flight path for a fixed receiver location. As the vertical dipole is omnidirectional in azimuth, no optimization is required and direction of flight would be immaterial.

The computer results for the dominant electric field components in the sea for the horizontal ( $E_\phi$ ) and the vertical dipole ( $E_r$ ) at a propagation frequency of 15 kc are shown in Figures 6 and 7, respectively.  $E_\phi$  has a definite gain with antenna altitude of 20 db per decade up to a height of 5 miles while  $E_r$  is relatively unchanged. At an altitude of 5 miles, a comparison of  $E_r$  and  $E_\phi$  indicates that they are of the same order of magnitude but orthogonal in space with  $E_\phi$  lagging in amplitude at large distances.

It can be concluded that, at VLF and up to altitudes of 5 miles, for the quasi-longitudinal approximation of the

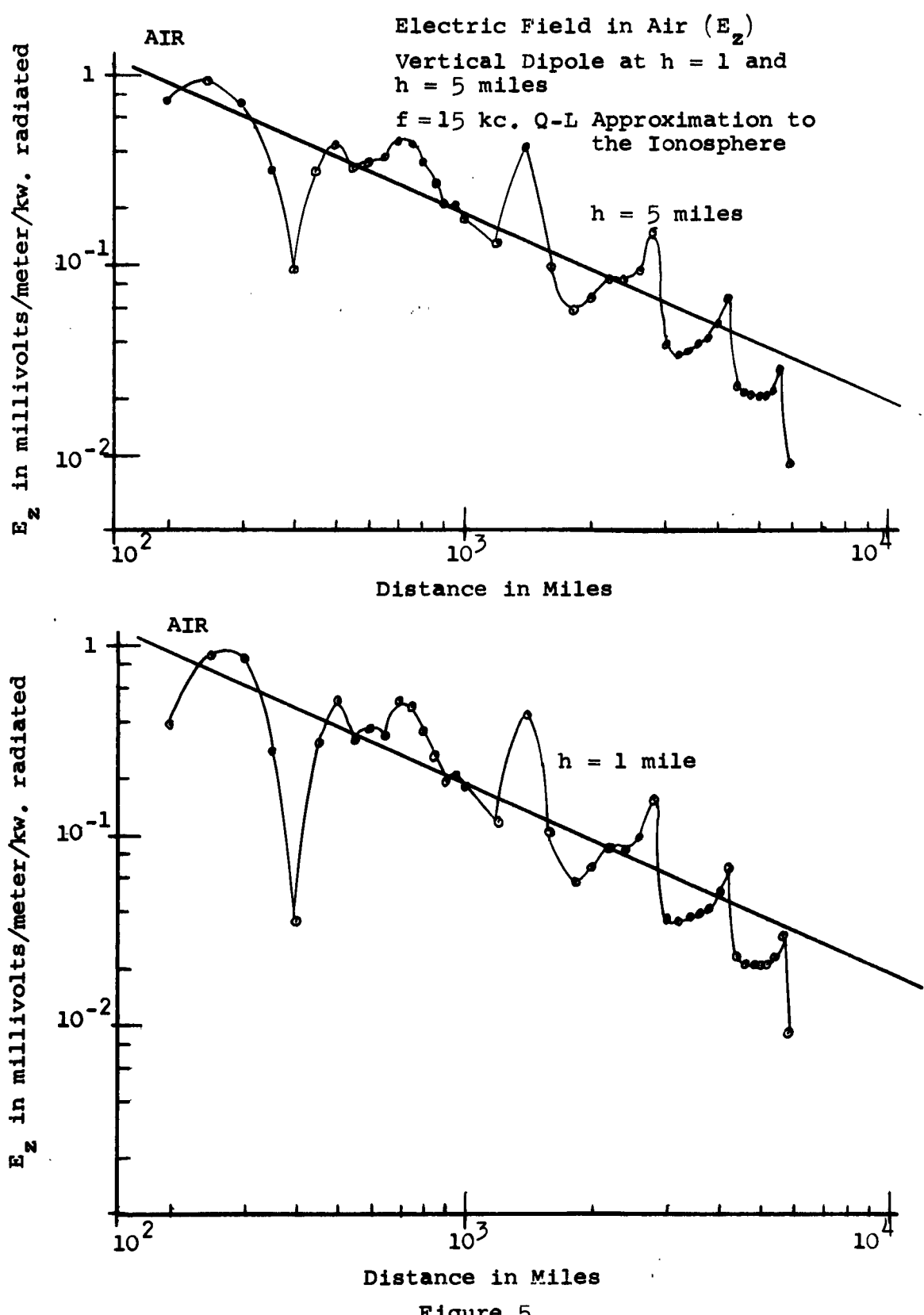


Figure 5.

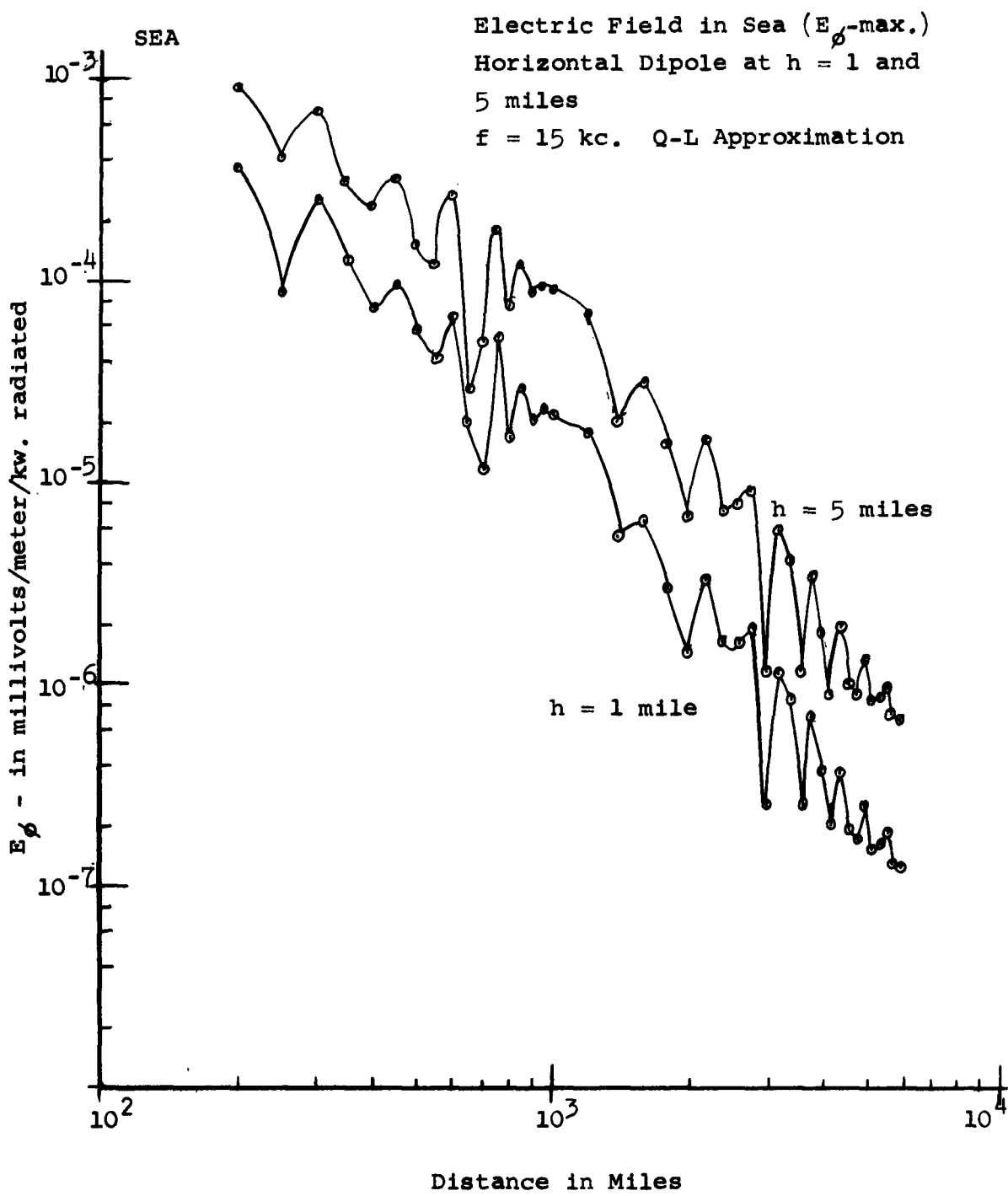


Figure 6.

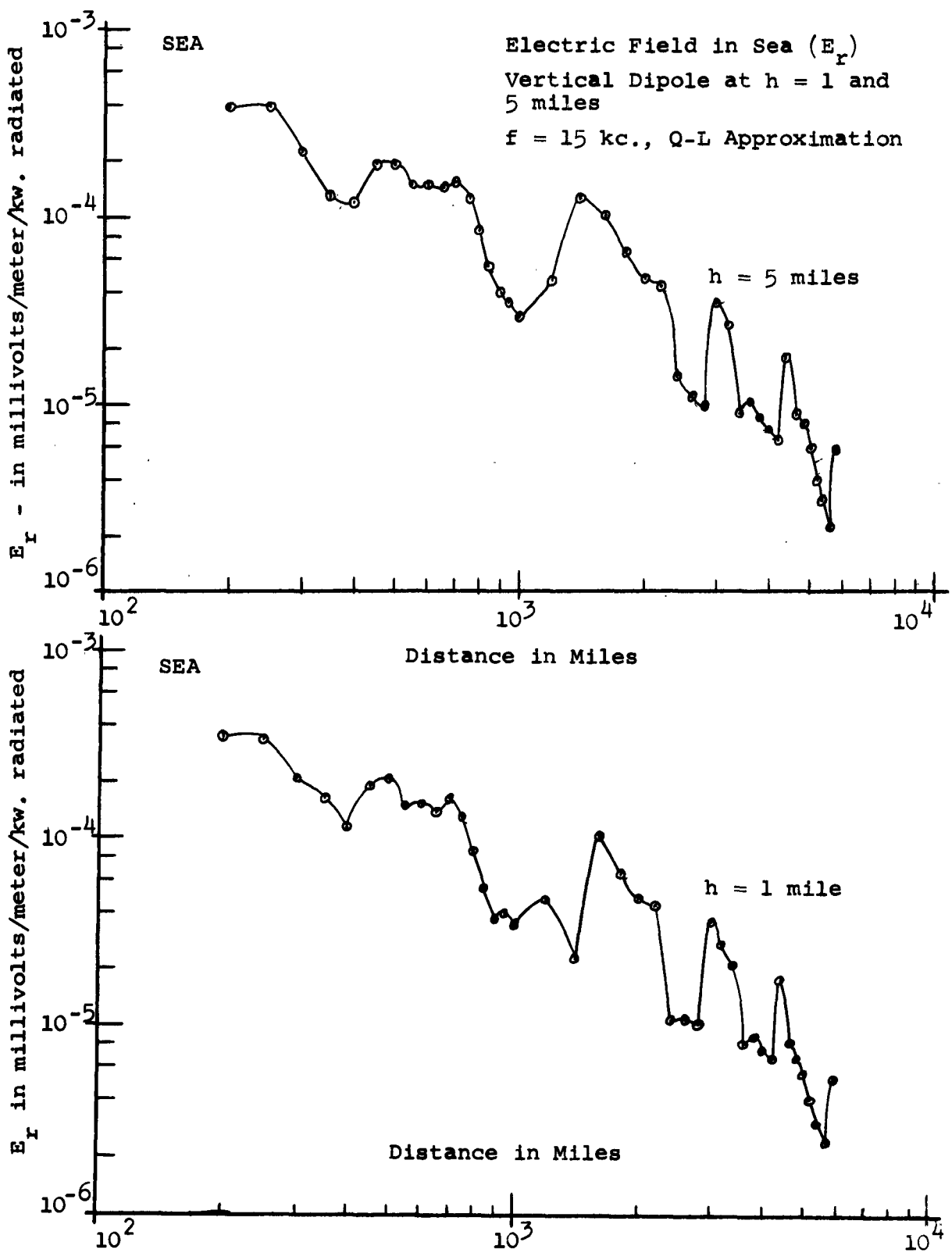


Figure 7.

ionospheric reflection coefficients, the airborne vertical dipole is the more efficient radiator to communicate with submarines (or surface vessels). However, the horizontal dipole experiences a height-gain as the antenna elevation is increased which results in a horizontally-polarized electric field component in the sea which approaches that obtained from the vertical dipole.

The horizontal component of the airborne horizontal antenna experiences a definite antenna gain of approximately 20 db per decade for altitudes greater than a skin depth in the earth in the vicinity of the antenna. The airborne vertical dipole on the other hand is relatively insensitive to antenna height at VLF.

At VLF, the electric field components tangent to the sea surface (the horizontally-polarized electric field and the tangential component of the vertically-polarized electric field) are the only components of measurable significance in the sea. The total tangential electric field measured in air which is equivalent to the tangential electric field in the sea is the difference in magnitude of the incident and reflected tangential fields. At VLF, this value is of the order of  $2|n|$  where  $n$  is the ratio of the propagation constant of air to that of sea water (or earth). The magnitude of  $n$  is approximately  $10^{-4}$  at VLF. The electric field in air normal to the sea surface (from the vertically-polarized electric field) is approximately twice the incident field for all angles of incidence less than the pseudo-Brewster angle

(between 89° to 90° at VLF). However in the sea because of the small value of the index of refraction, the normal electric field component is  $|n|^2$  times the value in air. In summary, the normal component of the electric field is the only measurable component in air near the earth's surface and the tangential component is the only measurable component in the sea.

An actual airborne trailing-wire antenna is composed of both vertical and horizontal segments. The antenna can, therefore, be considered as a large effective horizontal dipole and a smaller effective vertical dipole. By appropriately shaping the trailing wire antenna, a desired ratio of horizontal to vertical can be achieved. As shown in Figures 6 and 7, the vertical dipole radiates a larger component ( $E_r$ ) than the horizontal dipole ( $E_\phi$ ) in the far field. However, the horizontal dipole component ( $E_\phi$ ) approaches  $E_r$  with increased antenna height and it is here suggested that these components can be made approximately equal for some receiver distance resulting in an elliptically-polarized field. If by chance the phase difference between the two orthogonal field components happened to be zero, a relocation of the submarine would introduce a phase angle. The elliptically-polarized electric field would enable a submarine to orient the null of its floating wire antenna to best suit tactical requirements and also to use sophisticated receiving techniques such as polarization diversity to obtain better signal to noise ratios.

The field component ( $E_z$ ) measured in air near the surface of the earth radiated from an airborne antenna will in all probability be due to the vertical segment of the trailing wire antenna. Inspection of Figures 4 and 5 indicates that if appropriate effective lengths are assigned to the horizontal and vertical dipole, for example 5/6 and 1/6, respectively, and a constant current distribution is assumed over the length of the antenna, the electric field of the vertical dipole would still be dominant. Doubling the length of the vertical segment will result in an increase of vertical electric field of 6 db. The actual current distribution is quite complex dependent upon the physical parameters of aircraft and antenna.

In conclusion, tests to determine the electric fields in the sea from a trailing wire antenna should be made with submerged antennas to determine the relative magnitude of  $E_\phi$  from a horizontal dipole and  $E_r$  from a vertical dipole. The ellipticity of the resultant field should be verified and if it exists as suggested, should be further investigated to obtain better signal to noise ratios and possible interference protection.

## REFERENCES

1. Bremmer, H., Terrestrial Radio Waves, Elsevier Publishing Co., Amsterdam, Netherlands; 1949.
2. Wait, J. R., Diffractive Corrections to the Geometrical Optics of Low Frequency Propagation, in Electromagnetic Wave Propagation, Academic Press, London, England; 1960.
3. Wait, J. R., and A. M. Conda, Pattern of an Antenna on a Curved Lossy Surface, IRE Transactions on Antennas and Propagation, AP-6, pp. 348-359; October, 1958.
4. Eckersley, T. L., and G. Millington, The Experimental Verification of the Diffraction Analysis of the Relation Between Height and Gain for Radio Waves of Medium Lengths, Physical Soc. of London--Proc., 51, pp. 805-809; 1939.
5. Wait, J. R., Excitation of Modes at Very Low Frequency in the Earth-Ionosphere Wave Guide, Jour. of Geo. Res., 67, No. 10, pp. 3823-3828; September, 1962.
6. Norton, K. A., The Physical Reality of Space and Surface Waves in the Radiation Field of Radio Antennas, Proc. IRE, 25, pp. 1122-1202; September, 1937.
7. Biggs, A. W., Radiation Fields from a Horizontal Electric Dipole in a Semi-Infinite Conducting Medium, IRE Trans. on Antennas and Propagation, AP-10, No. 4, pp. 358-362.
8. Bickel, J. E., J. L. Heritage, and S. Weisbrod, "A Study of Signal vs. Distance data at VLF," VLF Symposium, NBS, Boulder Labs, Vol. 4, pp. 29-39; January, 1957.

INVESTIGATION OF PARALLEL-WIRE AND COAXIAL  
SIDE-LOADED TRANSMISSION LINES AS A TRAILING WIRE ANTENNA

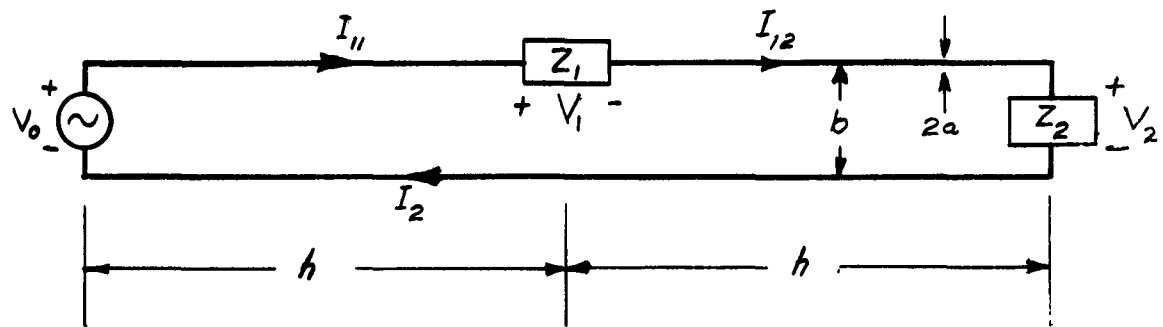
The purpose of this study, started in July, 1961, was to determine the advantages, if any, that a parallel-wire side-loaded transmission line might have when used as a trailing wire antenna, and to suggest a design for a practical form of this type of antenna for use in the VLF spectrum. This paper summarizes the results of the investigation.

With physically long airborne trailing wire antennas (lengths in the range of thousands of feet), there is an obvious mechanical advantage in end-feeding the antenna. Such an antenna operating in the VLF spectrum would probably be electrically short ( $\frac{2\pi h}{\lambda} < 1$ ). This would result in a large input reactance as compared to the input resistance. At high power levels such an input impedance would be difficult to match to a transmitter. It can be shown by an approximate method [1] that for electrically short, thin linear antennas, the input reactance of a center-fed antenna is less than that of an asymmetrically-fed antenna of the same length. Thus, the task of matching the impedance of a center-fed antenna to a transmitter should be easier than for an end-fed antenna.

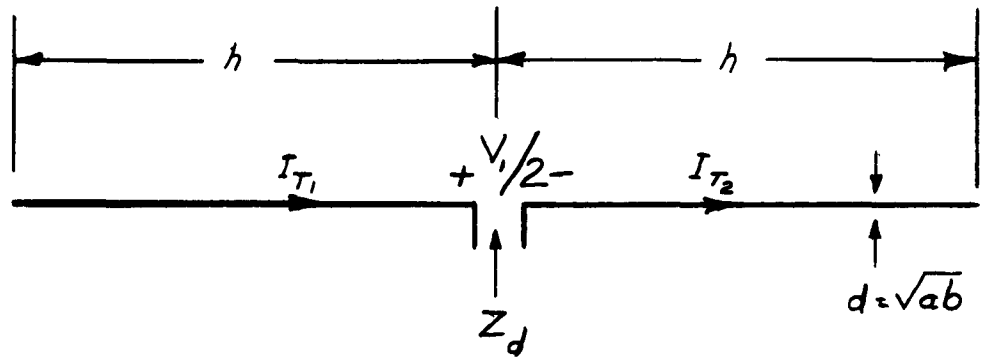
Theoretical studies by Harrison [2] and King and Harrison [3] show that the "radiation" currents  $I_{T1}$  and  $I_{T2}$  of the parallel-wire side-loaded transmission-line antenna

of Figure 1 have the same distribution as the current on the equivalent center-fed linear antenna. Thus, this parallel-wire side-loaded transmission-line antenna should have the same radiation properties as a center-fed linear antenna. King and Harrison [3] point out that such a structure may be of little practical value since it has no point of symmetry. In many situations it would be impossible to approximate the antenna input voltage,  $V_o$ , by coupling to a tank coil or by connecting a transmission line across the input terminals without altering the circuit appreciably. In the VLF trailing-wire application, however, a relatively short aircraft would be towing an antenna several thousand feet in length, and thus it becomes reasonable to approximate the aircraft and the transmitter by  $V_o$ , a point discontinuity in the scalar potential field. As a consequence of the similarity of the "radiation" current distribution in these two antennas the side-loaded transmission-line antenna should realize the electrical advantages of a center-fed antenna, while at the same time retaining the mechanical advantages of an end-fed antenna.

In this study, the results of King and Harrison [3] were extended in two directions: (1) the theoretical work was expanded to cover a general parallel-wire side-loaded transmission-line antenna with an arbitrary number of side loads located in an arbitrary manner along the line, and (2) numerical calculations were made on various side-load configurations, in order to select the most promising types for the trailing wire application.



(a) Single side-loaded transmission-line antenna

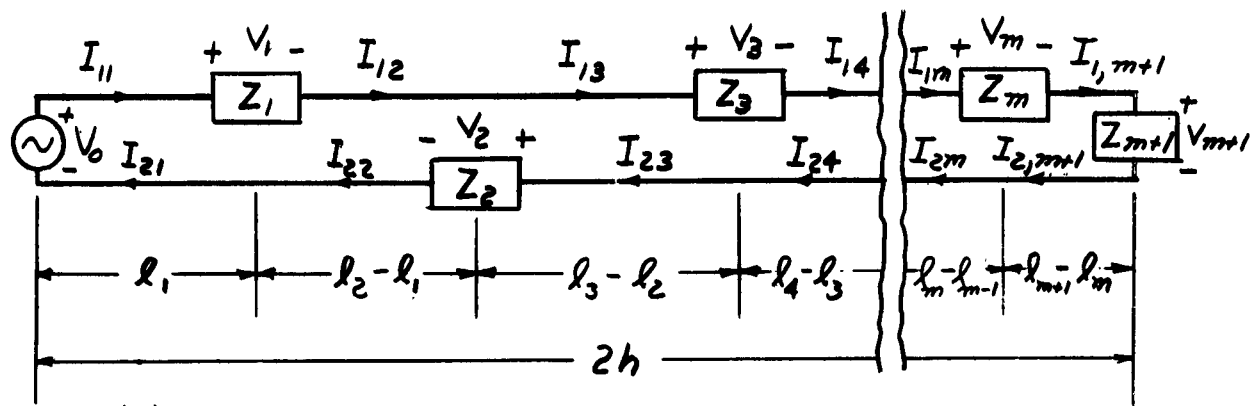


(b) The equivalent center-fed linear antenna

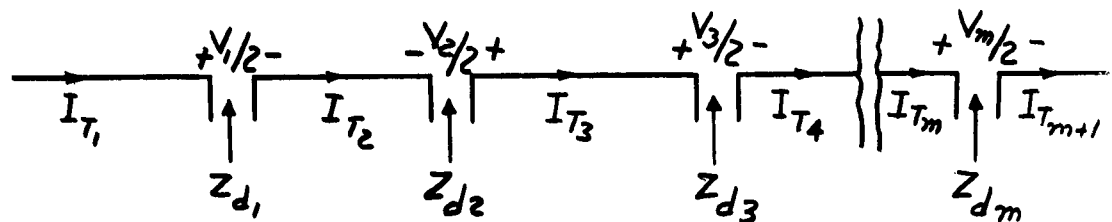
Figure 1.

The study of the general parallel-wire side-loaded transmission line revealed that its radiation properties can be described in terms of the radiation from a set of superimposed single-fed asymmetrical linear antennas [4]. This is illustrated in Figure 2. The theory shows that the "radiation" currents,  $I_{T1}$  and  $I_{T2}$ , as opposed to the transmission line currents,  $I_{11}$ ,  $I_{21}$ , and  $I_{12}$ , for the general side-loaded antenna have the same distribution as the current on the multiply-fed linear antenna. It can be shown that the current distribution on a multiply-fed linear antenna is equivalent to the superposition of the current distributions on a set of single-fed asymmetrical linear antennas. As a result of the linearity of the system, we can separate the multiply-fed antenna into an equivalent set of single-fed asymmetrical antennas. Thus, by using a general parallel-wire side-loaded transmission-line antenna, we should gain the same advantages that were described above for the single side-loaded transmission-line antenna.

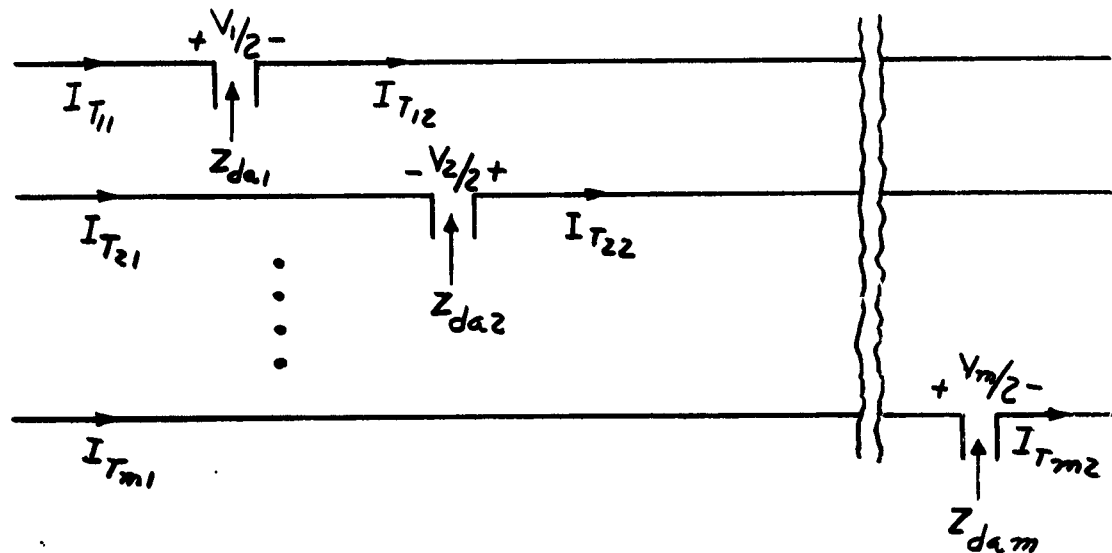
Another result of this study is the determination of an equivalent circuit of the general parallel-wire side-loaded transmission-line antenna. It was proven [4] that, for input impedance and efficiency calculations, the antenna shown in Figure 3a can be replaced by the equivalent circuit shown in Figure 3b. The equivalent circuit has basically the same configuration as the antenna. The main simplification is that the effects of radiation from the two-wire transmission line can be taken into account by lumped impedances in parallel



(a) General side-loaded transmission-line antenna



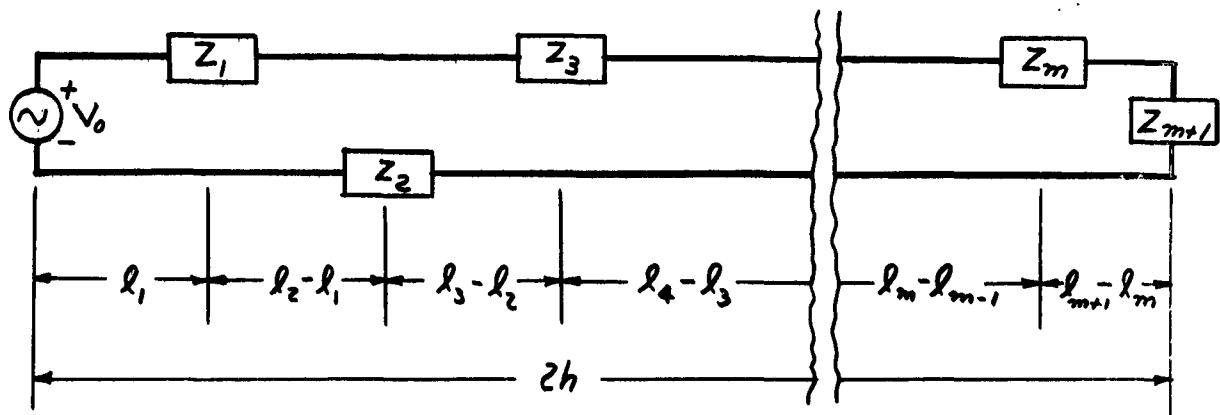
(b) Multiply-fed linear antenna



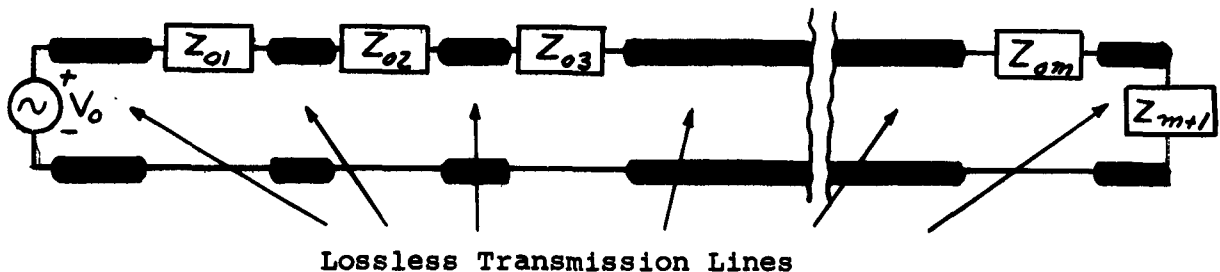
(c) Set of asymmetrically-driven linear antennas

$$I_{1n} - I_{2n} = I_{Tn} = \sum_{K=n}^{m+1} I_{T_{K1}} + \sum_{K=1}^{n-1} I_{T_{K2}} \quad n = 1, 2, \dots, m+1.$$

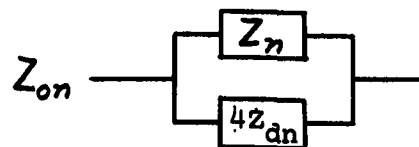
Figure 2



(a) General side-loaded transmission-line antenna



(b) Equivalent circuit



where  $Z_{dn}$  = input impedances of the equivalent multiply-fed linear antenna

where  $n = 1, 2, 3 \dots m$ .

Figure 3.

with the side loads, and the transmission line itself can be considered lossless. The impedances lumped in parallel with the side loads turn out to be  $4Z_{dn}$ , where  $Z_{dn}$  are the input impedances of the multiply-fed linear antenna of Figure 2 [4].

The next step in the study was to use the equivalent circuit to investigate in an approximate manner the whole family of parallel-wire side-loaded transmission lines to see which particular types appear most promising for the trailing wire antenna application. Numerical calculations were made for two configurations of the side loads. The first was the single side-loaded parallel-wire transmission-line antenna with an inductive end-load illustrated with its equivalent circuit in Figure 4. This antenna is the same antenna as that shown in Figure 1, except that the side-load does not necessarily have to be located at the center of the structure. By adjusting the value of the inductive impedance,  $Z_2$ , and the location of the inductive side-load,  $Z_1$ , the impedance,  $Z_A$ , which is the reflected impedance at point A-A' in the direction of  $Z_2$ , can be adjusted to have a large value at the frequency,  $f_1$ , shown in Figure 4c. Assuming that the antenna is electrically short ( $2\pi h/\lambda < 1$ ),  $Z_{da}$ , the input impedance of the equivalent asymmetrically-driven linear antenna, is capacitive. By varying the inductance of  $Z_1$ , the impedance  $Z_{o1}$  can be adjusted to have a large value at frequency  $f_2$ . Thus  $Z_B$ , which is the sum of  $Z_{o1}$  and  $Z_A$ , will have a large value at  $f_1$  and at  $f_2$  as illustrated in Figure 4c. The effect of the two-wire transmission line between the generator,  $V_o$ ,

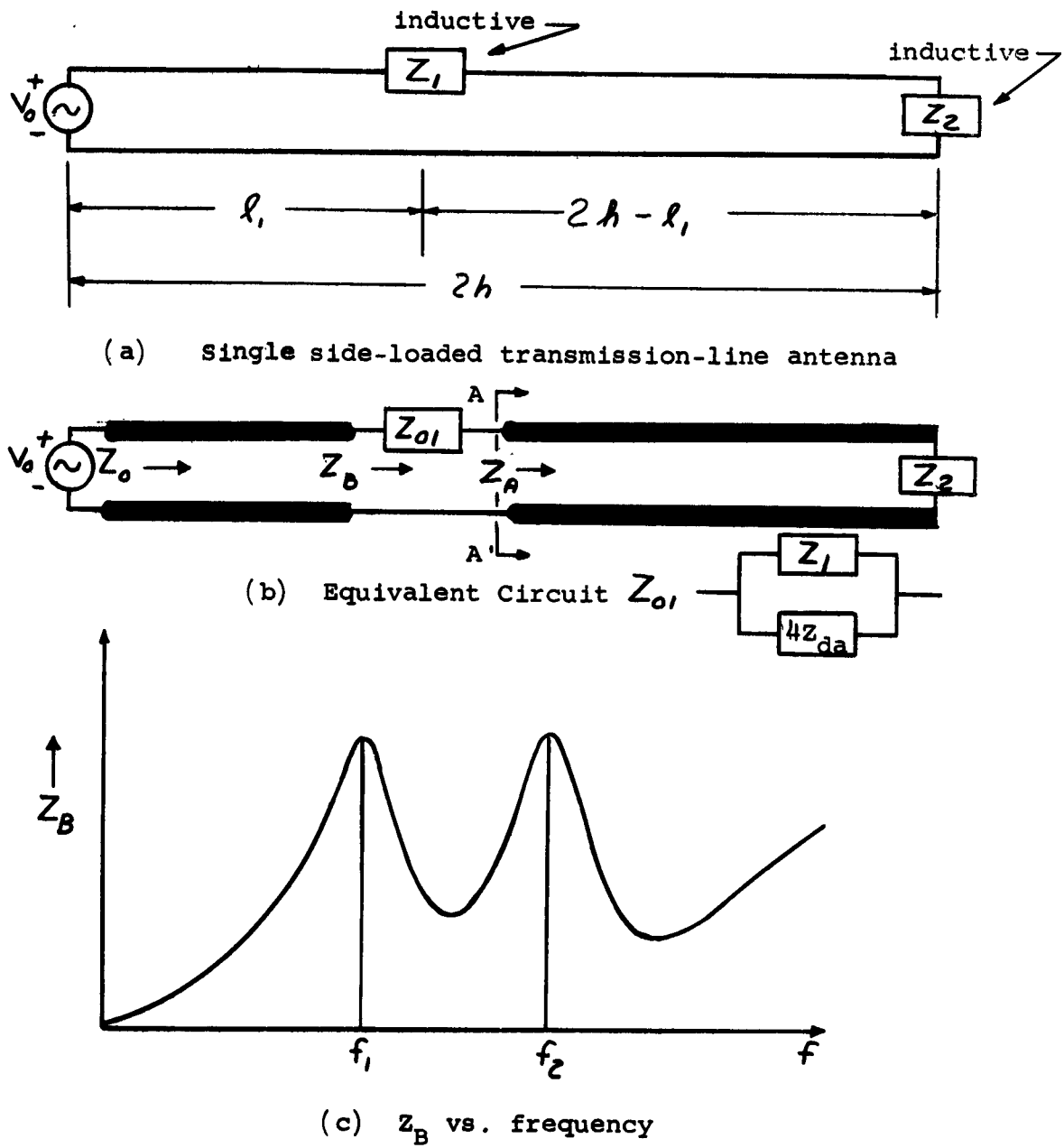


Figure 4.

and  $Z_1$  is simply to shift the frequencies where  $Z_B$  becomes large so that the resulting input resistance and reactance curves have the form shown in the graph of Figure 5.

It may be noted that in the region of  $f_3$  the input reactance,  $X_o$ , of the antenna is nearly zero, and its variation with frequency in that region is relatively small. In the same region,  $R_o$ , the input resistance of the antenna, is larger than  $R_{da}$ , the input resistance of the equivalent asymmetrically-driven linear antenna, and its variation with frequency is also relatively small. Thus, an operating point exists at which the antenna input impedance has little or no reactance to be balanced out. If the input resistance can be made sufficiently large, impedance-matching to a transmitter could be further simplified. Figure 6 shows curves of input resistance and reactance plotted against frequency for an antenna of the type just described. The length of the antenna is 2000 feet, the radius of the conductors is 1 inch, and the conductor spacing is 28 inches. The side load is an 0.840 millihenry inductance (with  $Q = 100$  at 78 kc) located at the center of the structure. Observing the curves of Figure 6, we see that at 65 kc the input resistance varies relatively slowly as a function of frequency and has the value of 15 ohms, in comparison to 15 ohms for  $R_d$ , the input resistance of the equivalent center-fed linear antenna. At the same frequency the input reactance also varies slowly as a function of frequency and has a value of -300 ohms. Thus, from an impedance matching standpoint, this frequency would be a good operating point.

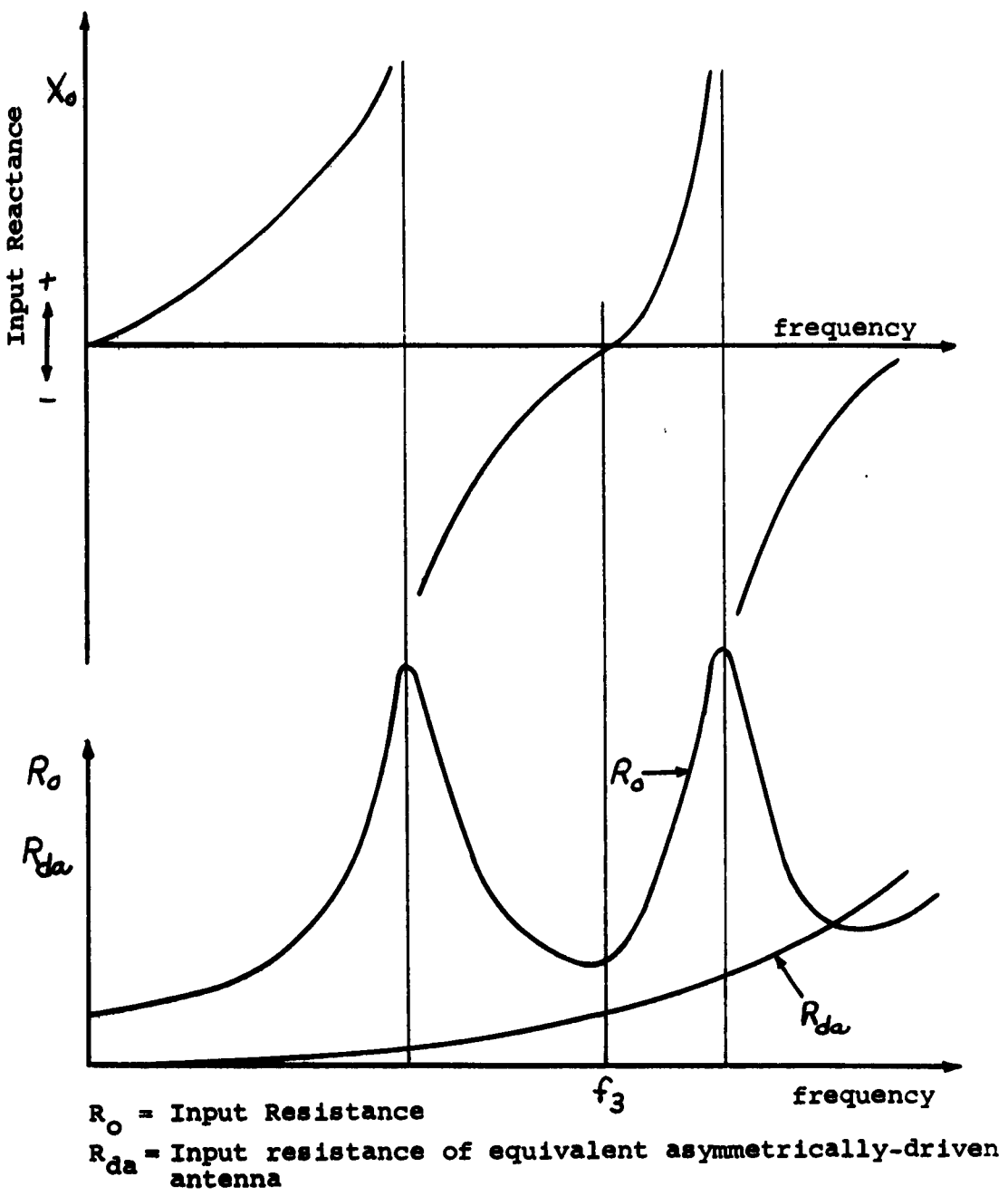


Figure 5. General characteristics of the input impedance for a single side-loaded transmission-line antenna

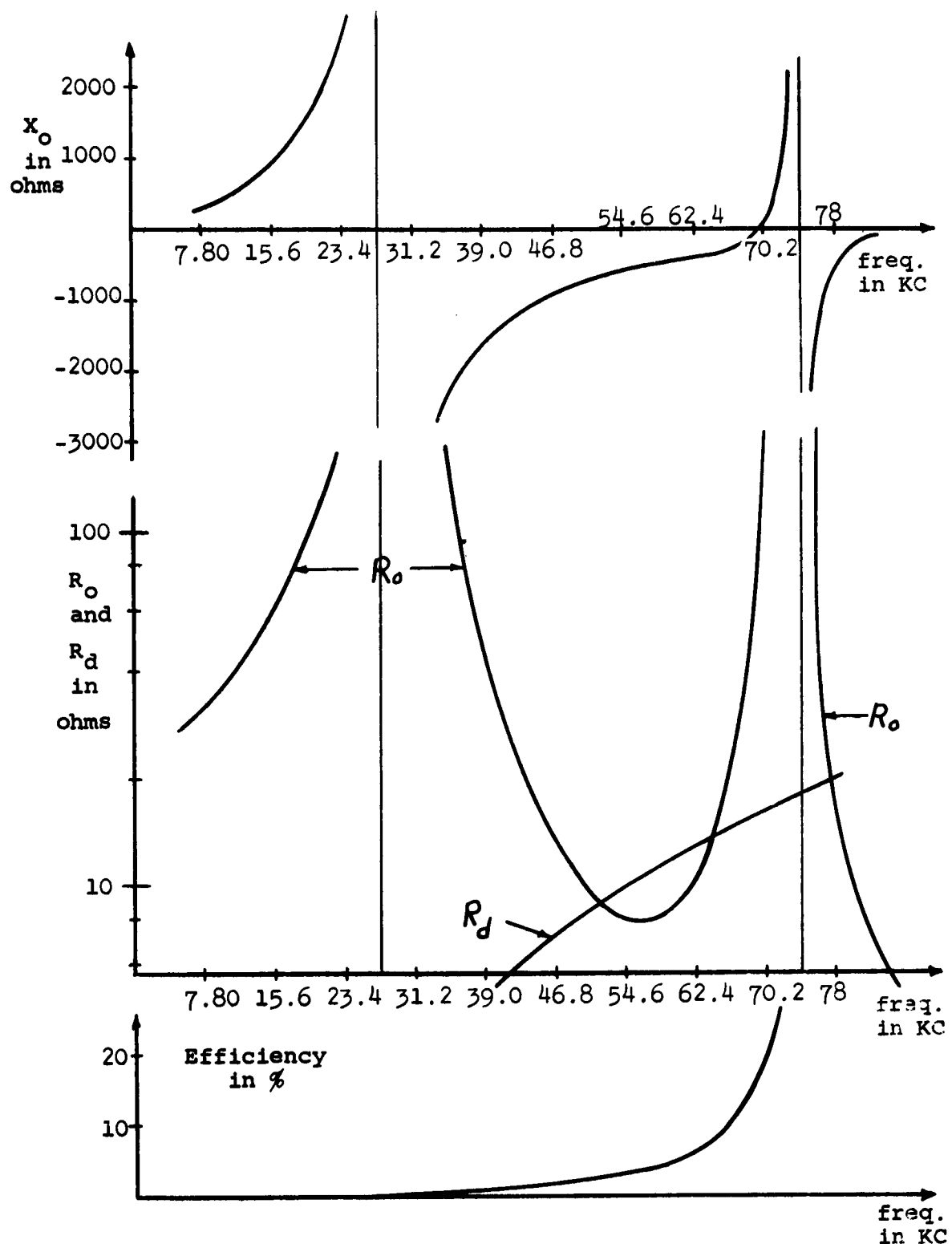


Figure 6. Theoretical input impedance and efficiency for a single side-loaded transmission-line antenna

Another factor to be considered is the power lost in the antenna due to the finite conductivity of the wires and the finite Q of the side and end loads. The theoretical expressions for the antenna input impedance and current distribution were derived under the assumption that the conductivity of the wires is infinite. If it is desired, these expressions can be modified in an approximate manner to include the finite conductivity of the wires [4]. The efficiency of an antenna is normally defined to be the ratio of the radiated power to the total power input to the antenna. In order to simplify the efficiency calculations, it is assumed that the power losses in the wires can be neglected in comparison with the radiated power and the losses in the side and end loads. The theoretical antenna efficiency shown in Figure 6 is the ratio of the radiated power to the sum of the radiated power plus the power lost in the side and end loads, which are assumed to have a  $Q = 100$  at 78 kc. At the chosen operating frequency, 65 kc, this efficiency is 8%. The "overall" antenna efficiency, which must also include any network required to match the antenna impedance to the transmitter output impedance, will be less than 8% due to losses in the matching network.

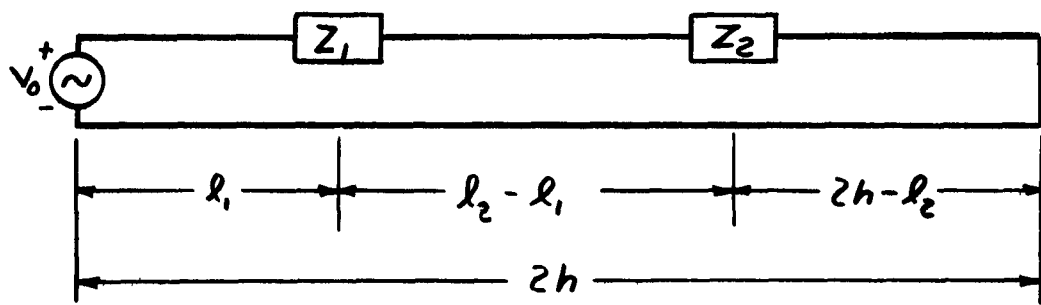
The antenna in this example could also be operated at 70.2 kc, where the input reactance is zero and the efficiency is about 20%. For this case, the input resistance is larger (although not as stable with respect to frequency), and any

required matching network should be simpler and more efficient than the network required to match the same transmitter to other VLF antennas, which may have a large reactive part in the input impedance.

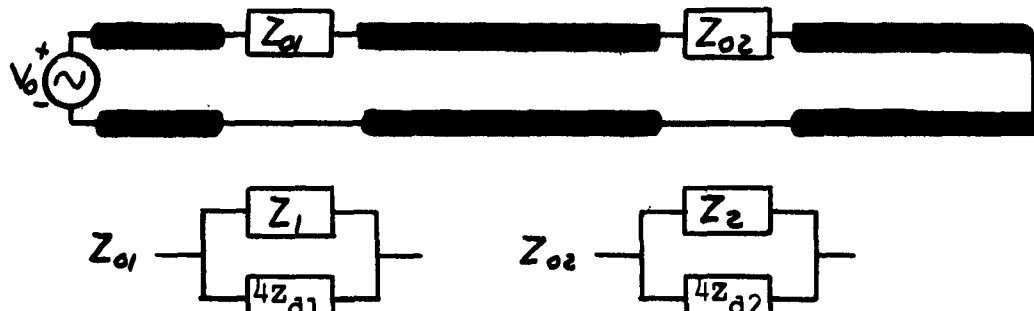
From the above modified definition of antenna efficiency, it might appear that a higher antenna efficiency could be obtained with no side loads. This is not the case, since it can be shown that with no side loads, a parallel-wire transmission line with spacing small compared to a wavelength does not radiate appreciably because of the cancellation of equal and opposite currents in the wires. The side loads create an unbalance in the currents, which results in radiation from the structure. The losses in the wires are still present even if there are no side loads.

The second configuration chosen for numerical investigation is the double side-loaded parallel-wire transmission line shown in Figure 7. In this case the far end is short circuited. A qualitative description of the variation of the input impedance with respect to frequency is not as straightforward as for the first case considered. This is basically because the two side loads operate as a coupled system. The theoretical expressions, however, predict that the input impedance becomes large at two frequencies which can be adjusted by adjusting the size and location of the side loads.

Figure 8 shows the curves of input resistance, input reactance, and antenna efficiency calculated for an antenna



Double Side-Loaded Transmission-Line Antenna



Equivalent Circuit

**Figure 7.** Double side-loaded transmission-line antenna and the equivalent circuit

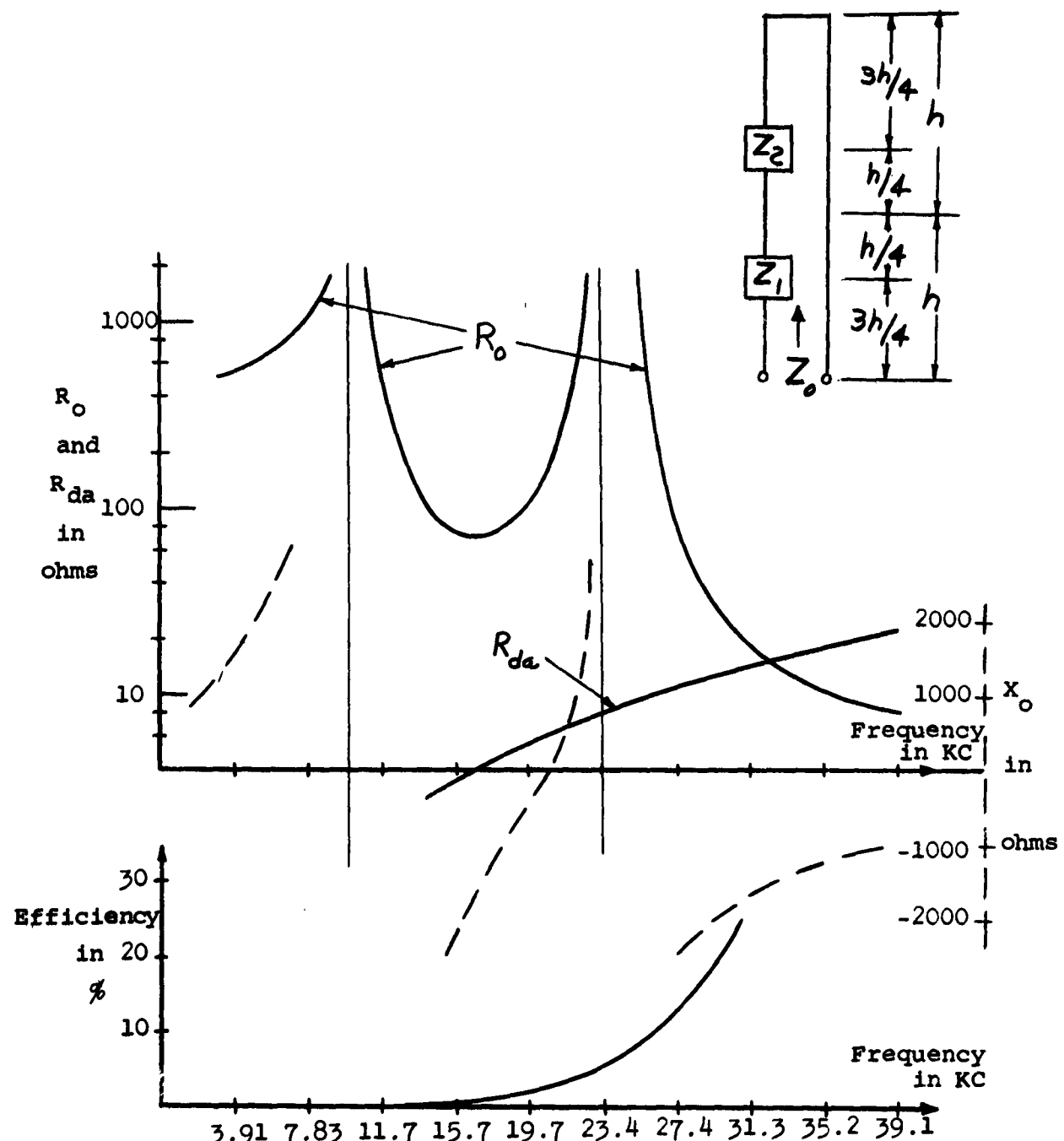


Figure 8. Theoretical input impedance and efficiency for a double side-loaded transmission-line antenna

of this type. The length of the antenna is 8000 feet, the conductors have a radius of 1/8 inch, the conductor separation is 3.5 inches, and the side loads are inductances of 6.1 millihenrys (with  $Q = 100$  at 18 kc). The location of these side loads is illustrated in the figure. Again we find a desirable operating point where the input resistance is 100 ohms, the input reactance is essentially zero, and the antenna efficiency, neglecting the power loss in the wires, is 2%. Even with high quality inductive side loads ( $Q = 100$  at 18 kc), at this operating frequency, the efficiency is low because of the small unbalance of the transmission-line currents. It should be noted that, while large currents may be flowing in the transmission-line antenna, it is only the net unbalanced current which produces the radiation; hence we can have a power loss in the high-Q side loads and no appreciable radiation (and hence low efficiency) if the current unbalance is small.

Experimental verification of the theory for a parallel-wire double side-loaded transmission-line antenna is presented in Figure 9. The experimental model is scaled down from the antenna of Figure 8. We note from Figure 9 that we have a desirable operating point in the region of 124 mc. The high frequency is the result of frequency scaling. This scaling is done in inverse proportion to the dimensional scaling in order to retain the electrical properties of the actual VLF antenna.

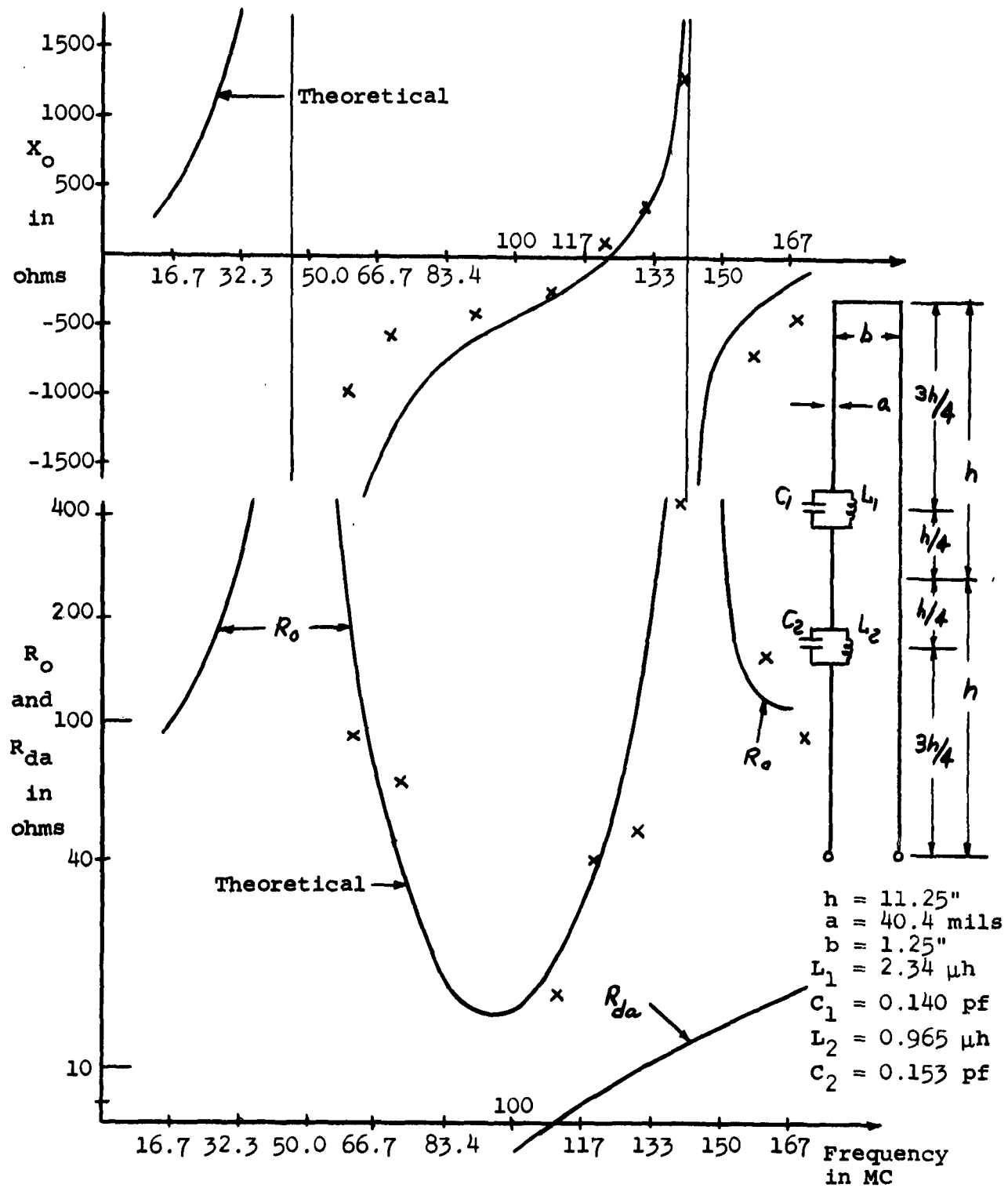


Figure 9. Comparison of theory and experiment for a double side-loaded transmission-line antenna

It should be mentioned at this point that there are many factors to consider in choosing an optimum operating point. For example, in Figure 8 the frequency for which  $X_o = 0$  is in a region in which the behavior of  $R_o$  is not the best from the stability point of view. Moreover, considerably better antenna efficiencies could be obtained at higher frequencies, at the expense of larger input reactance. In any practical design, all of the design parameters cannot be simultaneously optimized, and compromises must be made.

The parallel-wire transmission-line antennas for which theoretical characteristics are shown in Figures 6 and 8 are not suggested as designs for a practical VLF trailing-wire antenna. The physical size of an antenna with 2-inch diameter conductors and 28-inch spacing prohibits its use in the VLF trailing-wire application. An antenna with 1/4-inch diameter conductors and 3.5-inch spacing is somewhat more feasible; however, problems of maintaining the required spacing of the conductors and preventing the twisting of this antenna in flight are anticipated. The dimensions for these antennas were chosen in order to facilitate the computer calculations of the antenna characteristics.

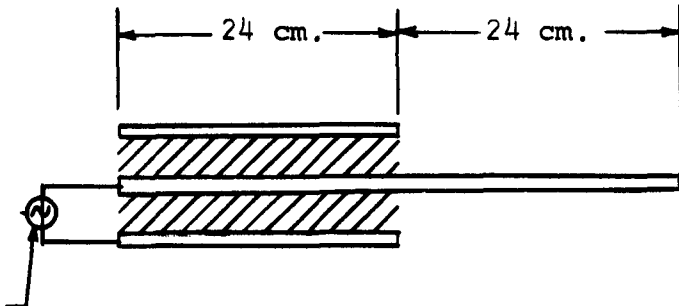
The theory developed for this class of antennas shows that the input impedance is relatively insensitive to the  $(l/a)$  and  $(l/b)$  ratios (here,  $l$  = antenna length,  $a$  = conductor radius, and  $b$  = conductor spacing), provided that these ratios are very large. Another theoretical result is

that the overall impedance level is directly proportional to  $\ln(b/a)$  [4]. Consequently, the input impedance characteristics shown in Figures 6 and 8 should be realizable in an antenna with smaller conductors and spacing, provided that the original  $(b/a)$  ratio is maintained. From theoretical considerations alone, it should be possible to design a parallel-wire transmission-line antenna with input impedance characteristics similar to those of Figures 6 and 8 in the form of a parallel-wire line embedded in a dielectric, with the outside dimension of the dielectric being of the order of 1/2 inch or less. In practice, however, the conductor diameter would necessarily be small to maintain the required  $(b/a)$  ratio, thereby increasing the  $I^2R$  power losses in the wires for a given antenna current. For the case of driving this antenna from a 10 kw transmitter, the antenna current may be of the order of 30 amperes or more. Such a current flowing in small conductors would lower the antenna efficiency. The  $I^2R$  power loss problem is decreased with lower transmitter power; however, the communication range is also decreased.

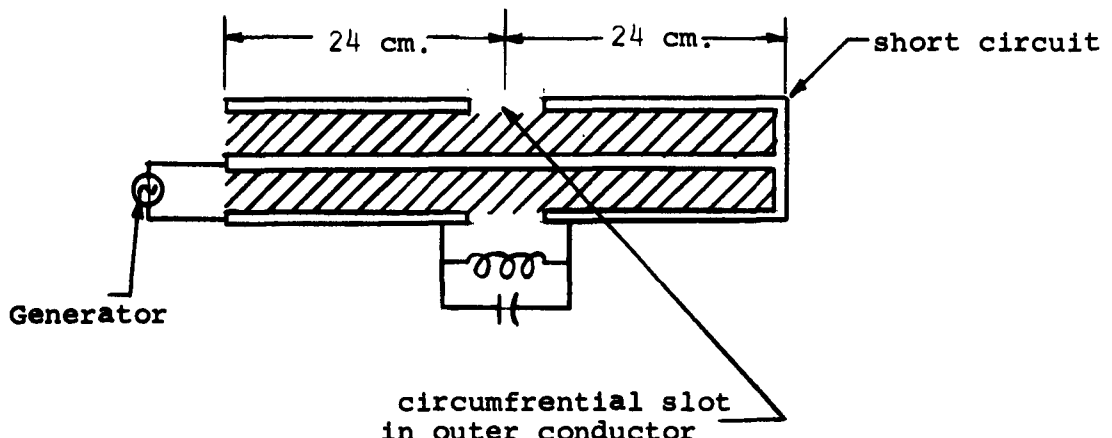
As a possible solution to the problem of size and aerodynamic instability which may be associated with the parallel-wire side-loaded transmission-line antenna, a coaxial side-loaded transmission-line antenna is being investigated. As a means of determining the feasibility of such an antenna, relative field intensity measurements were made for a coaxial side-loaded antenna and a coaxial sleeve antenna

shown in Figure 10. The relative field intensity with equal and constant power input to both antennas is shown in Figure 11. The field radiated from a length of shorted coaxial cable is also shown to indicate that no appreciable antenna mode exists for the coaxial configuration with no side load or slot. Much of the erratic nature of the relative field intensity data can be attributed to the fact that the measurements were made in a room with the shortest dimension equal to only a few wavelengths. The high frequencies are a result of frequency scaling. From Figure 11 it can be seen that over an appreciable frequency range, the coaxial side-loaded antenna radiates nearly as well as the sleeve antenna of the same length. Since a theory for the general case of the coaxial side-loaded antenna was not available at the time of the experiment, no attempt could be made to predict the behavior of the relative field intensity for the side-loaded antenna.

An approximate analysis of a coaxial single side-loaded transmission-line antenna was made in a manner similar to that made for the parallel-wire antenna. With the assumption that the outer conductor diameter,  $d_o$ , is much larger than the inner conductor diameter,  $d_i$ , it was found that the expression for the input impedance has the same form as for the parallel-wire case. The overall input impedance level for the coaxial case is directly proportional to  $\ln(\frac{d_o}{d_i})$  for  $d_o \gg d_i$ . The realization of a practical coaxial trailing wire antenna with  $d_o \gg d_i$  and small  $d_o$  would be difficult



**Generator Sleeve Antenna - RG58U (Not to Scale)**



**Side-loaded Antenna - RG58U (Not to Scale)**

**Figure 10**

**Experimental Models of a Coaxial Single Side Loaded Antenna and a Coaxial Sleeve Antenna**

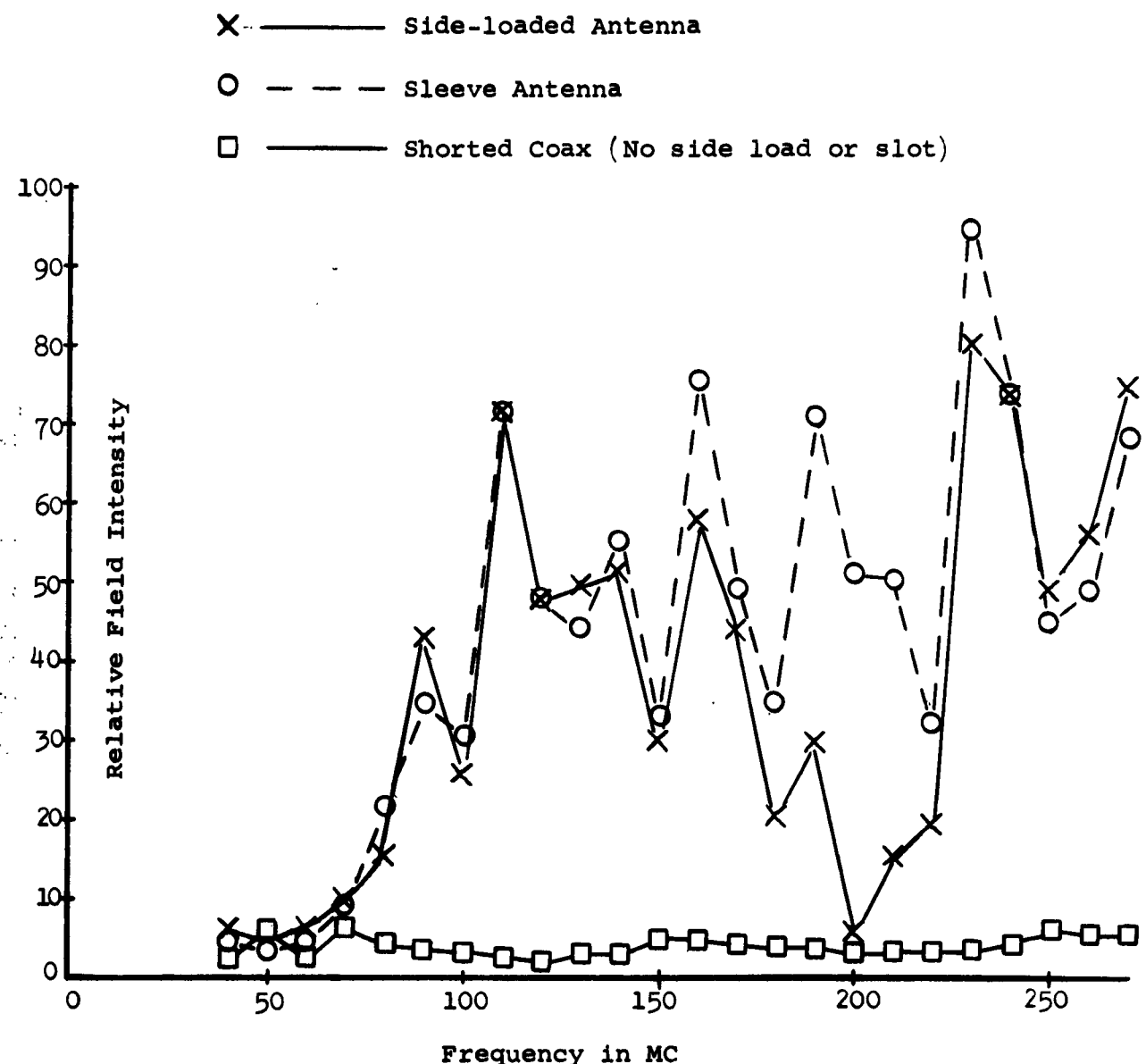


Figure 11

Relative Field Intensity for Coaxial Single Side-Loaded Antenna and Coaxial Sleeve Antenna

for 10 kw input to the antenna because of  $I^2R$  losses due to the large current flowing in the small inner conductor. An analysis of the coaxial side-loaded transmission-line antenna in the general case (i.e.,  $d_o$  is not necessarily much less than  $d_i$ ) will require a more general method since the method of Kulterman [4] becomes too approximate in the general case.

The various mechanical restrictions (weight, space, tensile strength, stability in flight, etc.) associated with the construction and deployment in flight of either the parallel-wire or the coaxial form of the side-loaded transmission-line antenna will impose limitations on the range of electrical properties which are theoretically possible. Admittedly, the mechanical problems associated with a side-loaded transmission-line trailing wire antenna will be greater than those for a single bare trailing wire antenna of the same length; however, desirable electrical properties are theoretically obtainable with the side-loaded antenna (at least for the parallel-wire case) for relatively short lengths.

## REFERENCES

1. King, R. W. P., "The Theory of Linear Antennas,"  
Harvard University Press, 1956, p. 192, p. 404.
2. Harrison, C. W., Jr., "Hybrid Transmission Lines,"  
Sandia Corp., Albuquerque, N. M., Technical  
Memorandum 157-58(14); May, 1958.
3. Harrison, C. W., and R. W. P. King, "Folded Dipoles  
and Loops," I. R. E. Transactions on Antennas  
and Propagation, March, 1961.
4. Kulterman, Robert W., "Linear Side-Loaded Transmission-  
Line Antennas," Technical Report EE-78, Engineering  
Experiment Station, University of New Mexico,  
Albuquerque, New Mexico, August, 1962.

## EXPERIMENTAL INVESTIGATIONS

During the past year the experimental program on the project has changed. Several experiments were completed; others were started. There were six areas in which experimental investigations played an important role. These are:

1. Subterranean Communication Experiment (completed).
2. ELF Noise Measurements (closed).
3. Two-Layer, Sea-Air Model (completed).
4. Coaxial and Toroidal Antenna Impedance Measurements (active).
5. Side-Loaded Transmission-Line Antenna (active).
6. Three-Layer Model (active).

Several of the new areas of investigation involve the effects of the ionosphere, including its anisotropic nature; however, at the present time, there has been no attempt to include the anisotropy of the ionosphere in any of the modeling experiments. The theoretical analyses of the ionospheric reflections indicate that it may be possible to model the effects of the ionosphere for such radiators as the trailing-wire antenna by proper phasing of the signals on a two-section antenna. There are problems confronting the construction of the basic three-layer model which must be solved before determining if this anisotropic modeling is feasible.

Some of the experiments have met with great success, while others have presented formidable problems which are

only partially solved. In order to facilitate a discussion of all of the experiments, each is individually discussed in the following topics.

1. Subterranean Communication Experiment. This task, now considered completed, sought to determine the feasibility of communicating from a shore station to a submerged submarine utilizing the earth's crust as the propagating medium (see Report EE-83). One full-scale field experiment was performed in two mine shafts located in the Manzano Mountains, which provided a measurement of the earth's effective conductivity. Based upon these measurements and subsequent calculations, it became apparent that a system utilizing the earth's crust as the path of propagation would not provide satisfactory ranges of communication.

The theoretical model employed in the analysis mentioned above consisted of a low-conductivity layer situated between two other layers of higher conductivity (Figure 1). Specific dimensions and conductivities were assumed for the various layers for the purpose of the analysis. The low-conductivity layer was assumed to be 20 kilometers thick and to possess a conductivity of  $4 \times 10^{-6}$  mhos per meter. The conductivity of the upper or sedimentary layer was assumed to be  $10^{-2}$  mhos per meter and its thickness was considered to be about 1 kilometer. The lower layer extending toward the center of the earth was considered to have the same conductivity as the upper layer; i.e.,  $10^{-2}$  mhos per meter, and to

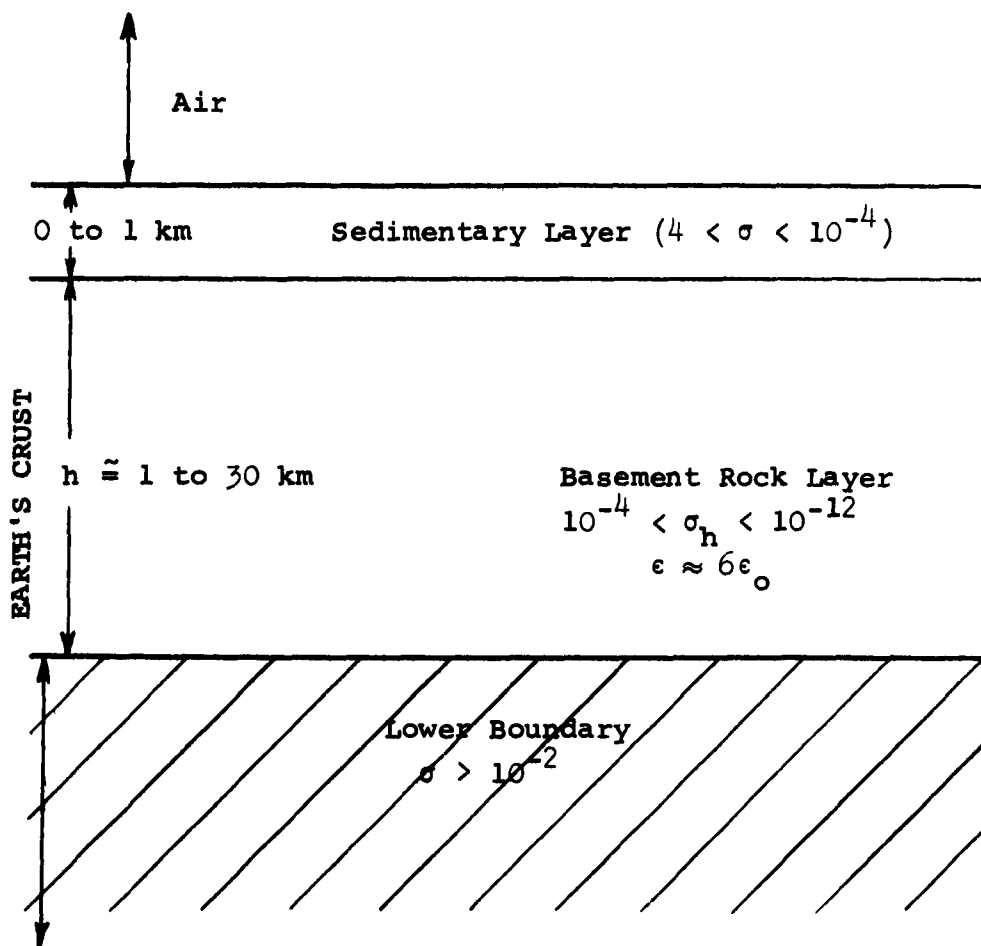


Figure 1.

Model used in determining propagation of Electromagnetic Waves in Earth's Crust.

be of sufficient thickness so that it could be considered infinite in extent. Assuming the electromagnetic wave to be propagated in the low-conductivity (center) layer, the distance required for the wave to be attenuated by 100 db was calculated for various frequencies and for various modes of propagation ( $TM_{oo}$ ,  $TE_{ol}$ , and  $TM_{ol}$ ). The results of these calculations are presented in Table I and Table II.

The quantities presented in Table I consider the mode of propagation to be  $TM_{oo}$  which provides the least attenuation of the possible modes.  $TE_{ol}$  and  $TM_{ol}$  modes were computed; however, as evident from Table II they experience greater attenuation than the  $TM_{oo}$ . Another advantage of the  $TM_{oo}$  mode is that the attenuation does not vary appreciably with  $h$ , the thickness of the low-conductivity center layer, whereas the other modes are highly dependent upon  $h$ .

Table I -  $TM_{oo}$  Mode

<u>freq.</u>	<u>DB<sub><math>\lambda_1</math></sub></u>	<u><math>\lambda_1</math> (KM)</u>	<u>S 100 db distance (KM)</u>
100	55	158	290
500	50.3	68.2	135
1000	49.4	47.0	95.4
1500	48.3	38.5	80
3000	42.5	25.6	60

Table II -  $TE_{01}$  and  $TM_{01}$  Modes

freq.	$DB_{\lambda_1}$	$\lambda_1$ (KM)	100 db distance (KM)
100	860	636	73.6
500	181	129	71.0
1000	103	68.4	66.3
1500	80.3	49.5	61.5
3000	55	28.9	52.6

These calculations indicate that useable signals can be received at considerable distances (e.g., at 100 cps a signal will travel 290 km before it is attenuated 100 db). The distance through the basement strata for which transmission appears feasible, while appreciable, is an order of magnitude less than desired for long range communication; and this does not take into account the additional losses which would be encountered in penetrating the upper layer to reach the submarine receiver. Because of these disadvantages this method is considered impractical for long range communications.

The scheme employed to measure the effective earth conductivity is new and useful, and deserves some consideration. A pulsed transmitter was employed to obtain high peak dipole moments. A receiver employing a loop antenna, an oscilloscope, and a photographic recording camera was used. The transmsitting and receiving units are illustrated in block-diagram form in Figure 2. By measuring the vertical and horizontal components of the received signal near the earth's surface, a ratio of the

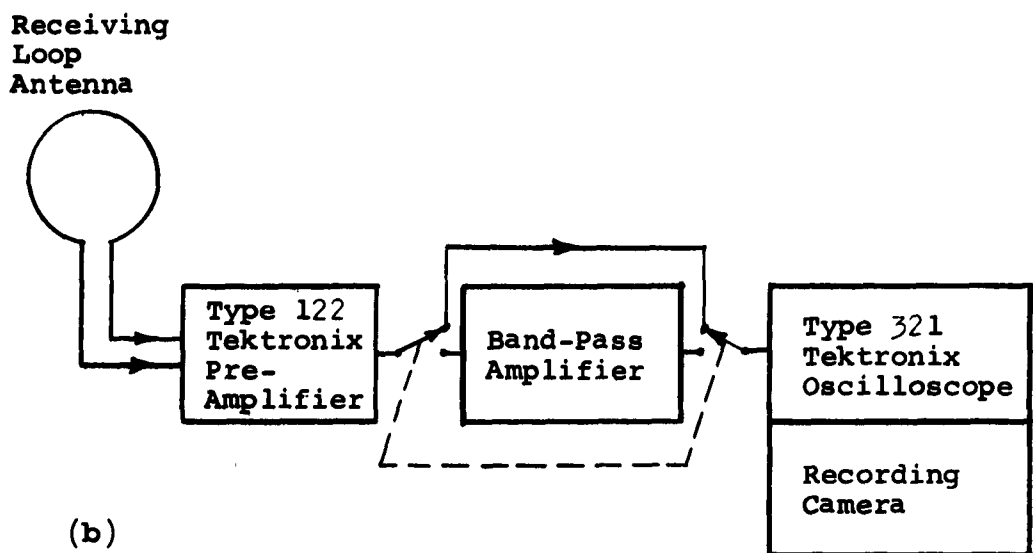
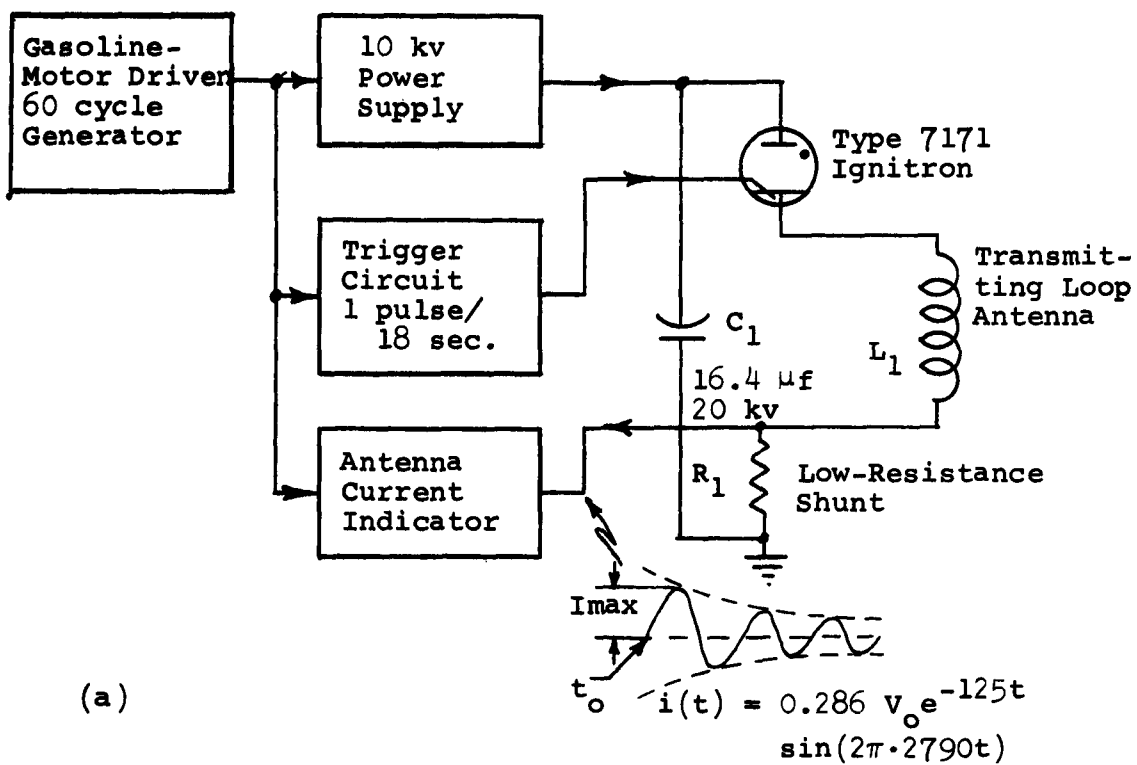


Figure 2. (a) Block Diagram of 3 kc Pulsed Transmitter.  
 (b) Block Diagram of 3 kc Pulse Receiver.

two can be formed which allows one to determine the effective conductivity of the earth's crust in the vicinity of operation. By using this ratio, it is not necessary to know the magnitude of the transmitted signal since this term drops out of the calculations. This new technique may prove to be valuable in measuring the earth's conductivity for use in other problems. A complete description of the system and the theory upon which it is based is presented in the final report on the subterranean experiment (EE-83).

2. ELF Noise Measurements. This experimental investigation, now inactive, was to consist of two phases. The initial phase was primarily concerned with the development of instrumentation and data-reduction equipment for use in obtaining ELF electromagnetic noise measurements. Also in this phase some field measurements were to be made and the data reduced in order to evaluate the overall system. The second phase of the investigation was to have concerned the improvement of the instrumentation and data-reduction systems and the continuation of the field measurements and their evaluation on a regularly scheduled basis. The first phase of the experiment was completed and two reports (EE-69 and EE-70) were prepared which describe the results of this initial investigation. Continued work on the second phase of this experiment would require considerably more sophisticated equipment, additional personnel, etc. Since other agencies which are better equipped to pursue this work are

concerned with this problem, the task has been set aside and it will not be resumed unless there is a desire for its continuation. A summary of the initial phase of this experiment is presented below.

Phase I of this task consisted of the design and construction of electronic instrumentation for the purpose of obtaining electric field strength measurements in the 5 to 50 cps spectrum. The completed system (Figure 3) was placed in the field and recordings were made over extended periods during both the daylight and night-time hours. The results of the experiment, as evaluated with the data-reduction system illustrated in Figure 4, indicated the presence of the various mode frequencies in the 5 - 30 cps region as predicted by Schumann and Wait<sup>1</sup>, although none were extremely pronounced. A mode frequency of about 15.5 cps was identified; however, the other modes that should correspond to the ionospheric situation resulting in the 15.5 cps mode frequency (8.47, 22.57, and 29.7 cps), were present but not as discernible as was the 15.5 cps signal. The field intensity at 15.5 cps was less than at the other mode frequencies. A typical plot of the data is shown in Figure 5. A better data-reduction system (a larger number of narrow-band filters) might have been

---

<sup>1</sup>Wait, J. R., "Terrestrial Propagation of Very-Low-Frequency Radio Waves," Journal of Research, NBS, Vol. 64D, No. 2, March-April, 1960, and

Schumann, W. O., "Über die Dämpfung der elektromagnetischen Eigenschwingungen des Systems Erde-Luft-Ionosphäre," Z. Naturforsch 7A, 250, (1952).

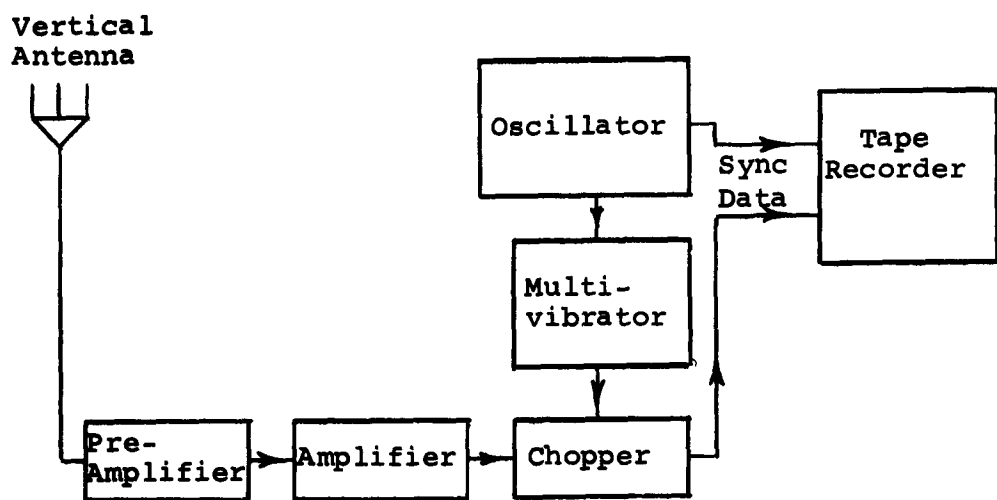


Figure 3. Block Diagram of ELF Noise Receiver.

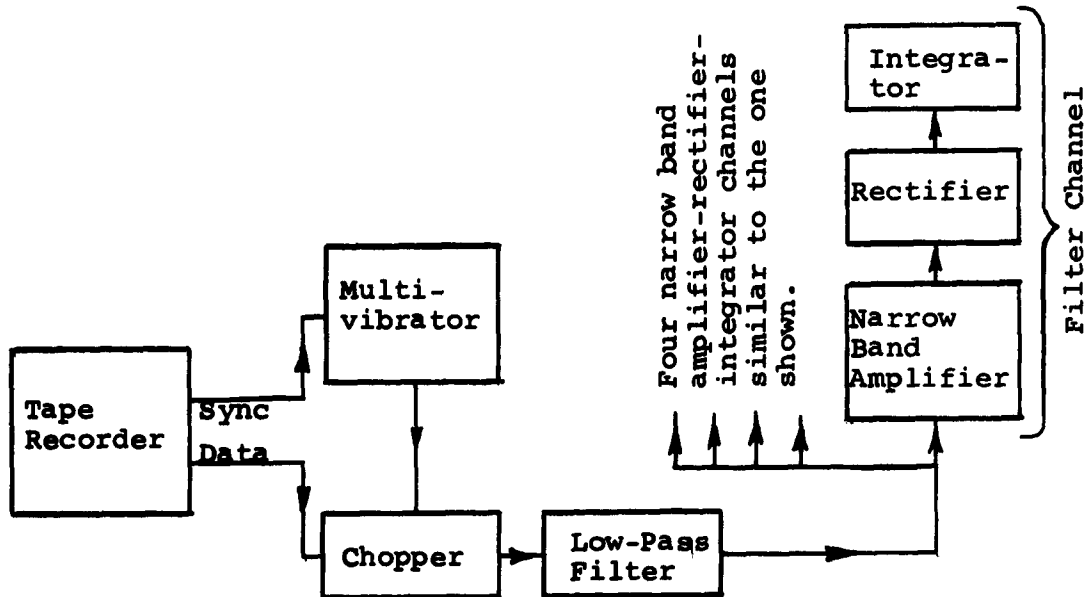


Figure 4. Block Diagram of the ELF Noise Data Reduction System.

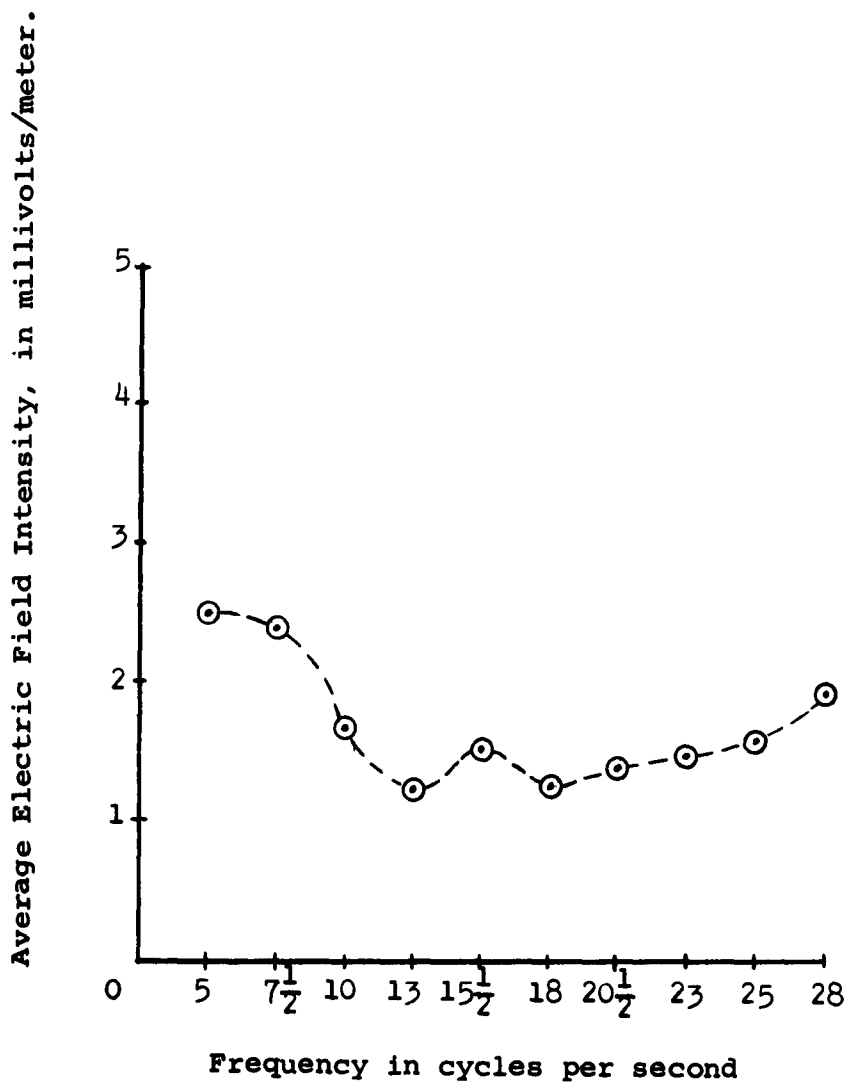


Figure 5. Average value of observed field strength during 1000-1100 (MST) for period 31 July to 8 September, 1961.

able to give better resolution of the data. The equipment used in performing the experiment is being stored in case this task is to be re-activated.

3. Two-Layer Model (Sea-Atmosphere). The two-layer model described in Report EE-59, "A Modeling Technique for Experimental Verification of Dipole Radiation in a Conducting Half-Space," is a successful model for use in evaluating the field magnitude and field patterns of various submerged antenna configurations.\* It, of course, provides a means for making impedance measurements on the various submerged antenna configurations; however, a large salt water tank is available and is normally used for making these measurements. The model, consisting of a wading pool (12 ft., diameter x 3 feet, depth) filled with salt water, was equipped with a set of frames constructed from dielectric or insulating material which served as supports for positioning the transmitting and receiving antennas at various locations and depths throughout the pool. The use of this configuration allowed frequencies in the order of 50 mc/s to 250 mc/s to be employed in the model to represent actual frequencies of 5 kc/s to 25 kc/s and model antennas of 10 cm to 20 cm length to represent actual antenna lengths of 20 meters to 40 meters. The model, which was operated atop a dormitory to eliminate reflection problems, was dismantled after it had been used to make

\* A paper covering this investigation, entitled "Experimental Verification of Dipole Radiation in a Conducting Half Space," by W. E. Blair, will be published soon in PGAP Transactions.

all the desired measurements. The model is readily available should other problems require its use. The emphasis now has been shifted to the problem of perfecting a model which will provide some properties of the ionosphere (see Three-Layer Model).

#### 4. Coaxial and Toroidal Antenna Impedance Measurements.

The experimental and theoretical work on the coaxial and the toroidal antennas is still active. After a summary of the work was prepared covering these experimental measurements and the corresponding theoretical analyses, it was apparent that some of the assumptions which were made in the analysis of the toroidal antenna were not demonstrated to be valid. Before the work is continued these assumptions are being checked out experimentally. A description of the two antennas is presented below.

The coaxial antenna consists of a length of submerged coaxial cable whose jacket, sheath, and dielectric has been removed, allowing each part to be exposed to the water as illustrated in Figure 6. The center conductor is allowed to extend beyond the end of the dielectric at least  $\frac{\lambda_w}{8}$ , where  $\lambda_w$  is the wavelength in sea water. The original analysis by Moore<sup>2</sup> used assumptions that were equivalent to placing parallel metallic plates perpendicular to the cable at both ends of the antenna, with the plates making contact to the center conductor

---

<sup>2</sup> Moore, Richard K., "The Theory of Radio Communications Between Submerged Submarines," Sc. D. Thesis at Cornell University, 1951.

and the sheath, respectively. In an experiment which employed the plates, the theoretical and experimental results seemed in apparent agreement although the experimental data was not consistent. A new set of measurements is being made to see if the impedance of the actual antenna configuration can be predicted by using a reflection coefficient for the length of bare center conductor that contacts the sea water. If this can be done, it will be superior to the present approximate solution.

The toroidal antenna, initially described by Anderson, consists of a multi-turn winding on a magnetic toroid which girds the center of an elongated conductor. Essentially the antenna appears as a submerged transformer with one single-turn winding and another multi-turn winding (Figure 7). Anderson<sup>3</sup> analyzed the toroidal antenna as a receiving antenna and demonstrated that it possessed some very desirable characteristics. The analysis as a receiving antenna is based upon an analogous solution of an electrostatic problem by Stratton<sup>4</sup>. The results show that the presence of the elongated conductor placed through the center of the toroid improves the receiving characteristics by as much as 34 db, depending upon the length of the elongated conductor. These representative numbers are based upon the open circuit voltage of the multi-turn winding and do not involve the internal impedance of the antenna.

<sup>3</sup>Anderson, Wallace L., "Submerged Antennas," Technical Memorandum #2, Engineering Experiment Station, University of New Mexico, June 12, 1961.

<sup>4</sup>Stratton, Julius Adams, Electromagnetic Theory, p. 214, McGraw-Hill, New York, 1941.

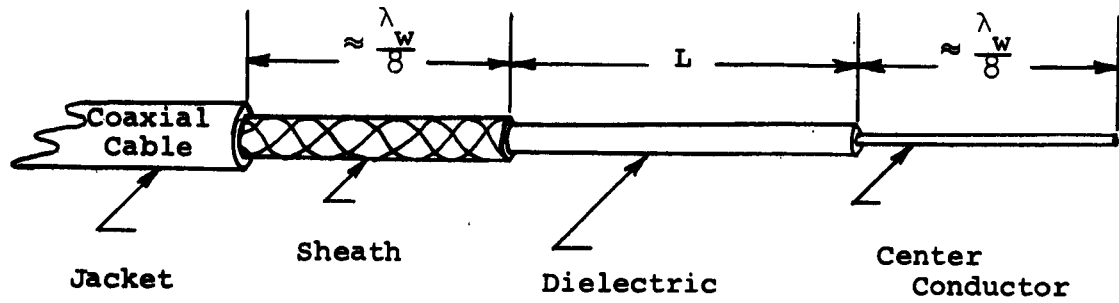


Figure 6. Coaxial Antenna.

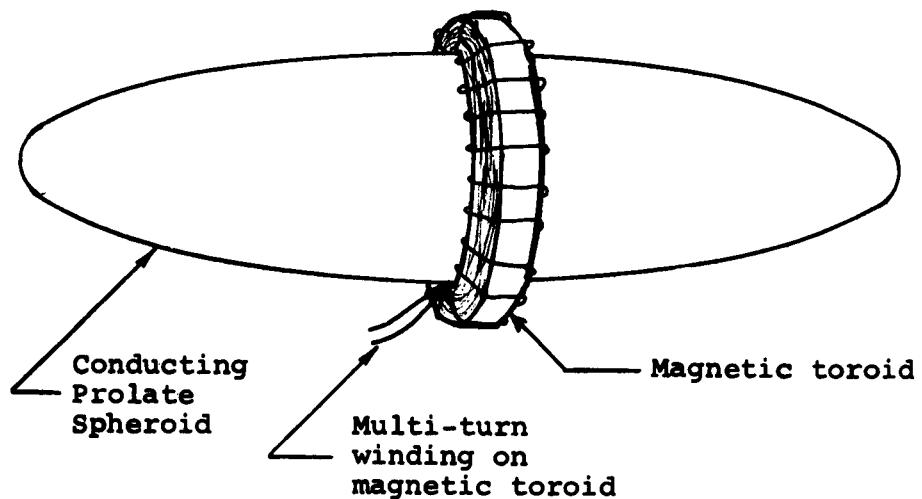


Figure 7. Toroidal Antenna.

When the toroidal antenna, threaded by the elongated conductor, is evaluated as a transmitting antenna, the results of the solution of the electrostatic problem by Stratton are no longer applicable. The determination of the impedance is, therefore, a difficult problem which has been attacked by finding the upper and lower bounds on the impedance without considering the presence of the elongated conductor through the toroidal axis. As yet, no satisfactory solution to the problem, including the elongated conductor, has been found. An experimental measurement did verify the gain relationship existing between the toroidal antenna operating with and without the elongated conductor's presence. The publication of the report on these antenna measurements will be postponed until these problems are solved.

5. Side-Loaded Transmission-Line Antenna. Experimental work is being continued on the side-loaded transmission-line antenna in an attempt to find a geometry which will lend itself to being towed by an aircraft. The antenna configuration which was first evaluated was that of a parallel-wire transmission line (Figure 8). The large physical size and poor aerodynamic properties of such an antenna make it undesirable if not impractical for conventional use. The configuration now being investigated is coaxial in nature. It is being experimentally compared with a sleeve antenna of identical size (Figure 9) to see if it has sufficient merit to warrant

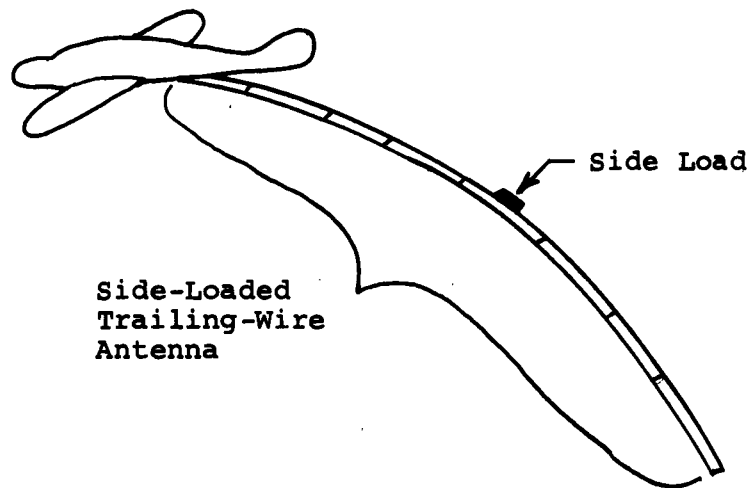


Figure 8. A parallel-wire, side-loaded, trailing-wire antenna being towed by an aircraft.

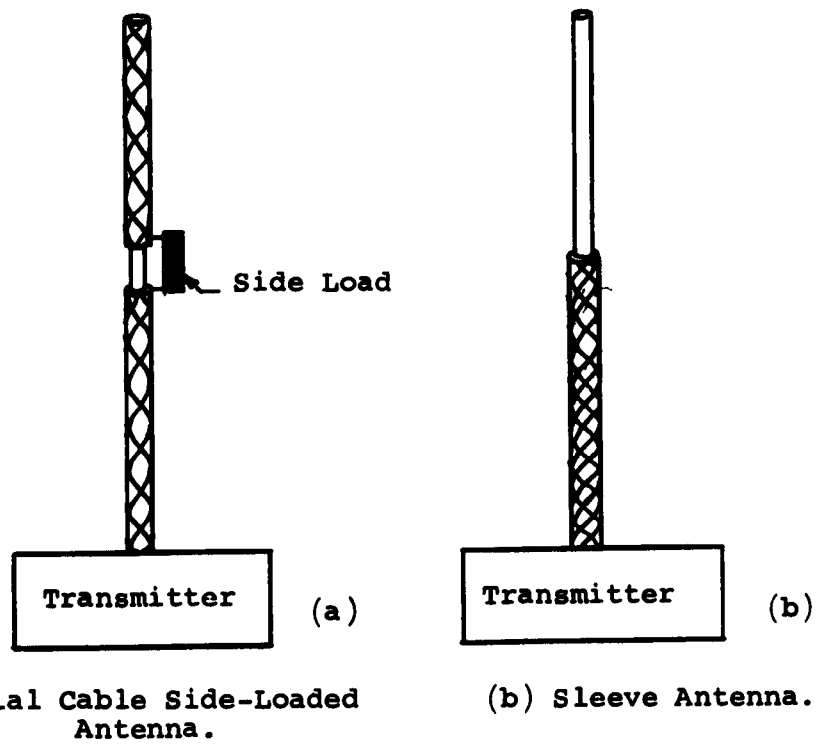


Figure 9.

a theoretical evaluation. If the results of the experimental test show that it does possess characteristics superior to the sleeve antenna, the theory will be developed and a practical design attempted.

6. Three-Layer Model (Sea-Air-Ionosphere). The design of a three-layer model is the next logical step following the two-layer model described above. The results obtained from the two-layer model are valid only for a flat sea when the ionosphere can be neglected.

The first approach to the design of a three-layer model is the flat-earth configuration. Initially this configuration was to consist of two layers of salt water separated by a thin layer of low-loss dielectric. With this arrangement one layer of water represents the sea, the other the ionosphere; and the sandwiched layer of dielectric represents the air. Because of the low dielectric constant of the styrafoam used to represent the air, the model is not large in wavelengths even though it was to be physically large for a laboratory model (16 feet in diameter). Consequently, the reflections from the edges of the model were too large to be neglected. After numerous attempts to alleviate the reflection problems on smaller models were unsuccessful, the configuration was discarded in favor of a different scheme.

If the dielectric to represent the air possessed a large relative dielectric constant, the model could be many wavelengths in extent for the same physical size mentioned above.

With this idea in mind, distilled water was selected as the dielectric to represent the air. Assuming the relative dielectric constant of distilled water to be 80 and other parameters the same of those of the air (i.e., the losses in distilled water can be considered negligible), the electrical size of the model will be approximately nine times as large as the model which employs styrafoam.

Preliminary tests were performed on a small model consisting of parallel aluminum plates separated by distilled water contained in a plastic liner (Figure 10). The results indicate that edge reflections are not a serious problem; however, the evaluation of these initial tests is not complete. If the edge reflections are negligible, the next step will be to replace the upper aluminum plate with a salt water layer contained in another plastic liner. This configuration may allow the trailing-wire antenna to be modeled and to take into consideration the anisotropy of the ionosphere by the proper phasing of two perpendicular antennas.

A large model based upon the use of water in each of the three layers can allow the curvature of the earth to be considered. A sketch of such a model is illustrated in Figure 11. Two concentric hemispherical plastic liners are forced to assume the proper shape by a slight hydrostatic pressure produced by filling the respective layers to slightly different levels.

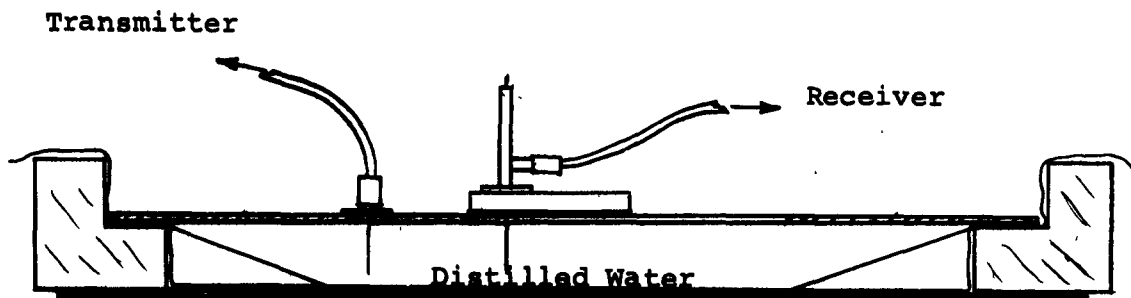


Figure 10. A cutaway view of a small model which employs distilled water as a dielectric.

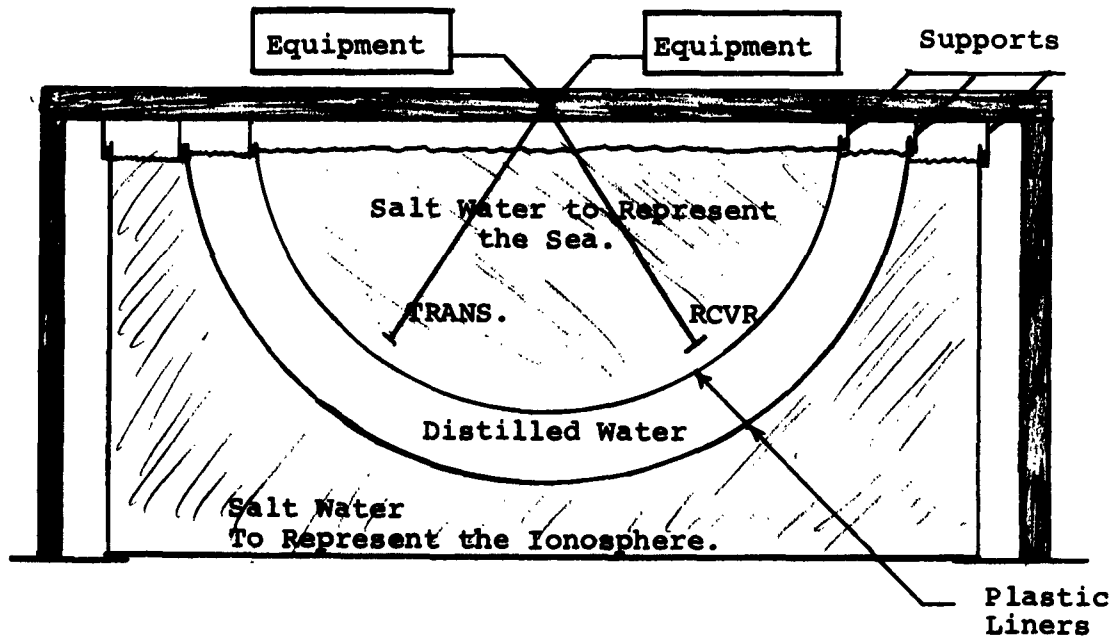


Figure 11. A possible scheme for obtaining a spherical configuration in the three-layer model.

## PLANS FOR 1963

During 1963 we propose to continue in general the tasks that were under way at the end of 1962, but with particular emphasis on the ELF portion of the spectrum.

### I. ELF/VLF Propagation

In the area of ELF/VLF propagation we propose to continue working on the extension of the theory of communications between stations in the ionosphere, in the air and on the surface of the earth and submerged submarines. We will continue to investigate the effects which could enhance ELF/VLF propagation and could lead to improvements in submarine communication or to a better understanding of its problems.

Air-to-Submarine Propagation. Work will continue on the evaluation of electromagnetic fields at VLF caused by airborne antennas and received by submerged dipoles. This will be extended to the ELF portion of the spectrum. The effects caused by an anisotropic ionosphere will be included. The main objective of this task will be to provide a theory of computational procedures for predicting field strengths in the sea for an arbitrary propagation path, arbitrary antenna height and orientation, varying characteristics of the ionosphere and for any other significant parameters.

The Effect of the Sea State on Air-to-Sea and Sea-to-Air Propagation. Now that it has been determined that only the gross features of the sea surface are required to describe such a surface for the purpose of solving this problem, the effort will center on a search for mathematical methods to evaluate the expressions resulting from Maxwell's equations near a rough air-sea interface. At present the finite difference method appears to be the best mathematical approach available for the solution of such expressions. The simple two-dimensional case on which this method was tried checked with the results obtained by others. The use of this method will be extended to rougher surfaces and to three-dimensional problems, although it is not yet at all clear as to whether this can be accomplished or how it could be done. Such calculations are expected to be quite involved, and extensive use of computers is anticipated.

Submarine-to-Air Propagation. In the initial study of the sea-air ionosphere problem at ELF, ideal conditions were assumed (flat boundaries, isotropic ionosphere, etc.), and the field strengths in the sea, resulting from submerged electric vertical and horizontal transmitting dipoles, were computed. The results obtained were restricted to very large ranges to satisfy the constraints in approximating some of the integrals. It appeared, at that time, that some kind of a numerical process could be used to remove these limitations.

An attempt was made to determine the feasibility of solving numerically the integrals associated with a submerged electric dipole. The preliminary investigation showed that the problem was much more complicated than at first anticipated. It has been shown that, although these integrals can be evaluated numerically, a considerable effort would be required. It appears that other approaches to the problem are available which should be superior and more direct than the evaluation of the integrals. It is proposed to investigate these approaches further.

Satellite-to-Submarine Propagation. It is assumed that a satellite may be used to propagate ELF/VLF to the earth either from the ionosphere or from beyond the F-layer of the ionosphere. To investigate the feasibility of this method of communication it is proposed to continue the study of propagation from or beyond the ionosphere to points on the earth's surface and into the sea. To accomplish this, the recently completed work for obtaining the far-zone VLF radiated power for current sources in a homogeneous anisotropic ionosphere will be extended to the near field and to the air-ionosphere interface. Particular emphasis will be placed on the extension of this theory to ELF.

## II. ELF/VLF Antennas

In the area of antenna studies we will continue looking for new approaches to the development of antennas for communication with or between submarines. Particular attention will

be devoted to those antennas that offer the most promise in the enhancement of submarine communication in the ELF portion of the spectrum. Some attention will be given to the establishment of controlled directivity of totally submerged antennas.

Submerged Antennas. The theoretical investigation of fundamental properties and limitations of submerged electric and magnetic sensors will continue and will be extended to electric and magnetic antennas as receiving elements. It is anticipated that this task should determine whether directivity can be obtained with a submerged antenna or prove that, on the basis of the current level of the state of the art, submerged directivity is not practical.

Air-to-Submarine Antennas. The effort on this task will continue on the investigation of side-loaded transmission lines used as trailing-wire antennas. It is proposed to extend the experimental investigation of the coaxial form of the side-loaded transmission line in order to establish a better correlation between the radiating properties and the input impedance. Previous attempts to determine this correlation have been hampered by masking effects of reflections from walls and an undetermined amount of radiation from the model due to an unloaded side-slot. It should be possible to obtain the desired correlation by means of further input impedance and field intensity measurements at a higher power level in an outdoor open area. It

should be possible to determine from these measurements whether a more detailed analysis of the coaxial side-loaded transmission-line antenna is justified. Since experimental work using a single bare wire as an airborne trailing-wire antenna is now under way, it is proposed that a theoretical study of the current distribution, input impedance and efficiency of such an antenna be undertaken and the results compared with those obtained on transmission-line antennas. An investigation of the use of a second trailing-wire antenna as a director should also be undertaken.

ELF Antenna for Launching Waves in Air. The search for a suitable antenna for launching ELF signals in air will continue in order to find the best method for reliably getting signals from the shore to a submarine at long ranges. Calculations of impedance, current distribution, the effect of earth conductivity and permittivity, as well as field strengths, should continue. If the initial study shows promising results, limited verification of the theory should follow. It appears that the toroidal type of antenna buried in a conducting soil offers promise, and it is proposed to continue investigating this type of an antenna.

Antennas in or beyond the Ionosphere. Theoretical investigation to determine practical expressions for the driving-point impedance of an electric antenna at VLF in the ionosphere will continue. It is anticipated that the

impedance will show the effects of the antenna's orientation with respect to the earth's magnetic field. The initial task will be on a bare antenna in a homogeneous anisotropic ionosphere. Once this problem is solved it will be extended to an insulated antenna in an inhomogeneous anisotropic ionosphere. The effect that a sheath of electrons near the antenna may have on antenna performance will also be considered.

### III. Experimentation, Modeling and Testing

When all the variables are considered, the problem of ELF/VLF propagation and antenna design is one of great complexity. To obtain experimental data at this frequency is time-consuming and costly. When conditions such as these prevail it is often helpful to scale the experimental set-up so that a simulated picture of the problem can be obtained. This of course leads to modeling. It may be possible in a model to represent to some extent the sea, the air and the ionosphere and their effects on electromagnetic propagation and antenna performance. Even though such models are not to exact scale they are often helpful to the understanding of the problem as they may indicate the order of magnitude of one parameter when another is made to change. Often the direction of such a change may be significant. As is true of any model, the analogy generally holds only for a restricted range of operating conditions, but within such a range it may give useful answers. This is the

reason why modeling is considered so important in a study of ELF/VLF propagation and antennas.

We now have a useful technique to simulate two-layer, sea-air problems; however, extrapolating such experimental data to the three-layer problem (sea-air-ionosphere) has presented a number of difficulties. For this reason we propose to continue working on the three-layer model, feeling that the study of the model itself may help us understand some of the difficulties involved in ELF/VLF propagation and antenna investigations.

When the requirement arises we propose to model, if this is at all possible, antennas buried in the ground or submerged in the sea, and any novel type of an antenna. We feel that this may help in understanding the problems connected with submarine communications and provide indications as to possible avenues of attacking them.

INDEX OF REPORTS PREPARED UNDER  
CONTRACT Nonr 2798(01)(FBM)

Technical Reports

- EE-59 "Experimental Verification of Horizontal Electric Dipole Radiation in a Conducting Half-Space," by W. E. Blair, June 1962.
- EE-60 "Transmission Coefficients for Electromagnetic Plane Wave Radiation into a Conducting Half-Space," by Elizabeth B. Simmons, December 1961.
- EE-69 "A System for Recording Electromagnetic Atmospheric Noise in the 3-50 cps Region," by James F. White, January 1962.
- EE-70 "Measurements of Electromagnetic Atmospheric Noise in the 3-50 cps Region," by James F. White, February 1962.
- EE-74 "A Study of the Electrical Dipole Moment and the Far Fields from a Trailing Wire Antenna," by R. W. Kulterman, June 1962.
- EE-76 "Electromagnetic Radiation in Magneto-Ionic Media for VLF and VHF Spectra," by Kenneth R. Cook, July 1962.
- EE-78 "Linear Side-Loaded Transmission-Line Antennas," by Robert W. Kulterman, August 1962.
- EE-83 "Experimental and Theoretical Investigations of the Feasibility of Wave Propagation in the Earth's Crust," by C. J. Benning, K. R. Cook and R. D. Kelly, October 1962.

Technical Memoranda

- TM #5 "On Norgorden's Refraction Coefficient," by R. H. Williams, January 1962.
- TM #6 "A Note on the Use of an Island as an ELF or VLF Transmitting Antenna," by Kenneth R. Weiner, August 1962.

List of Publications

Durrani, S. H., "Air-to-Sea Communication -- Electro-magnetic Fields in the Two Media Caused by Vertical and Horizontal Electric Dipoles in Air," a paper presented at the URSI meeting held October 23 to 25, 1962, at Austin, Texas.

Cook, K. R. and R. D. Kelly, "Quasi-Static Response of a Magnetic Dipole Near the Air-Earth Interface," a paper presented at the URSI meeting held October 23 to 25, 1962, at Austin, Texas.

Durrani, S. H., "Air-to-Undersea Communication with Electric Dipoles," PGAP Transactions, Vol. AP-10, Number 5, September 1962.